# Towards the Characterization of Enzymes Involved in the Metabolism of Tyrosine and Tyrosine Derivatives

Prajwalini Vijaykumar Mehere

Dissertation submitted to the faculty of the Virginia Polytechnic Institute and State University in partial fulfillment of the requirements for the degree of

Doctor of Philosophy
In
Biochemistry

Jianyong Li
David R. Bevan
Timothy R. Larson
Jinsong Zhu

December 6, 2010
Blacksburg, Virginia

Keywords: Tyrosine, aminotransferase, arylalkylamine, acetyltransferases

# Towards the Characterization of Enzymes Involved in the Metabolism of Tyrosine and Tyrosine Derivatives

Prajwalini Vijaykumar Mehere

# ABSTRACT

Tyrosine is involved in many biological processes including protein synthesis. This dissertation is focused on two different aspects: tyrosine catabolism and tyrosine derivative metabolism. Tyrosine undergoes degradation via tyrosine aminotransferase (TAT). Deficiency of TAT leads to some disease conditions or tyrosinemia type II. TAT has been characterized in several species, including humans. Mouse tyrosine aminotransferase was used as a model protein for the tyrosine catabolism portion of this study. Characterization of TAT included its expression in a bacterial expression system, purification using various chromatographic techniques, crystallization under different conditions, and its kinetic analysis, and molecular dynamics simulations. Based on sequence, structure, and kinetic data we have shown that mouse TAT behaves like human TAT. Our crystallization studies added new insights into the mechanism of TAT by shedding light on involvement of a disulfide bond in the regulation of mTAT. Molecular dynamics analysis provided perspective on the differences (preferences) in the substrate specificities of mouse and *Trypanosome cruzi* TAT.

Tyrosine is a precursor of several key neurotransmitters. These neurotransmitters must be regulated in order to function properly. The hypothetical *N*-acetyltransferases from *Aedes aegypti* were used as model proteins for investigation of tyrosine derivative metabolism. We found nine potential arylalkylamine *N*-acetyltransferase (AANAT) genes in *Ae. aegypti*. Phylogenetic analysis suggests that these *Ae. aegypti* AANATs (AeAANATs) can be further divided into three clusters. Phylogenetic analysis suggests that insect AANATs may have different functions as compared with the mammalian AANATs, for which function is specific to circadian rhythm regulation. PCR amplification indicates that eight of the nine putative AeAANATs are expressed in the mosquito. Expression of the eight putative AeAANATs and substrate screening of their recombinant proteins against dopamine, octopamine, tyramine, epinephrine, tryptamine, 5-hydroxytryptamine, and methoxytryptamine established that five of the eight putative AeAANATs are true AANATs.

The discontinuous expression profiles of AeAANAT genes were studied in detail. Six of the AeAANATs were expressed in the head before and after blood feeding, suggesting their potential role in neurotransmission inactivation. Down-regulation of these genes after blood feeding suggests that blood feeding or factors related to blood feeding impact on the regulation of these genes. Kinetic studies determined that two AeAANAT proteins are highly efficient in mediating the acetylation of dopamine and 5-hydroxytryptamine. Substrate analysis of AeAANATs supports the notion that acetylation of arylalkylamines is vital to the biology of mosquito species, and that these genes emerged in response to specific pressures related to necessities for biogenic amine acetylation.

## Dedication

In the loving memory of my late grandparents Mr. and Mrs. Babulalji Mehere

# Acknowledgements

First and foremost I would like to thank to my advisor, Dr.Jianyong Li, for letting me chose subjects which were my areas of interest for this dissertation. While going through the process of Ph.D. I know that I would not be successful without his support and motivation when I needed the most. I learnt from him that science requires dedication and perseverance. I appreciate the time he spent to make me strong on profession level.

My sincere thanks to my committee members Dr. Timothy Larson, Dr. Jingsong Zhu, and Dr. David Bevan for their insightful comments and encouragements.

I would like to thank Justin Lemkul for running the molecular dynamic studies for this dissertation. Thanks to other members of the faculty, especially Dr. Pablo Sobrado for chairing my preliminary examination committee. Thanks to Dr. Qian Han for his mentorship during the program. Also my special thanks to Haizhen Ding for all the help she provided since I joined the Li laboratory. My sincere thanks to Kim Harich for his help with mass spectrophotometry analysis on metabolite project. I am very thankful to Laurie Good and Elizabeth Watson for their suggestions on writing this dissertation.

I cannot express my gratitude towards Stephanie Lewis-Huff in words for her constant support for last two years professionally as well as personally. My special thanks to my friends at Virginia Tech Dr. Vidhya Sivakumaran, Dr. Elizabeth Prittchet, and Ana Mercedes for their constant support not only on personal level but also on professional level. Thanks to my friends Sanghmitra, Kavvya, Janani, Marlyn, Arjun, and Steve for their constant support throughout the degree.

I can’t forget to thank my friends, Dr. Sejian Veeraswami, Dr. Shashikant Jadhav, and Dr. Shilpashree Shinde for being on my side in ups and downs of my life. Last but not least I would like to thank my family, my brothers Vikal, Vinal, and Ajay. I would like to thank to my mother for giving me the strength to complete this degree. Last but not the least many thanks to the almighty for giving me the courage and strength to take such a huge step in my life.

# Table of Contents

# List of Figures

## Chapter 1



## Chapter 2



## Chapter 3

## Chapter 4



## Chapter 5



## Appendix I

## Appendix II

# List of Tables

## Chapter 2



## Chapter 3



## Chapter 5



## Appendix II

# Chapter 1. Introduction

Tyrosine is an aromatic amino acid, which not only is required for protein synthesis, but also is a precursor of many neurotransmitters that play roles in many significant physiological functions (e.g., stress-induced mood regulation and stimulation of the nervous system) through signaling cascades. In many animal species, including mammals, tyrosine is typically derived via two mechanisms: (1) via the hydrolysis of tyrosine-containing proteins, and (2) hydroxylation of phenylalanine that is obtained mainly from the ingestion of protein-rich foods. In mammals, tyrosine is linked to the production of vital brain chemicals that participate in the regulation of appetite, pain sensitivity, and the body's response to stress. Tyrosine is also needed for normal functioning of the thyroid, pituitary, and adrenal glands. Any living species with a nervous system needs tyrosine to produce epinephrine, dopamine, and norepinephrine—three important neurotransmitters that control the way one perceives and interacts with the environment (*1*). In humans, a shortage of tyrosine can lead to a numbers of mental disorders such as depression, anxiety, and chronic fatigue (*2*).

Several evolutionary differences between the specific function of tyrosine metabolism in insects and mammals have been reported. For example, the reward system in insects uses octopamine instead of dopamine, which is associated with the mammalian reward system (*3*). Additionally, dopamine has been linked to the development of aversive memories in insects (*4*). However, a common link in all animals is the use of tyrosine for the biosynthesis of catecholamines, 3, 4-dihydroxy derivatives of phenylethylamine (L-DOPA) (Figure 1.1) (*5*). The biosynthesis of catecholamines begins with the enzymatic hydroxylation of tyrosine to L-DOPA by tyrosine hydroxylase (*5*). The subsequent decarboxylation of L-DOPA by dopa decarboxylase (DDC) leads to the formation of dopamine, a key signaling molecule located primarily in the striatum of mammals (*5*). Dopamine appears to have multiple functions, relating to movement, reward-related behaviors, motivation, cognition, and learning. The hydroxylation of dopamine by dopamine-β-hydroxylase (DBH) produces norepinephrine (*5*). Phenylethanolamine-*N*-methyltransferase (PNMT) methylates norepinephrine to epinephrine, which is an important hormone for the peripheral nervous system (*5*). Both the aromatic phenol ring of tyrosine and the catechol ring absorb light strongly in the UV-region, making them easy to detect. In insects, tyrosine is also linked to the production of tyramine by tyrosine hydroxylase, which is a rate-

limiting enzyme used in octopamine synthesis (*6*). Tyramine is vital for insects since it controls several physiological functions such as oviposition (*7*). This compound is also a direct precursor for the synthesis of octopamine, which plays a significant role in the fight-or-flight response (*8*). Tyramine, octopamine, and dopamine are associated with important physiological functions in insects, but an over-accumulation of these aromatic amines could be problematic for in insects. This means that specific mechanisms must be equipped to inactivate or prevent the over-accumulation of these bioactive amines. In insects, for example, aromatic amines may undergo *N*-acetylation, *O*-sulphation, and *N*-methylation in the presence of different enzymes. These modifications may prevent their excessive accumulation, thereby maintaining normal physiological functions of the insect nervous system. The *N*-acetylation of biogenic amines describes the reaction that introduces an acetyl group on amino group of biogenic amines in a chemical reaction that uses acetyl coenzyme A (AcCoA) as an acetyl group donor. The enzymes that catalyze the acetylation of biogenic amines are generally known as *N*-acetyltransferases (NATs). However, a number of function-related names have been assigned to NATs according to the structural property of their acetyl group acceptors. For example, NATs that catalyze the acetylation of arylamine and arylalkylamine are named arylamine *N*-acetyltransferase (ANAT) and arylalkylamine *N*-acetyltransferase (AANAT), respectively. The latter is particularly important since AANATs are present in many species from bacteria to humans. In mammals, AANAT plays an important role in circadian rhythm regulation (*9*). In insects, however, there are more AANANT or putative AANAT sequences, and these enzymes appear to be involved in a variety of functions such as cuticle sclerotization (*10*) and aromatic amine inactivation. In general, much is known about mammalian AANATs, but research, investigating insect AANAT—(and particularly studies targeting mosquitoes)—has largely been neglected.

Another common link that exists among all the mammals and most of the insect species is related to the catabolism of tyrosine via tyrosine transaminases/tyrosine aminotransferase. Tyrosine transaminase mediates this key reaction by converting tyrosine to *p*-hydroxyphenylpyruvate, which is subsequently converted into glucogenic and ketogenetic substrates via a series of enzymes, and is then utilized in the Krebs cycle. Interestingly, tyrosine aminotransferases (TAT) is not ubiquitously present. For example, although it is present in most insect species, it is conspicuously not found in the pea aphid (*Pea aphide) (11)*.

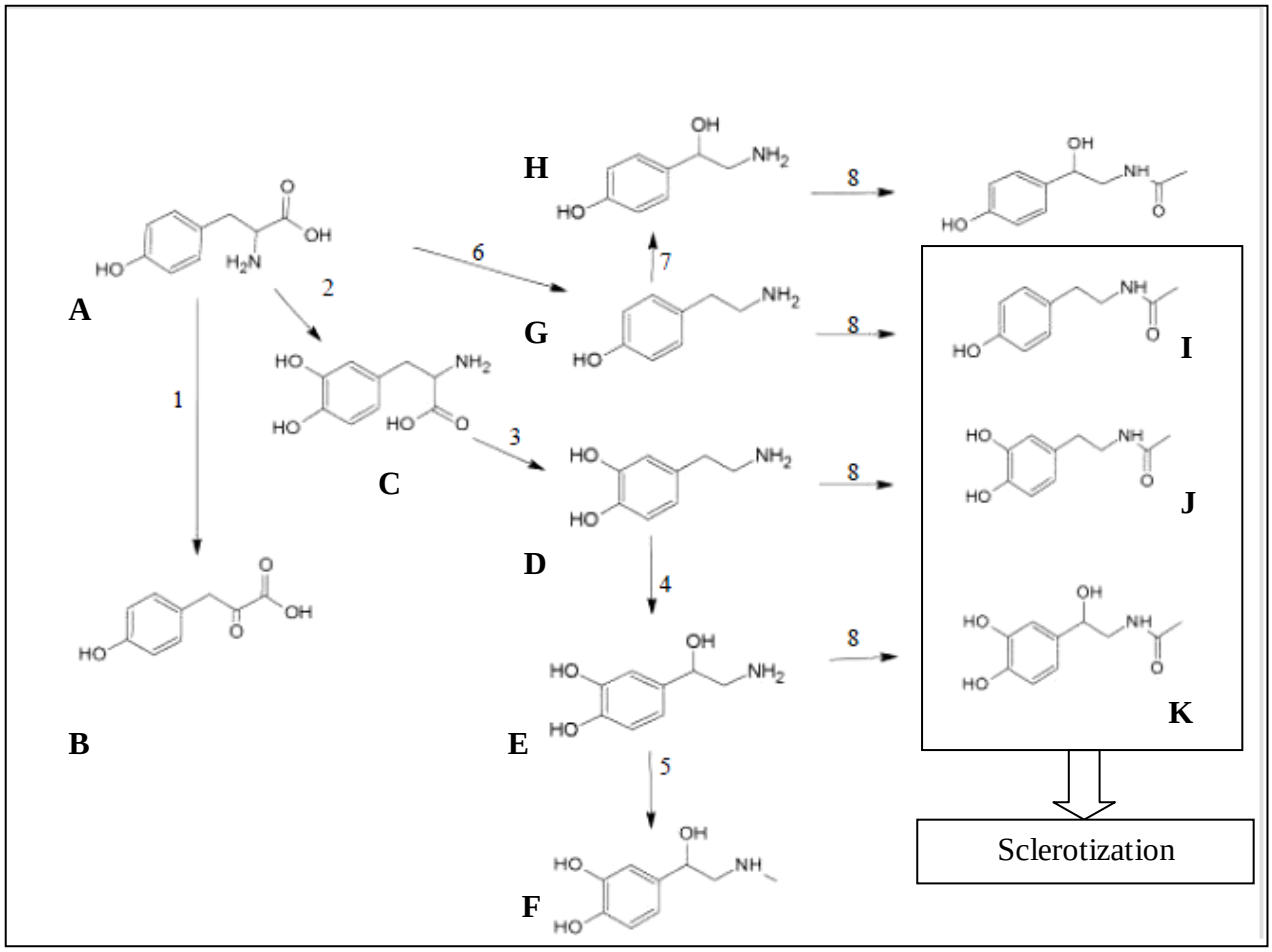


**Figure 1.1 Tyrosine metabolic pathway**.
Numbers refer to different enzymes in the pathway. (1) tyrosine aminotransferase; (2) tyrosine hydroxylase; (3) dopa-decarboxylase; (4) dopamine β-hydroxylase; (5) phenylethanolamine-*N*-methyltransferas; (6) tyrosine decarboxylase; (7) tyrosine β-hydroxylase; (8) arylalkylamine *N*-acetyltransferases. Letters refer to different compounds in the pathway: (A) Tyrosine; (B) *p*-hydroxyphenylpyruvate; (C) 3,4 dihydroxyphenylalanine; (D) Dopamine; (E) norepinephrine; (F) epinephrine; (G) Tyramine; (H) Octopamine; (I) *N*-acetyloctopamine; (J) *N*-acetyldopamine; (K) *N*-acetylnorepinephrine.

Conversely, an over-accumulation of tyrosine in the absence of functional TAT (which is essential for the degradation of this amino acid) may cause diseases such as type II tyrosinemia in mammals (12). Type II tyrosinemia, with an incidence frequency of less than 1 in 250,000 (13), is often associated with consanguinity, or shared genetic material. Abnormalities that affect the eye, skin, and neurological systems are primarily associated with this disease. When type II tyrosinemia involves the central nervous system (CNS), its outcomes can range from slight decreases in intelligence to severe mental retardation. The disease has also been linked to microcephaly, tremors, ataxia, self-mutilating behavior, fine-motor coordination disturbances, language deficits, and convulsions (14, 15).

TAT has been mainly studied in bacteria (*Escherichia coli)*, parasites (*Trypanosoma cruzi)*, rats, and humans. Although its gene from different species varies in levels of sequence identity and gene organization, all of them use pyridoxial 5'-phosphate (PLP) as a cofactor. Despite the wealth of information on mammalian TATs, their structural and functional aspects—as well as their relationship with mutations in tyrosinemia—remain to be established.

The major goal of this Ph.D. research, therefore, was to study the structure and functions of certain enzymes involved in tyrosine metabolism. Of particular emphasis was [1] the enzyme involved in tyrosine transamination using mouse TAT as a model protein, and [2] the AANATs involved in the acetylation of arylalkylamines using mosquito AANATs as model proteins. In the first study, the biochemical, structural, and computational characterization of mouse TAT is described. In the second study, the biochemical and molecular characterization of mosquito AANAT was performed using the model species, *Aedes aegypti*, which is a biological vector responsible for transmitting yellow fever. The remainder of this introductory chapter provides a brief overview of the chapters included in this dissertation.

Chapter 2 features a literature review of studies pertaining to TATs. Specifically, it summarizes previous TAT-related research in different species—with a primary emphasis, however, on mammalian TAT. This review is followed by a discussion of the evolutionary background of TAT and its place in the PLP family. Although the majority of this overview emphasizes the biochemical features, structure, and suggested functional roles of mammalian TAT, it also includes an examination of the structural and functional roles of prokaryote TAT as well. Finally, a brief discussion regarding the direction of future research on mammalian TAT is also provided.

Chapter 3 is a manuscript that describes the biochemical and structural characteristics of mouse TAT—with a special focus on the differences in substrate specificity of mammalian TAT versus TAT from invertebrate species. Particularly worth noting is the detection of intra-molecular disulfide bond formation in TAT, which helps explains previous observations regarding inactivation and reactivation of TAT under oxidative and reductive conditions, respectively.

Chapter 4 provides a review of the acetylation of tyrosine-derived aromatic amines. It summarizes current knowledge of the general control mechanisms associated with the amino acid metabolism via ubiquitous GCN5-related *N*-acetyltransferase family (GNAT). These proteins catalyze acetylation of biogenic amines using acetyl CoA as the acetyl group donor. This discussion is followed by a detailed review of important members of the NAT subfamily and their functions in eukaryotes. For example, a review of the potential roles AANATs play in insects in general, as well as physiology behaviors such as blood feeding and role of blood feeding in egg development in mosquitoes in particular, is also included. This chapter also includes a discussion regarding the roles of biogenic amines in insects. An overview of gene duplication and its importance is also reported. This chapter ends with a summary of the importance of AANAT studies in mosquitoes.

Chapter 5 describes the identification of putative AANATs in *Ae. aegypti* through (1) molecular biology approaches, (2) verification of their AANAT identity through expression of their putative AANAT coding sequences and screening of their recombinant proteins against arylalkylamines, and (3) evaluation of their expression during mosquito development. Results of this work provide an important basis for predicting the function of these enzymes in *Ae. aegypti* and possibly in other mosquitoes.

Chapter 6 summarizes the findings associated with the various components of this comprehensive study, discusses the major conclusions drawn from our experimental results, and suggests future studies that could be undertaken on aspects of this research.

Two appendices follow the main body of this dissertation. Appendix (A) provides a discussion of some initial problems encountered with TAT crystallization, as well as supplementary material on the full length mTAT protein. Appendix (B) provides an analysis of catecholamines from the brain and body extracts *of Ae. aegypti* by positive-ion electrospray

tandem mass spectrometry. The present findings in appendix (B) suggest that the *N*-acetylation pathway may be localized to the brain and body of *Ae. aegypti* mosquitoes.

## References


1. Rasmussen, D. D., Ishizuka, B., Quigley, M. E., and Yen, S. S. (1983) Effects of tyrosine and tryptophan ingestion on plasma catecholamine and 3,4-dihydroxyphenylacetic acid concentrations, *J Clin Endocrinol Metab 57*, 760-763.

2. Leyton, M., Young, S. N., Pihl, R. O., Etezadi, S., Lauze, C., Blier, P., Baker, G. B., and Benkelfat, C. (1999) A comparison of the effects of acute tryptophan depletion and acute phenylalanine/tyrosine depletion in healthy women, *Adv Exp Med Biol 467*, 67-71.

3. Barron, A. B., Maleszka, R., Vander Meer, R. K., and Robinson, G. E. (2007) Octopamine modulates honey bee dance behavior, *Proc Natl Acad Sci U S A 104*, 1703-1707.

4. Selcho, M., Pauls, D., Han, K. A., Stocker, R. F., and Thum, A. S. (2009) The role of dopamine in Drosophila larval classical olfactory conditioning, *PLoS One 4*, e5897.

5. Molinoff, P. B., and Axelrod, J. (1971) Biochemistry of catecholamines, *Annu Rev Biochem 40*, 465-500.

6. Gruntenko, N. E., Karpova, E. K., Chentsova, N. A., Adonyeva, N. V., and Rauschenbach, I. Y. (2009) 20-hydroxyecdysone and juvenile hormone influence tyrosine hydroxylase activity in *Drosophila* females under normal and heat stress conditions, *Arch Insect Biochem Physiol 72*, 263-272.

7. Raushenbakh, I., Gruntenko, N. E., Karpova, K., Adon'eva, N. V., Alekseev, A. A., Chentsova, N. A., Shumnaia, L. V., and Faddeeva, N. V. (2006) [The mechanism of the effect of apterous56f mutation on the reproductive function of *Drosophila melanogaster*], *Genetika 42*, 169-176.

8. Roeder, T., and Gewecke, M. (1990) Octopamine receptors in locust nervous tissue, *Biochem Pharmacol 39*, 1793-1797.

9. Klein, D. C. (2007) Arylalkylamine *N*-acetyltransferase: "the Timezyme", *J Biol Chem 282*, 4233-4237.

10. Andersen, S. O. (2008) Quantitative determination of catecholic degradation products from insect sclerotized cuticles, *Insect Biochem Mol Biol 38*, 877-882.

11. Wilson, A. C., Ashton, P. D., Calevro, F., Charles, H., Colella, S., Febvay, G., Jander, G., Kushlan, P. F., Macdonald, S. J., Schwartz, J. F., Thomas, G. H., and Douglas, A. E.

(2010) Genomic insight into the amino acid relations of the pea aphid, *Acyrthosiphon pisum*, with its symbiotic bacterium *Buchnera aphidicola*, *Insect Mol Biol 19 Suppl 2*, 249-258.

12. Sivaraman, S., and Kirsch, J. F. (2006) The narrow substrate specificity of human tyrosine aminotransferase--the enzyme deficient in tyrosinemia type II, *FEBS J 273*, 1920-1929.

13. Macsai, M. S., Schwartz, T. L., Hinkle, D., Hummel, M. B., Mulhern, M. G., and Rootman, D. (2001) Tyrosinemia type II: nine cases of ocular signs and symptoms, *Am J Ophthalmol 132*, 522-527.

14. Bein, N. N., and Goldsmith, H. S. (1977) Recurrent massive haemorrhage from benign hepatic tumours secondary to oral contraceptives, *Br J Surg 64*, 433-435.

15. Cavelier-Balloy, B., Venencie, P. Y., Lemonnier, V., Verola, O., Servant, J. M., Puissant, A., and Civatte, J. (1985) [*Histiocytoid hemangioma* of the scalp], *Ann Dermatol Venereol 112*, 965-972.

# Chapter 2. Literature Review on Tyrosine Aminotransferase (TAT)

Tyrosine is an aromatic amino acid that is involved in many important biological processes. Accumulation of tyrosine in blood can lead to several disorders, hence the importance of closely regulating its metabolism. The degradation of L-tyrosine begins with an α-ketoglutarate-dependent transamination through tyrosine aminotransferase (TAT) to para-hydroxyphenylpyruvate (*p*-hydroxyphenylpyruvate). The subsequent oxidation step, that is catalyzed by *p*-hydroxyphenylpyruvate-dioxygenase, breaks off 2, 5-dihydroxyphenyl-1-acetate. Next, homogentistate-oxygenase is required to split the aromatic ring of homogentisate. Thus, through the incorporation of a further $O_2$ molecule, maleylacetoacetate is created. Fumarylacetate is produced by maleylacetoacetate-*cis-trans*-isomerase from end to end rotation of the carboxyl group created from the hydroxyl group via oxidation. This *cis-trans*-isomerase contains glutathione as a coenzyme. Fumarylacetoacetate is finally divided via by fumarylacetoacetate-hydrolase through the addition of a water molecule, liberating fumarate (also a metabolite of the citric acid cycle) and acetoacetate (3-ketobutyroate) (Figure 2.1). Acetoacetate is a ketone body, which, after activation with succinyl-coenzyme A (CoA), can be converted into acetyl-CoA which can, in turn, be oxidized by the Krebs cycle or used for fatty acid synthesis.

Impaired tyrosine catabolism resulting in increased plasma tyrosine, is typically associated with certain genetic disorders and is due to defects in the enzymes involved in the catabolism of tyrosine (*1*). Tyrosine catabolism occurs through a series of enzymatic reactions that yield acetoacetate, which is ketogenic, and the Krebs cycle intermediate fumarate, which is glucogenic. Liver and kidney cells are the only two cell types that express the complete tyrosine catabolic enzymes and can completely oxidase tyrosine to carbon dioxide and water. A deficiency of these enzymes results in the hereditary tyrosenimias types 1 (*2*), 2 (*1, 3-5*), and 3 (*6*)**. The focus of this literature review is TAT (tyrosine aminotransferase), which is a rate determining enzyme in the tyrosine catabolic pathway present in the liver, and is involved in breaking down the amino acid tyrosine into *p*- hydroxyphenylpyruvate** (*1*).

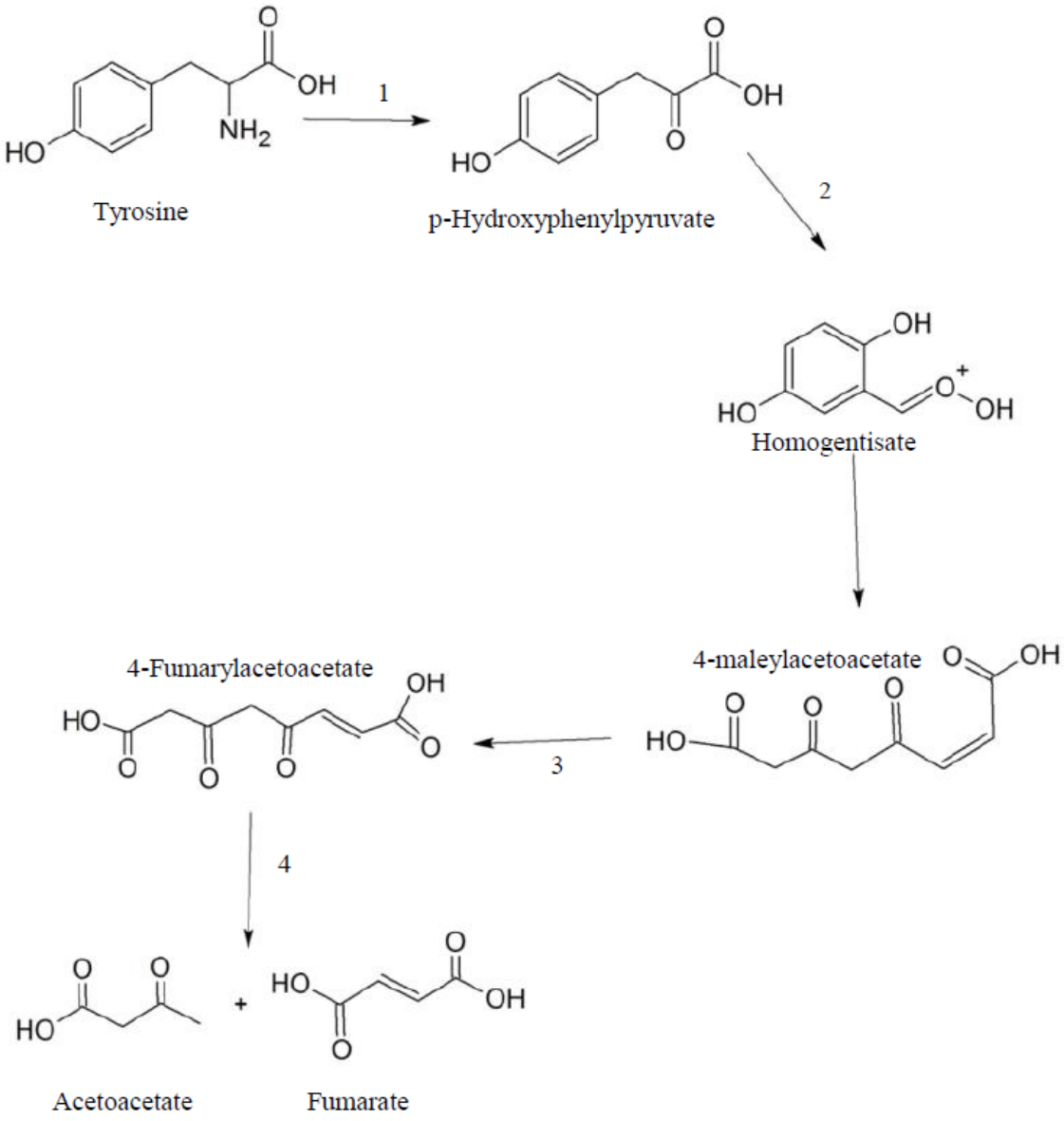


**Figure 2.1 Tyrosine degradation pathway representing the degradation of tyrosine to acetoacetate and fumarate**.

Numbers 1-4 represent the enzymes required in the pathway to carry out the successive reactions. (1. -Tyrosine aminotransferase; 2. -*p*-Hydroxyphenylpyruvate-dioxygenase; 3 -.Maleylacetoacetate *–cis –trans* –isomerase; 4 -.4-Fumaryl-acetoacetate). (Adapted from http://en.wikipedia.org/wiki/Tyrosine (2010)

## 2.1 TAT, the enzyme involved in tyrosine catabolism

TAT has been found in both eukaryotes and prokaryotes (*7*) including in bacteria (*8*), fungi (*9*), plants (*10*), animals (*11*), parasites (*12*), and flies (*13*).

In *Escherichia coli,* TATs catalyze the final step in the biosynthesis of the aromatic amino acids tyrosine, phenylalanine, and tryptophan from the common intermediate chorismate. For tyrosine biosynthesis, *tyrA* encodes the bifunctional enzyme chorismate mutase/ prephenate dehydrogenase, which catalyzes the conversion of chorismate to *p*-hydroxyphenylpyruvate. Further, the enzyme TAT, encoded as *tyrB*, catalyzes the final step in tyrosine and phenylalanine biosynthesis by converting *p*-hydroxyphenylpyruvate and phenylpyruvate to tyrosine and phenylalanine, respectively. Aspartate aminotransferases (AATs) and branched-chain aminotransferases are also involved in tyrosine and phenylalanine biosynthesis as these enzymes have overlapping activities with *tyrB* in *E. coli* and *Pseudomonas aeruginosa* (*10*). Additionally, in the bacteria, *Klebsiella pneumoniae,* it has been found that TAT plays an important role by catalyzing in the rate limiting step in the conversion of methylthioribosephosphate to α-ketomethiobutyrate. *K. pneumoniae* is responsible for urinary and respiratory tract infections as well as blood infections in humans (*14*).

In plants, tyrosine and phenylalanine biosynthesis proceeds via the intermediate, chorismate. TATs are not involved in tyrosine metabolism in plants. Rather, they are involved in the synthesis of secondary metabolites. There are seven paralogs of TATs that have been found in *Arabidopsis thaliana,* but only two enzymes have been characterized (*10, 15*).

Mammalian TATs were first discovered in the late 1950s. In humans, TAT is the rate-limiting enzyme in the tyrosine degradation pathway. Specifically, TAT, the liver-specific protein breaks down tyrosine. The molecules generated as a result of degradation process are either excreted by the kidneys or used in energy production. It has been reported that the liver is the major site for tyrosine formation as well as degradation (*16*) and under normal conditions, intracellular tyrosine levels are tightly regulated by hormones (*16*).

## 2.2 Structural features of TATs

TATs are members of the pyridoxal -5'- phosphate (PLP) dependent enzyme family that contains at least five different fold types. Detailed structural classification of this family has made it possible to divide the superfamily based on fold type (*17*). Most of the research progress to date has been associated with the fold type I, or AAT family. This family was subsequently further divided into seven subfamilies, including Iγ, Iα, and Iβ (*17*). AAT and TAT, which are members of the Iα subfamily, represent thoroughly studied enzymes of the aminotransferase superfamily. Most of the prokaryotic aminotransferases in this subfamily have relatively broad specificity in that they react with a wide variety of amino acids. The Iγ subfamily of enzymes has been relatively less characterized. Furthermore scientists have determined that the Iγ subfamily contains a diverse membership including the kynurenine aminotransferase/ glutamine transaminases (*18, 19*), the highly thermophilic AAT (*20*), and a broadly substrate specific TAT from *Trypanosoma cruzi*. Mammalian TATs possess narrow substrate specificity compared to parasite (*12*) and bacterial TAT (*21*). Most of the crystal structures determined to date belong to the Iα subfamily (*22, 23*). Recently, however, more information has been obtained by the characterization and crystallization of the members of the Iγ subfamily from mammalian species including the kynurenine aminotransferases (KAT I, KAT II, and KAT III) (*18, 19, 24*). Thus far, the TATs have been expressed, purified, characterized, and crystallized in various species such as *E. coli* (*25*), *T. cruzi* (*12*), and human (Structural genomic consortium). The catalytic event remains uncertain in human and *T. cruzi* TATs due to the lack their complex structures with substrates or substrate analogs. But the known general reaction mechanism of PLP dependent enzymes suggests that active site residues for PLP binding may have been conserved throughout the PLP dependent enzyme family, which includes TATs (Figure 2.2).

## 2.3 General reaction mechanism of PLP dependent enzymes

It has been stated in the review of Eliot et al *(26)* that PLP catalyzed reaction types can be divided according to the position at which the reaction occurs. For instance, transamination, decarboxylation, racemization, elimination, and replacement of an electrophilic R-group occur at α position. (Figure 2.3) (*26*). The apoenzyme increases natural catalytic potential and impose

selectivity of the substrate binding and reaction type (*26*) (Figure 2.3). PLP functions to stabilize negative charge development at the alpha carbon (Cα) in the transition state formed after the condensation of the amino acid substrate with PLP to form an external aldimine (*26*). The fully formed carbanions are referred to as the quinoid intermediates. The pi system of the cofactor stabilizes the Cα anion by the delocalization of the negative charge. It is for this reason that PLP is often described as an electron sink (Figure 2.3) (*26*). This factor allows PLP in the absence of enzyme to catalyze several of the potential reactions slowly (*26*).

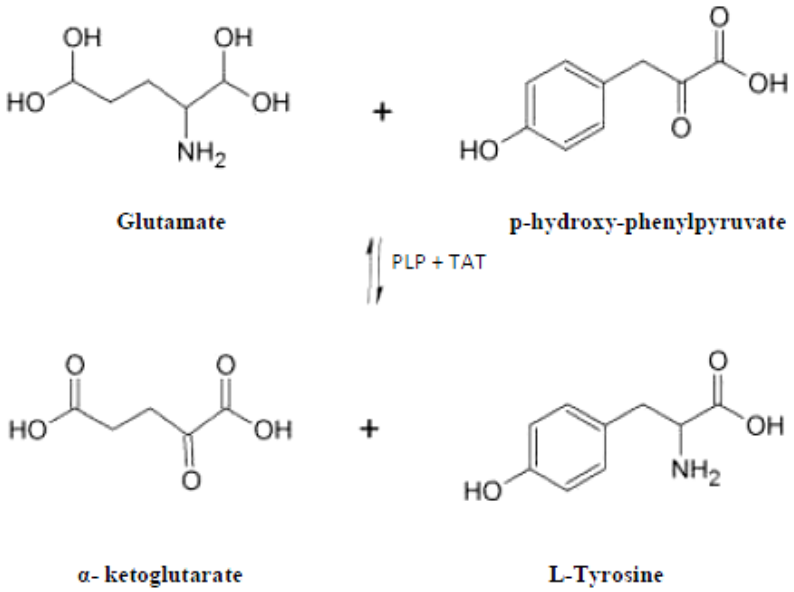


**Figure 2.2 The transamination of tyrosine and α-ketoglutarate in the presence of TAT and PLP**.

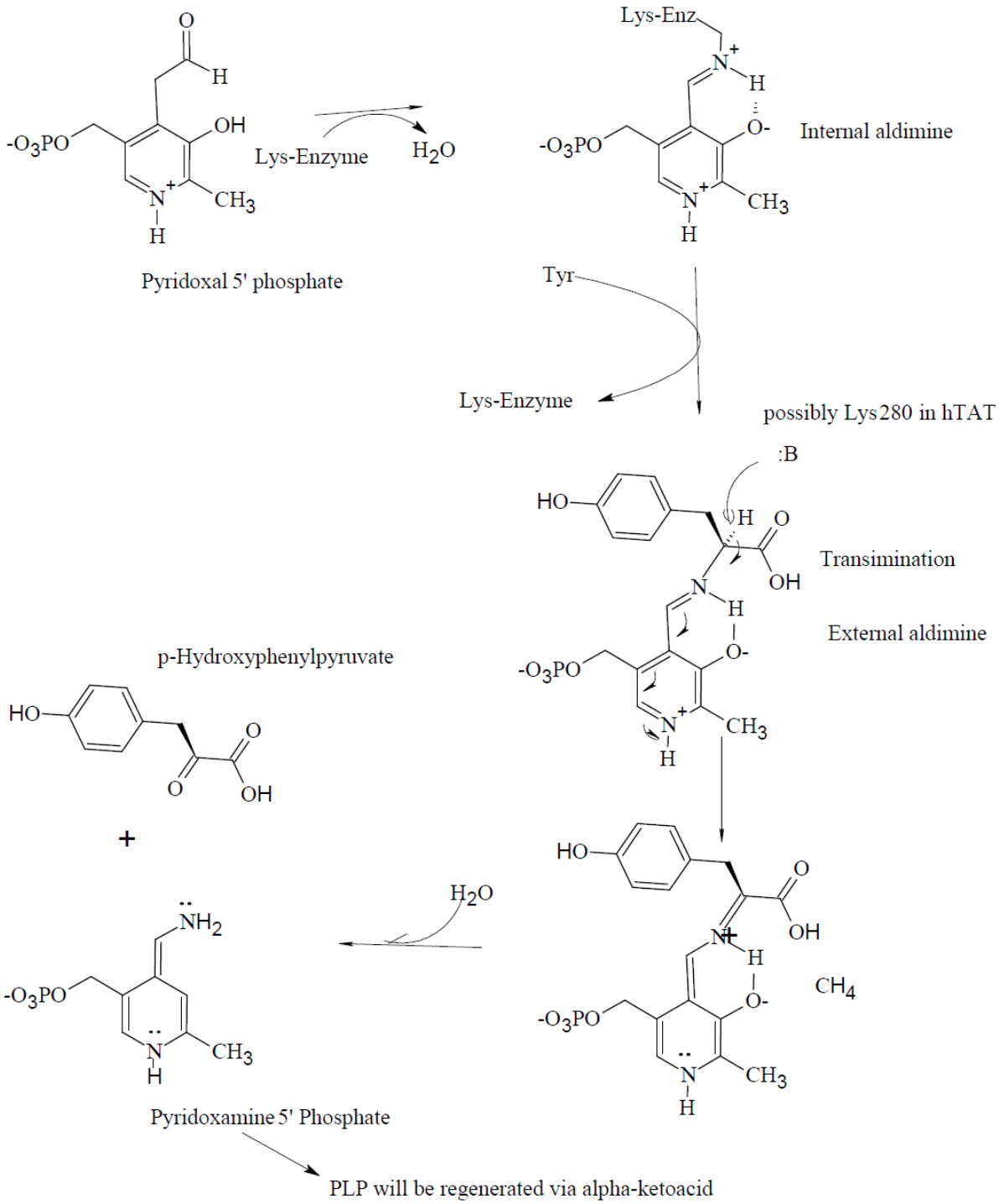


**Figure 2.3 General PLP-dependent mechanism.** This figure is adapted from http://en.wikipedia.org/wiki/Tyrosine_aminotransferase (2010). (This is the modified version of the figure).

## 2.4 Stability and regulation of TATs in mammals

It has been reported by Cienchanover et al. that in liver TATs are stable for 1-2 hours (*27*) . In the liver TAT is typically regulated by glucorticoids and ubiquitin enzymes. Ubiquitin enzymes are involved in the degradation mechanism of TAT, contrary to glucocorticoids that are involved in synthesis mechanism of TATs (*27*). It has been reported that two glucocorticoid response elements are essential for the stimulation of TAT transcription (*28*). It has also been reported by researchers that cyclic adenosine monophosphate (cAMP) also participates in the regulation of TAT activity via up-regulating its transcription (*28*). Insulin also plays a role in inducing TATs (*28*), but shown to have little effect on the process of transcription. It has been found that insulin slows the degradation rate of the enzyme and therefore it has major impact on stability of the protein. How insulin slows down the degradation rate of the enzymes (*27*) is yet to be understood.

In mammals TATs possess an additional 38 amino acids on the *N*-terminus in comparison to other TATs, e.g., *T. cruzi* and *E. coli* (Figure 2.4). The first 38 amino acids are involved in providing stability to this enzyme (*21*). It has been proven that this sequence is involved in ubiquitination and ultimately in the degradation of the TATs (*27, 28*). According to literature the *N*-terminus (33-RKKGRKAR-40) and C–terminus (450-EECDK-454) (Pro, Glu, Ser, Thr) are mainly responsible for degradation of mammalian TATs (*29*). In a report, Rogers et al. demonstrated, that TAT is protected by PLP from ubiquitin-mediated degradation. In the same report they also proposed that the binding of PLP co-factor to the enzyme may change the three-dimensional structure of the enzyme and, as a result ubiquitin–TAT ligase (E3) can not bind to lysine residues (*29*). Hypothetically, PLP may sterically hinder the Lys residues in the *N*-terminal domain that is involved in targeting TAT for degradation. However, the physiological significance of a PLP protection mechanism remains to be demonstrated and needs further investigation. This question may be answered by lower resolution TAT crystal structure along with ubiquitin binding domain.

## 2.5 Localization of TATs

Localization studies involving in rat model suggest that TAT is localized in the mitochondrial matrix in this species (*30*), whereas TAT has been found in the cytosol of humans

and frogs (*21, 31*). Mark et al. reported TAT localization in rat brain *(32).* Specifically, these researchers determined the distribution of tyrosine transaminase in the rat brain tissue (*32*). Their results indicated that brain tyrosine transaminase was primarily a mitochondrial enzyme, probably localized on the inner mitochondrial membrane. The results were discussed in relation to the function of tyrosine as a precursor of catecholamines in the central nervous system. It has been a matter of debate, however, whether or not soluble TAT is expressed in the brain, and it appears that the majority of the TAT activity in brain can be ascribed to the mitochondrial AAT. Nonetheless, one report did confirm the presence of low levels of soluble TAT in brain tissues (*33*).

**Table 2.1 Different factors/compounds/hormones that regulate TAT activity.**

| **Species** | **Factors/ compound/hormones** | **Effect on activity** | **References** |
|---|---|---|---|
| *Felis catus* | Vitamin B6 deficiency | Inhibit PLP binding to TAT | (*34*) |
| *Gallus gallus* | Heat stress | Increases TAT activity in the liver | (*35*) |
| *Rattus norvegicus* | Insulin | Increases TAT activity | (*36*) |
| *Rattus norvegicus* | Hydrocortison | Increases TAT activity | (*36*) |
| *Rattus norvegicus* | Adrenalin | Increases TAT activity | (*37*) |
| *Rattus norvegicus* | Dexamethazon | Increases TAT activity | (*38*) |
| *Rattus norvegicus* | Glucagon | Increases TAT activity | (*39, 40*) |
| *Rattus norvegicus* | Estradiol | Increases TAT activity | (*41*) |
| *Rattus norvegicus* | Ethanol (acute administration) | Induces TAT synthesis by downstream or upstream effectors | (*42*) |
| *Rattus norvegicus* | Ethanol (Chronic administration) | No change | (*42*) |

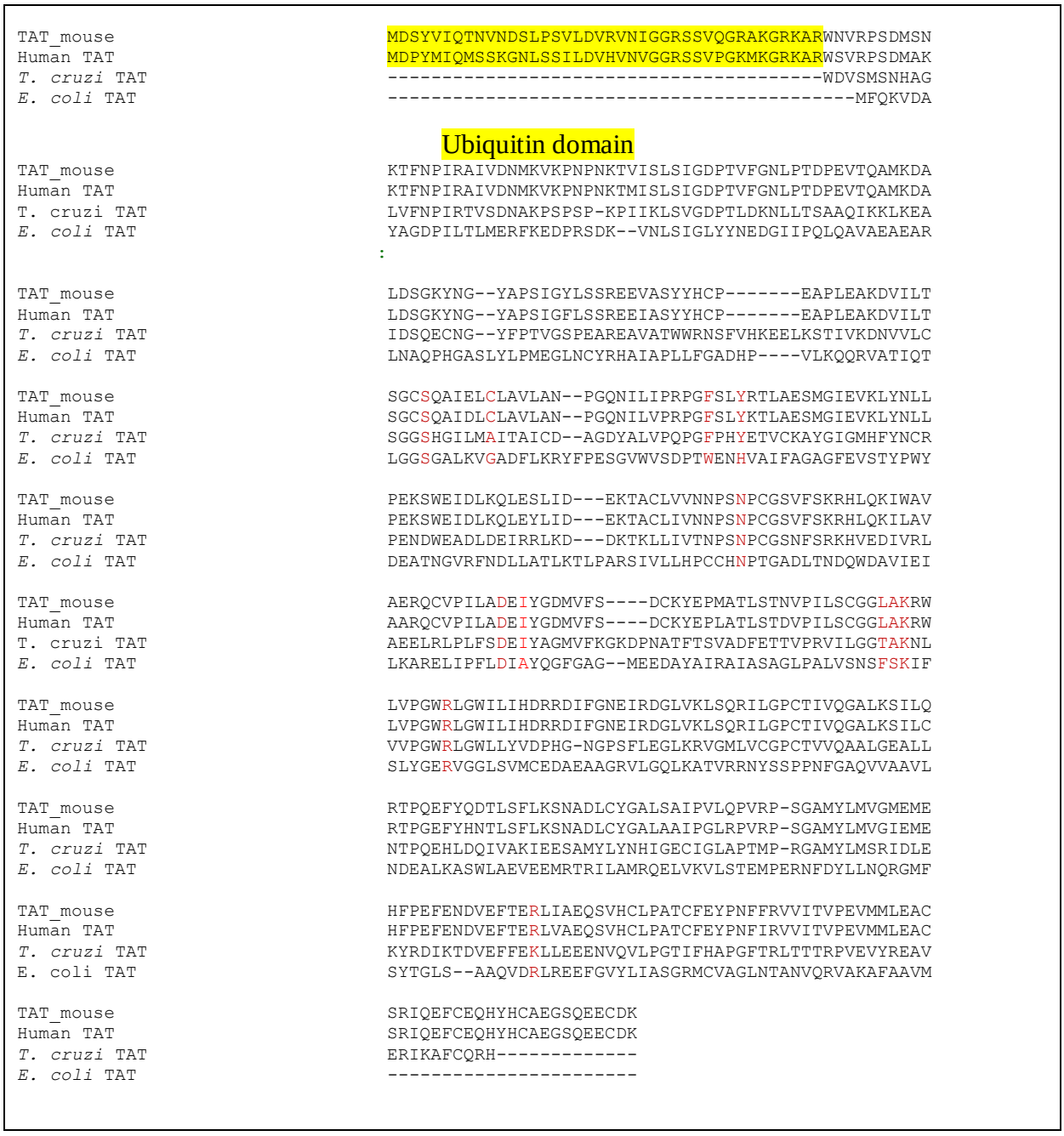


**Figure 2.4 Sequence alignment of mouse, human, *T. cruzi*, and *E. coli* TATs.**
The active site residues are colored in red. The first 38 amino acids of the *N*-terminus (Yellow) in human TAT and mouse TAT represent the TAT-ubiquitin binding domain. Potential active site residues are shown in red. Sequence alignment using was done using ClustalW (*43*).

## 2.6 Diseases and genetic conditions related to TATs in humans

The human TAT (hTAT) gene is located on the long arm of chromosome 16 at position 22.1 (*44*). Mutations in TAT gene may cause a shortage of the enzyme leading to a toxic accumulation of tyrosine and its byproducts, which are capable of damaging the liver, kidneys, nervous system, and other organs. TAT mutations lead to an autosomal disorder commonly known as Richner –Hanhart syndrome (Online Mendelian Inheritance in Man (OMIM) no. 276,600). It is a rare autosomal disorder caused by deficiency of hepatic cytosolic TAT, which is the rate limiting enzyme of tyrosine catabolism. Thus far, 15 mutations in the hTAT gene have been identified in tyrosinemia type II patients from families in Italy, France, the USA, and UK. These mutations are scattered over the entire gene including six missense, four nonsense, two splice mutations, and one silent mutation (*21, 45*). A complete deletion of both TAT alleles in a single patient has also been reported (*46*). No literature has been available, which states a clear correlation in the clinical phenotype of tyrosinemia type II patients with any particular hTAT gene mutation. The clinical symptoms for tyrosinemia type II include elevated plasma tyrosine levels and skin and eye lesions (*1, 47-49*). Affected individuals usually have painful, non-pruritic, and hyperkeratotic plaques on the soles and palms. The plantar surface of the digits may show marked yellowish thickening associated with hyperkeratosis. Ophthalmologic involvement is recalcitrant pseudodendritic keratitis (*50*). Several studies indicated that the skin and eye symptoms often present within the first year of life and include excessive tearing, photophobia, eye pain, and redness. Skin lesions may present from the first few weeks of life to the second decade. Tyrosinemia type II also leads to mental retardation in more than 50% of reported cases, but the mechanism behind it is unknown (*51*). According to several studies, tyrosine restricted and phenylalanine restricted diet offer rapid recovery of the oculocutaneous signs and symptoms of Richner and Hanhart syndrome and may prevent mental retardation (*50, 52*). .Recently Fu et al. showed that TAT is a novel suppressor gene of the development and progression of hepatocellular carcinoma, and its deactivation caused by gene deletion and hypermethylation contributes to the pathogenesis of hepatocellular carcinoma (*44*). It has been reported that TAT deficiency leads to corneal dystrophies (*53*). Activity for TATs has been induced in neoplasm, and in liver by hepatotropic poison (*40, 54*). Besides these, several examples in the literature describe the interrelationship of TAT and various diseases or conditions (Table 2.2)

**Table 2.2 Examples of diseases/conditions, causes and effect of/on TAT.**

.

| Diseases / Condition | Causes | Effect of/on TAT | References |
|---|---|---|---|
| Arthritis | Induced /experimental | Induction of TAT in liver of rat | (*55*) |
| Asbestosis | Asbestos | TAT acts as a marker | (*56*) |
| Burns | Irradiation or flash burn injuries | TAT induced in liver | (*57*) |
| Carbon tetrachloride poisoning | Animal was treated with CCL4 | Induced TAT activity in the liver | (*58*) |
| Carcinoma 256 walker | Transplanted in rats | Induced TAT activity in liver | (*59*) |
| Hepatocellular carcinoma | Superinduction by actinomyosite, amphotericin B | Induced TAT activity | (*60*) |
| Chagas disease | Caused by *T.cruzi* a parasite | TATs were expressed in all benzaldehyde-resistant strains; and thus considered as potential target for chemotherapy | (*61*) |
| Cholera | Induced | Blocking of promoter by Cholera toxin | (*62*) |
| Craniopharygioma | hormonal | Induced TAT activity | (*63*) |
| Cystinosis | CHST6, KRT3, KRT12, PIP5K3, SLC4A11, TACSTD2, TGFBI, and UBIAD1 genes | TAT deficiency | (*53*) |
| Diabetes mellitus | Thyroid hormones and alloxan | Induced TAT activity | (*64*) |
| Maple syrup disorder | Phenylketone bodies in the urine | Defect in TAT | (*65*) |
| Hemangioblastoma | Induced | Induced TAT activity | (*63*) |

## 2.7 Substrate specificity of TATs in different species

According to Jensen and Gu (*17*) classification, the *E.coli* TATs, which belong to the Iα subfamily, transaminate both aromatic amino acids efficiently and also accept dicarboxylic amino acids (*66*). The *T. cruzi* (tcTAT) shows broad substrate specificity including leucine, methionine, alanine and the aromatic amino acids as amino acid donors, and several 2-oxoacids, such as pyruvate and 2-oxoisocaproate as amino acceptors (*21*). Valine, isoleucine, and dicarboxylic amino acids are poor substrates for tcTAT (*21*). In contrast, hTAT shows narrow substrate specificity in spite of sharing 40 % sequence identity with tcTAT (*21*). hTAT did not show any activity to aspartate and does not utilize other cosubstrates, such as pyruvate, oxaloacetate, or α-ketoisocaproate (*21*).

## 2.8 Structural studies of TATs

To date, three crystal structures of TATs have been available in the Research Collaboratory for Structural Bioinformatics (RCSB) protein data bank. These structures are from *E. coli (25)*, *T. cruzi* (*25*), and human (Figure 2.5). The crystal structure of *E.coli* TAT was determined in the late 1990s by molecular-replacement methods at 3.5 Å resolution. The overall fold of *E. coli* TAT resembles the aspartate aminotransferases with two identical subunits forming a dimer in which each monomer binds a PLP molecule via a covalent bond linked to the epsilon-$NH_2$ group of Lys258. In comparing with the structure of *E.coli* TAT with those of the open, half-open or closed forms of chicken or *E. coli* aspartate aminotransferases, it showed that the *E.coli* TAT structure to be in the open conformation (*25*). *E.coli* TAT belongs to the Iα subfamily with 3.5 Å resolution. The second TAT crystal structure was solved in the late 1990s from *T. cruzi* (tcTAT) (*12*). The structure of tcTAT, which belongs to subfamily Iγ, was determined at 2.5 Å resolution. This structure shares 70% sequence similarity with mammalian TATs. TcTAT is responsible for pathogenesis of Chagas disease (American trypanosomiasis) in human, which has been linked to congestive heart failure (*67*). Chagas disease is transmitted to animals and humans by insect vectors that are found primarily in the Americas. Chagas disease occurs in two phases: an acute phase characterized by focal or diffuse inflammation mainly affecting the myocardium, and a chronic phase marked by an inflammatory fibrotic reaction that

damages the cardiac muscle, conduction network, and enteric nervous system. Dutra and Gollob (*68*) reported that the disease is due to a multifactorial, persistent, and variable interaction between the pathogen and host. It has been shown that tcTAT may be involved in drug resistance to benznidazole, a drug currently being used in chemotherapy of Chagas disease (*61*). The tcTAT structure was solved using the molecular replacement method. The crystal structure of tcTAT shows two major differences from the AAT in the Iα family. Blankenfieldt et al. (*12*) reported that tcTAT contains a loop protruding from the enzyme surface in the larger cofactor binding domain, whereas the AAT have a kinked alpha helix. Second is the smaller substrate binding domain. The tcTAT has a four stranded antiparallel beta sheet instead of the two stranded beta sheet seen in AAT (*12*). The position of the aromatic ring of the tcTAT PLP cofactor is similar to that seen in AAT, but the phosphate group is closer to the substrate-binding site with one of its oxygen atoms pointing towards the substrate (*12*). The crystal structure of TAT has also been deciphered in humans, but no discussion is available on this structure. Further research is also needed to elucidate the relationship between the crystal structure of TAT and mutations thereof that lead to tyrosinemia type II.

## 2.9 Summary

Despite rapid progress over the past few decades in our understanding of the various roles of the TAT enzyme plays in diverse species, the exact mechanism of interaction between TAT and its substrates is unclear. It is poorly understood why there is a difference in the substrate specificity in spite of the high protein sequence similarity between tcTAT and mTAT or hTAT. Moreover, despite documented evidence of the involvement of active site residues in the catalysis of mammalian TATs, these reports lack important details concerning structural information. For example, the presence of disulfide bonds in mTAT was predicted under oxidative conditions, but not demonstrated in earlier studies (*69*). In this dissertation, detailed structural characterizations of mTAT in cofactor binding mode are elucidated—along with molecular dynamic studies, which shed light on possible residues responsible for the stability of the mTAT-Tyr complex. Additional molecular dynamic studies were carried out to differentiate between two very similar structures, as well as to shed light on how small molecules (e.g., alanine) are accommodated in tcTAT, but not in hTAT.

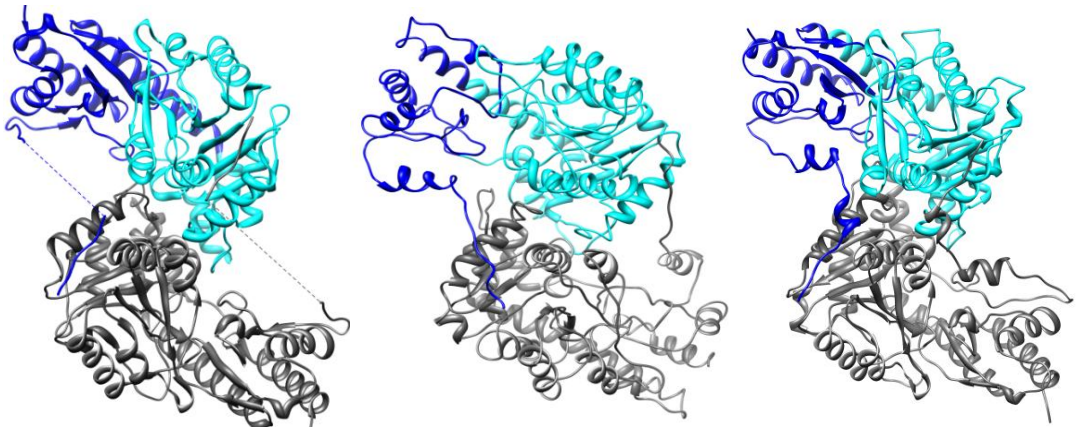


**Figure 2.5 The crystal structures of TATs from different species: human (A), *E. coli* (B), and *T.cruzi* (C).**
The small and large domains are depicted in two different colors in each structure. The small domain (along with *N*-terminus) is shown in blue; the large domain is shown in cyan. One of the two subunits is shown in gray.

## References


1. Natt, E., Kao, F. T., Rettenmeier, R., and Scherer, G. (1986) Assignment of the human tyrosine aminotransferase gene to chromosome 16, *Hum Genet 72*, 225-228.

2. Aponte, J. L., Sega, G. A., Hauser, L. J., Dhar, M. S., Withrow, C. M., Carpenter, D. A., Rinchik, E. M., Culiat, C. T., and Johnson, D. K. (2001) Point mutations in the murine fumarylacetoacetate hydrolase gene: Animal models for the human genetic disorder hereditary tyrosinemia type 1, *Proc Natl Acad Sci U S A 98*, 641-645.

3. Bohnert, A., and Anton-Lamprecht, I. (1982) Richner-Hanhart's syndrome: ultrastructural abnormalities of epidermal keratinization indicating a causal relationship to high intracellular tyrosine levels, *J Invest Dermatol 79*, 68-74.

4. Chitayat, D., Balbul, A., Hani, V., Mamer, O. A., Clow, C., and Scriver, C. R. (1992) Hereditary tyrosinaemia type II in a consanguineous Ashkenazi Jewish family: intrafamilial variation in phenotype; absence of parental phenotype effects on the fetus, *J Inherit Metab Dis 15*, 198-203.

5. Fellman, J. H., Vanbellinghen, P. J., Jones, R. T., and Koler, R. D. (1969) Soluble and mitochondrial forms of tyrosine aminotransferase. Relationship to human tyrosinemia, *Biochemistry 8*, 615-622.

6. Endo, F., Awata, H., Katoh, H., and Matsuda, I. (1995) A nonsense mutation in the 4-hydroxyphenylpyruvic acid dioxygenase gene (Hpd) causes skipping of the constitutive exon and hypertyrosinemia in mouse strain III, *Genomics 25*, 164-169.

7. Canellakis, Z. N., and Cohen, P. P. (1956) Kinetic and substrate specificity study of tyrosine-alpha-ketoglutaric acid transaminase, *J Biol Chem 222*, 63-71.

8. Mavrides, C., and Orr, W. (1975) Multispecific aspartate and aromatic amino acid aminotransferases in *Escherichia coli*, *J Biol Chem 250*, 4128-4133.

9. Sim, S. K., and Choi, Y. K. (1971) Tyrosine aminotransferase activity in a soluble extract of ergot fungus, *J Pharm Pharmacol 23*, 78-80.

10. Mikkelsen, M. D., Naur, P., and Halkier, B. A. (2004) Arabidopsis mutants in the C-S lyase of glucosinolate biosynthesis establish a critical role for indole-3-acetaldoxime in auxin homeostasis, *Plant J 37*, 770-777.

11. Prieur, D. J., Gorham, J. R., and Wood, R. K. (2001) Distribution of tyrosine aminotransferase activity in mink (*Mustela vison*), *Comp Biochem Physiol B Biochem Mol Biol 130*, 251-256.

12. Blankenfeldt, W., Nowicki, C., Montemartini-Kalisz, M., Kalisz, H. M., and Hecht, H. J. (1999) Crystal structure of *Trypanosoma cruzi* tyrosine aminotransferase: substrate specificity is influenced by cofactor binding mode, *Protein Sci 8*, 2406-2417.

13. Vass, E., Nappi, A. J., and Carton, Y. (1993) Alterations in the activities of tyrosinase, *N*-acetyltransferase, and tyrosine aminotransferase in immune reactive larvae of *Drosophila melanogaster*, *Dev Comp Immunol 17*, 109-118.

14. Heilbronn, J., Wilson, J., and Berger, B. J. (1999) Tyrosine aminotransferase catalyzes the final step of methionine recycling in *Klebsiella pneumoniae*, *J Bacteriol 181*, 1739-1747.

15. Lopukhina, A., Dettenberg, M., Weiler, E. W., and Hollander-Czytko, H. (2001) Cloning and characterization of a coronatine-regulated tyrosine aminotransferase from Arabidopsis, *Plant Physiol 126*, 1678-1687.

16. Groenewald, J. V., Terblanche, S. E., and Oelofsen, W. (1984) Tyrosine aminotransferase: characteristics and properties, *Int J Biochem 16*, 1-18.

17. Jensen, R. A., and Gu, W. (1996) Evolutionary recruitment of biochemically specialized subdivisions of Family I within the protein superfamily of aminotransferases, *J Bacteriol 178*, 2161-2171.

18. Han, Q., Cai, T., Tagle, D. A., and Li, J. (2010) Structure, expression, and function of kynurenine aminotransferases in human and rodent brains, *Cell Mol Life Sci 67*, 353-368.

19. Han, Q., Cai, T., Tagle, D. A., and Li, J. (2010) Thermal stability, pH dependence and inhibition of four murine kynurenine aminotransferases, *BMC Biochem 11*, 19.

20. Zhou, H., Hong, Y., Yan, M., and Xu, L. (2007) [Expression, purification and enzymatic characterization of Thermus thermophilus HB8 aspartate aminotransferase in *Escherichia coli*], *Sheng Wu Gong Cheng Xue Bao 23*, 278-283.

21. Sivaraman, S., and Kirsch, J. F. (2006) The narrow substrate specificity of human tyrosine aminotransferase--the enzyme deficient in tyrosinemia type II, *FEBS J 273*, 1920-1929.

22. Malashkevich, V. N., Jager, J., Ziak, M., Sauder, U., Gehring, H., Christen, P., and Jansonius, J. N. (1995) Structural basis for the catalytic activity of aspartate aminotransferase K258H lacking the pyridoxal 5'-phosphate-binding lysine residue, *Biochemistry 34*, 405-414.

23. Rhee, S., Silva, M. M., Hyde, C. C., Rogers, P. H., Metzler, C. M., Metzler, D. E., and Arnone, A. (1997) Refinement and comparisons of the crystal structures of pig cytosolic

aspartate aminotransferase and its complex with 2-methylaspartate, *J Biol Chem 272*, 17293-17302.

24. Han, Q., Robinson, H., Cai, T., Tagle, D. A., and Li, J. (2009) Biochemical and structural properties of mouse kynurenine aminotransferase III, *Mol Cell Biol 29*, 784-793.

25. Ko, T. P., Wu, S. P., Yang, W. Z., Tsai, H., and Yuan, H. S. (1999) Crystallization and preliminary crystallographic analysis of the *Escherichia coli* tyrosine aminotransferase, *Acta Crystallogr D Biol Crystallogr 55*, 1474-1477.

26. Eliot, A. C., and Kirsch, J. F. (2004) Pyridoxal phosphate enzymes: mechanistic, structural, and evolutionary considerations, *Annu Rev Biochem 73*, 383-415.

27. Ciechanover, A., Hargrove, J. L., and Gross-Mesilaty, S. (1997) Ubiquitin-mediated degradation of tyrosine aminotransferase (TAT) in vitro and in vivo, *Mol Biol Rep 24*, 27-33.

28. Onoagbe, I. O. (1994) Effects of glucocorticosteroids and insulin on tyrosine aminotransferase activity in isolated chick embryo hepatocytes and in intact embryos in ovo, *Arch Biochem Biophys 309*, 58-61.

29. Rogers, S., Wells, R., and Rechsteiner, M. (1986) Amino acid sequences common to rapidly degraded proteins: the PEST hypothesis, *Science 234*, 364-368.

30. Ohisalo, J. J., and Pispa, J. P. (1976) Heterogeneity of hepatic tyrosine aminotransferase. Separation of the multiple forms from rat and frog liver by isoelectric focussing and hydroxylapatite column chromatography and their partial characterization, *Acta Chem Scand B 30*, 491-500.

31. Minami-Hori, M., Ishida-Yamamoto, A., Katoh, N., Takahashi, H., and Iizuka, H. (2006) Richner-Hanhart syndrome: report of a case with a novel mutation of tyrosine aminotransferase, *J Dermatol Sci 41*, 82-84.

32. Mark, J., Pugge, H., and Mandel, P. (1970) Localization of tyrosine transaminase in rat brain, *J Neurochem 17*, 1393-1401.

33. Neve, S., Aarenstrup, L., Tornehave, D., Rahbek-Nielsen, H., Corydon, T. J., Roepstorff, P., and Kristiansen, K. (2003) Tissue distribution, intracellular localization and proteolytic processing of rat 4-hydroxyphenylpyruvate dioxygenase, *Cell Biol Int 27*, 611-624.

34. Bai, S. C., Rogers, Q. R., Wong, D. L., Sampson, D. A., and Morris, J. G. (1998) Vitamin B-6 deficiency and level of dietary protein affect hepatic tyrosine aminotransferase activity in cats, *J Nutr 128*, 1995-2000.

35. Tabiri, H. Y., Sato, K., Takahashi, K., Toyomizu, M., and Akiba, Y. (2002) Hepatic tyrosine aminotransferase activity is affected by chronic heat stress and dietary tyrosine in broiler chickens, *Br Poult Sci 43*, 629-634.

36. Iwasaki, Y., Lamar, C., Danenberg, K., and Pitot, H. C. (1973) Studies on the induction and repression of enzymes in rat liver. Characterization and metabolic regulation of multiple forms of tyrosine aminotransferase, *Eur J Biochem 34*, 347-357.

37. Ghisalberti, A. V., Steele, J. G., Cake, M. H., McGrath, M. C., and Oliver, I. T. (1980) Role of adrenaline and cyclic AMP in appearance of tyrosine aminotransferase in perinatal rat liver, *The Biochemical journal 190*, 685-690.

38. Paolicchi, A., Chieli, E., and Tongiani, R. (1990) Dexamethasone induction of gamma-glutamyl transferase in primary cultures of hepatocytes is enhanced by metyrapone, *Res Commun Chem Pathol Pharmacol 70*, 49-60.

39. Reynolds, R. D., Scott, D. F., Potter, V. R., and Morris, H. P. (1970) Further studies on the induction of tyrosine aminotransferase in Morris hepatoma 9618A, *Adv Enzyme Regul 9*, 335-347.

40. Sudilovsky, O., and Gunter, R. (1975) Induction of enzymes by glucagon, glucose repression, adenosine 3',5'-monophosphate concentration during carcinogenesis and in Morris 6918A hepatoma, *Cancer Res 35*, 1069-1074.

41. Presch, I., Birnbacher, R., Herkner, K., and Lubec, G. (1997) The effect of estradiol and ovariectomy on tyrosine hydroxylase, tyrosine aminotransferase and phenylalanine hydroxylase, *Life Sci 60*, 479-484.

42. Donohue, T. M., Jr., Drey, M. L., and Zetterman, R. K. (1998) Contrasting effects of acute and chronic ethanol administration on rat liver tyrosine aminotransferase, *Alcohol 15*, 141-146.

43. Thompson, J. D., Gibson, T. J., and Higgins, D. G. (2002) Multiple sequence alignment using ClustalW and ClustalX, *Curr Protoc Bioinformatics Chapter 2*, Unit 2 3.

44. Fu, L., Dong, S. S., Xie, Y. W., Tai, L. S., Chen, L., Kong, K. L., Man, K., Xie, D., Li, Y., Cheng, Y., Tao, Q., and Guan, X. Y. (2010) Down-regulation of tyrosine aminotransferase at a frequently deleted region 16q22 contributes to the pathogenesis of hepatocellular carcinoma, *Hepatology 51*, 1624-1634.

45. Natt, E., Kida, K., Odievre, M., Di Rocco, M., and Scherer, G. (1992) Point mutations in the tyrosine aminotransferase gene in tyrosinemia type II, *Proc Natl Acad Sci U S A 89*, 9297-9301.

46. Natt, E., Westphal, E. M., Toth-Fejel, S. E., Magenis, R. E., Buist, N. R., Rettenmeier, R., and Scherer, G. (1987) Inherited and de novo deletion of the tyrosine aminotransferase gene locus at 16q22.1----q22.3 in a patient with tyrosinemia type II, *Hum Genet 77*, 352-358.

47. Endo, F. (1998) [Hereditary tyrosinemia type II], *Ryoikibetsu Shokogun Shirizu*, 134-136.

48. Goldsmith, L. A., Kang, E., Bienfang, D. C., Jimbow, K., Gerald, P., and Baden, H. P. (1973) Tyrosinemia with plantar and palmar keratosis and keratitis, *J Pediatr 83*, 798-805.

49. al-Hemidan, A. I., and al-Hazzaa, S. A. (1995) Richner-Hanhart syndrome (tyrosinemia type II). Case report and literature review, *Ophthalmic Genet 16*, 21-26.

50. Macsai, M. S., Schwartz, T. L., Hinkle, D., Hummel, M. B., Mulhern, M. G., and Rootman, D. (2001) Tyrosinemia type II: nine cases of ocular signs and symptoms, *Am J Ophthalmol 132*, 522-527.

51. Godde-Jolly, D., Larregue, M., Roussat, B., and Van Effenterre, G. (1979) [A case of Richner-Hanhart syndrome (tyrosinosis with ocular, cutaneous and mental manifestations], *J Fr Ophtalmol 2*, 23-28.

52. Rabinowitz, L. G., Williams, L. R., Anderson, C. E., Mazur, A., and Kaplan, P. (1995) Painful keratoderma and photophobia: hallmarks of tyrosinemia type II, *J Pediatr 126*, 266-269.

53. Klintworth, G. K. (2009) Corneal dystrophies, *Orphanet J Rare Dis 4*, 7.

54. Sgibneva, O. V., Galaev Iu, V., and Goncharova, L. V. (1983) [Hormonal induction of liver tyrosine aminotransferase in animals with chronic poisoning by hepatotropic poisons], *Farmakol Toksikol 46*, 103-107.

55. Kroger, H., Dietrich, A., Gratz, R., Klewer, M., Wohlert, H., and Ehrlich, W. (1996) The influence of antagonists of poly(ADP-ribose)polymerase on the activity of antirheumatic drugs on the development of adjuvant arthritis in rats and on the induction of tyrosine aminotransferase in the liver of rats, *Adv Exp Med Biol 398*, 523-526.

56. Rahman, Q., Das, B., and Viswanathan, P. N. (1983) Biochemical mechanisms in asbestos toxicity, *Environ Health Perspect 51*, 299-303.

57. Henderson, T. R., and Jones, R. K. (1974) Tyrosine aminotransferase induction in rat liver as a response to irradiation or flash burn injuries, *J Trauma 14*, 317-324.

58. Iakobson, G. S., Sorokin, A. S., Gizatulin, Z., and Shorin Iu, P. (1977) [Tyrosine-alpha-ketoglutarate transaminase activity in the rat liver after partial hepatectomy and CCl4 poisoning], *Vopr Med Khim 23*, 701-703.

59. Girkin, G., and Kampschmidt, R. F. (1960) Changes in liver tyrosine-alpha-ketoglutarate transaminase activity during growth of *Walker carcinosarcoma* 256, *Proc Soc Exp Biol Med 105*, 221-223.

60. Donta, S. T. (1974) Alteration of tyrosine aminotransferase activity in hepatoma cells in tissue culture by amphotericin B, *Antimicrob Agents Chemother 5*, 240-246.

61. Rego, J. V., Murta, S. M., Nirde, P., Nogueira, F. B., de Andrade, H. M., and Romanha, A. J. (2008) *Trypanosoma cruzi*: characterisation of the gene encoding tyrosine aminotransferase in benznidazole-resistant and susceptible populations, *Exp Parasitol 118*, 111-117.

62. Van Lookeren Campagne, M. M., Wu, E., Fleischmann, R. D., Gottesman, M. M., Chason, K. W., and Kessin, R. H. (1990) Cyclic AMP responses are suppressed in mammalian cells expressing the yeast low Km cAMP-phosphodiesterase gene, *J Biol Chem 265*, 5840-5846.

63. Lee, L. S., Chi, C. W., Chang, T. J., Chou, M. D., Liu, H. C., and Liu, T. Y. (1989) Steroid hormone receptors in meningiomas of Chinese patients, *Neurosurgery 25*, 541-545.

64. Chatagner, F., Van Heijenoort, Y., and Portemer, C. (1968) Modification of the pyridoxine-induction of tyrosine transaminase in rat liver by thyroid hormones and by alloxan diabetes, *Nature 218*, 566-567.

65. Kindt, E., and Halvorsen, S. (1980) The need of essential amino acids in children. An evaluation based on the intake of phenylalanine, tyrosine, leucine, isoleucine, and valine in children with phenylketonuria, tyrosine amino transferase defect, and maple syrup urine disease, *Am J Clin Nutr 33*, 279-286.

66. Hayashi, H., Inoue, K., Nagata, T., Kuramitsu, S., and Kagamiyama, H. (1993) Escherichia coli aromatic amino acid aminotransferase: characterization and comparison with aspartate aminotransferase, *Biochemistry 32*, 12229-12239.

67. Nowicki, C., Hunter, G. R., Montemartini-Kalisz, M., Blankenfeldt, W., Hecht, H., and Kalisz, H. M. (2001) Recombinant tyrosine aminotransferase from *Trypanosoma cruzi:* structural characterization and site directed mutagenesis of a broad substrate specificity enzyme, *Biochim Biophys Acta 1546*, 268-281.

68. Dutra, W. O., and Gollob, K. J. (2008) Current concepts in immunoregulation and pathology of human Chagas disease, *Curr Opin Infect Dis 21*, 287-292.

69. Beneking, M., Schmidt, H., and Weiss, G. (1978) Subcellular distribution of a factor inactivating tyrosine aminotransferase. Study of its mechanism and relationship to different forms of the enzyme, *Eur J Biochem 82*, 235-243.

# Chapter 3. Tyrosine Aminotransferase: Biochemical and Structural Properties and Molecular Dynamics Simulations

Prajwalini Mehere[1], Qian Han[1], Justin A. Lemkul[1], Howard Robinson[2], David R. Bevan[1], Jianyong Li[1]

**Accepted in Protein and cell (2010)**

[1]Department of Biochemistry, Virginia Tech, Blacksburg, VA 24061

[2]Biology Department, Brookhaven National Laboratory, Upton, NY 11973

This article (Mehere et al. 2010) describes the biochemical, and structural properties, and molecular dynamics simulations of mouse tyrosine aminotransferase. I came up with the experimental design and concept for the manuscript. I was involved in expression, purification, and crystallization of mTAT. I was also involved in solving the crystal structure and docking studies. Qian Han was involved in kinetic characterization of this protein. Justin Lemkul was involved in running the molecular dynamic studies. Howard Robinson was involved in data collection for mTAT crystals.

## 3.1 Abstract

Tyrosine aminotransferase (TAT) catalyzes the transamination of tyrosine and other aromatic amino acids. The enzyme is thought to play roles in tyrosinemia type II, hepatitis, and hepatic carcinoma recovery. The objective of this study is to investigate its biochemical and structural characteristics and substrate specificity in order to provide insight into its involvement in these diseases. Mouse TAT (mTAT) was cloned from a mouse cDNA library, and its recombinant protein was produced using *Escherichia coli* cells and purified using various chromatographic techniques. The recombinant mTAT is able to catalyze the transamination of tyrosine using α-ketoglutaric acid as an amino group acceptor at neutral pH. The enzyme also catalyzes the transamination reactions of glutamate, phenylalanine, p-hydroxyphenylpyruvate, phenylpyruvate, and alpha-ketocaproic acid. Through macromolecular crystallography we have determined the mTAT crystal structure at 2.9 Angstrom resolution. The crystal structure revealed the interaction between the pyridoxal-5'-phosphate cofactor and the enzyme, as well as the formation of a disulfide bond. The detection of disulfide bond supports a previous suggestion regarding TAT inactivation by oxidants. Molecular dynamics simulations using the crystal structures of *Trypanosoma cruzi* TAT and human TAT provided further insight regarding the substrate-enzyme interactions and substrate specificity. The biochemical and structural properties of TAT, and the binding of its cofactor and the substrate may help in elucidating the mechanism of TAT inhibition and activation.

## 3.2 Introduction

Tyrosine aminotransferase (TAT) catalyzes reversible transamination of tyrosine and *p*-hydroxyphenylpyruvate (pHPP) (*1*). TAT deficiency leads to tyrosinemia type II in humans due to genetic mutation (*2*). In tyrosinemia type II, tyrosine accumulates in blood, eventually causing lesions in the patients (*1*). In humans, more than 15 mutations have been identified in the patients of tyrosinemia type II in Italy, France, the USA, and the UK (*3-9*). Tyrosinemia type II is often associated with consanguinity. The incidence is less than one in 250,000 (*10*). Eye, skin, and neurological symptoms are the foremost features of the disease (*6*). The disease is associated with microcephaly, tremor, ataxia, self-mutilating behavior, fine motor coordination disturbances, language deficits, and convulsions (*11, 12*).

*Trypanosoma cruzi* TAT (tcTAT) shares over 40% sequence identity with the mammalian TATs. *T. cruzi* causes Chagas disease, a parasitic disease that is endemic in Latin America. It has been shown that tcTAT may be involved in drug resistance to benznidazole, a drug currently used in chemotherapy of Chagas disease (*13*).

TAT is also considered as a marker of mature hepatocytes (*14*). Recently, Fu and colleagues demonstrated that TAT is a novel tumor suppressor gene and its inactivation, caused by gene deletion and hypermethylation, contributes to the pathogenesis of hepatocellular carcinoma (*15*).

Previous studies showed that TAT is a homodimer and is composed of two identical polypeptide chains (*16*). It is expressed not only in the liver but also in the kidneys (*17*) and brain (*17*). However the enzyme has the highest activity in the liver. In hTAT, the first 38 amino acids may not be involved in enzyme dimerization, and are not required in the active site stability and enzyme-substrate interactions (*18*). This N-terminal fragment, however, is required for being targeted by the ubiquitin-proteosome pathway (*19*), which degrades proteins to small peptides (*20*). So far crystal structures of TATs from *Escherichia coli* (*21*), *T. cruzi* (*16*), and *Homo sapiens* (Protein Data Bank code 3dyd) have been reported. In this study, we provide a mouse TAT (mTAT) crystal structure and its biochemical characteristics for comparative study. All crystal structures of TATs lack substrate binding information; therefore we used molecular dynamics simulations to provide further insight into substrate-enzyme interactions and substrate specificity.

## 3.3 Materials and Methods

**Expression and Purification of mTAT**

mTAT cDNA sequence was amplified from mouse liver cDNA pool using a forward primer (5'-CAT ATG AAG GCC AGG TGG AAT GT-3') and reverse primer (5'-CTC GAG CTA GTA GTG CTG TTC ACA GAA CTC-3') containing Nde1 and Xho1 restriction sites, respectively. The amplified sequence, encoding mTAT amino acid residues 41 to 442, was cloned into an Impact™-CN plasmid (pTYB12 vector) (New England Biolabs) for expression of a fusion protein containing a chitin-binding domain. Transformed *E. coli* cells were cultured at 37$^{o}$C. After induction with 0.2 mM isopropyl -1-thio-β-D-galactopyranoside, the cells were cultured at 15$^{o}$C for 24 hrs. Four liters of cells were harvested as the starting materials for affinity purification. The soluble fusion proteins were applied to a column packed with chitin beads and subsequently hydrolyzed under reducing conditions. The affinity purification resulted in the isolation of mTAT at around 80% purity. The recombinant mTAT was further purified by Source Q ion-exchange and gel-filtration chromatography. The purified recombinant mTAT was concentrated to 10 mg ml$^{-1}$ protein in 10 mM phosphate buffer (pH 7.5) containing 40 mM PLP using a Centricon YM-50 concentrator (Millipore). The concentrated protein was directly used in crystallization screening and optimization. Protein concentration was tested by a protein assay kit from Bio-Rad (Hercules, CA) using bovine serum albumin as a standard. Glycerol (10%) and 10 mM β-mercaptoethanol were added into the protein solution for the enzyme used in the biochemical characterization.

**Activity assay and enzyme kinetic study**

To determine the substrate specificity for α-keto acids, 16 α-keto acids were individually tested for their ability to function as an amino group acceptor for mTAT using tyrosine as an amino group donor. Those include glyoxylate, indo-3-pyruvate, KGA, α-keto-methylthiobutyric acid, α-ketoadipate, α-ketobutyrate, α-ketocaproic acid, α-ketoisoleucine, α-ketoleucine, α-ketovalerate, α-ketovaline, mercaptopyruvate, oxaloacetate, phenylpyruvate, pHPP, and pyruvate. Each of the 16 α-keto acids were assayed at 2 mM in the presence of 5 mM tyrosine and 40 μM PLP, prepared in 100 mM phosphate buffer at pH 7. The rate of pHPP production was determined using reversed phase high-performance liquid chromatography with ultraviolet detection (HPLC-UV) at 295 nm.

For enzyme kinetics studies, the transamination of tyrosine, phenylalanine, glutamate catalyzed by mTAT with phenylpyruvate, pHPP, KGA or α-ketocaproic acid as an amino group acceptor was tested using an assay mixture containing various concentrations of substrates, 40 mM PLP, 100 mM phosphate buffer (pH 7), and 1 μg enzyme in a total volume of 100 μl. The mixture was incubated for 15 min at 38$^{o}$C and stopped by adding an equal amount of absolute ethanol. The product was quantitated using HPLC with electrochemical detection (HPLC-ED) to measure the *o*-phthaldialdehyde thiol (OPT)-amino acid product conjugates after their corresponding reaction mixtures were derivatized by OPT reagent (*22*).

**Crystallization, data collection and processing, and structure determination**

The crystals were grown by the hanging-drop vapor diffusion method with the volume of reservoir solution at 500 μl and the drop volume at 2 μl, containing 1 μl of protein sample and 1 μl of reservoir solution. The optimized crystallization buffer consisted of 20% PEG 4000, 100 mM cacodylic acid buffer, pH 6.8, and 20% glycerol. Diffraction data of mTAT crystal was collected at the Brookhaven National Synchrotron Light Source beam line X29A (λ = 1.0908 Å). Data were collected using an ADSC CCD detector. All data were indexed and integrated using HKL-2000 software; scaling and merging of diffraction data were performed using the program SCALEPACK (*23*). The parameters of the crystals and data collection are listed in Table 2. The structure of mTAT was determined by the molecular replacement method using hTAT structure (Protein Data Bank code, 3dyd). The program Molrep (*24*) was employed to calculate both the cross-rotation and translation functions of the model. The initial model was subjected to iterative cycles of crystallographic refinement with the Refmac 5.2 (*25*) and graphic sessions for model building using Coot (*26*). The cofactor and substrate molecules were modeled before adding solvent molecules based on both the 2*F*o - *F*c and *F*o - *F*c electron density maps. Solvent molecules were manually added and refined with Refmac 5.2. Superposition of structures was done using "SSM Superposition" function in Coot (*26*). Figures were generated using Pymol (*27*). Protein and substrate interaction was also analyzed using Pymol (*27*).

**Docking and Molecular Dynamics Simulations**

mTAT and hTAT share 92% sequence identity, and exactly the same PLP binding sites. Since the hTAT crystal structure was determined at higher resolution than mTAT, we chose to use the hTAT structure (PDB code 3dyd) for the molecular dynamics simulations. The tcTAT structure (*16*) was selected for comparative purposes because both tcTAT and hTAT have a

highly conserved active site, but differ in that hTAT is very specific for tyrosine, and does not act upon alanine. The purpose of this work was to establish the molecular basis for this substrate difference using MD simulations. Complexes of both proteins with alanine and tyrosine bound were obtained by molecular docking using AutoDock (*28, 29*). The molecules for docking were prepared by using USCF Chimera (*30*) to add hydrogen atoms to the receptor and both ligands (alanine and tyrosine). AutoDock Tools 1.5.2 (ADT) was used to prepare the ligands and receptor, after which docking was performed using AutoDock 4.0 (*28, 29*). The X, Y, and Z dimensions of the grid were set to 45 x 45 x 51 Å with default grid spacing of 0.375 Å around the cofactor of both proteins. The Lamarckian Genetic Algorithm (LGA) was used to predict binding positions, orientations, and conformations of the ligands. Default parameters were used, except for the number of energy evaluations, which was set to 250,000. A total of 2,000 docking poses (500 for each ligand docked to each protein) were generated and clustered with a 2.0 Å threshold. The lowest energy configuration in the first cluster was considered the best docking pose for each ligand. These docked complexes were used as input for molecular dynamics simulations.

From each of these starting structures, three simulations were conducted. Systems were prepared and simulations conducted with GROMACS, version 4.0.5 (*31*). All structures were centered in a rhombic dodecahedral simulation cell filled with simple point charge (SPC) water (*32*) and sodium counter ions to give an electrically net neutral system. The force field used was GROMOS96 53A6 (*33*). Parameters for the covalently bound PLP cofactor were assigned based on analogous functional groups already present in the force field library. Following steepest descents minimization, the systems were equilibrated in two phases, during which position restraints were applied to all protein and cofactor heavy atoms. First, 100 picoseconds (ps) of constant volume (NVT) equilibration were performed at 310 K, with temperature maintained by the Berendsen weak coupling method (*34*). Next, 100 ps of constant pressure (NPT) equilibration were performed, with temperature controlled by the Nosé-Hoover thermostat (*35, 36*) and pressure controlled by the Parrinello-Rahman barostat (*37, 38*). Following this phase, position restraints were removed and production simulations conducted for 5 ns. During data collection, the same thermostat and barostat were used as in NPT equilibration. For all simulations, short-range non-bonded interactions were truncated at 1.2 nm for computational efficiency. Dispersion correction was applied to energy and pressure terms to account for truncation of van der Waals

terms. Long-range electrostatics were calculated with the Particle Mesh Ewald method (*39, 40*), using a cubic-spline interpolated grid, with 0.12-nm grid spacing. Constraints were applied to all bonds using the LINCS algorithm (*41*), allowing an integration time step of 2 fs.

## 3.4 Results

***Biophysical and biochemical characteristics***

Using affinity, Source-Q and gel-filtration chromatography, we purified the mTAT recombinant protein to a high purity as confirmed by SDS-PAGE (Figure 3.1). The purified mTAT showed high TAT activity using α-ketoglutaric acid (KGA) as an amino group acceptor. Among the temperature points tested, mTAT showed the highest TAT activity at 50 – 70 °C (Figure. 3.2a). When testing for optimum pH across a range of pH 6.0 – 11.0, achieved by adjusting the pH of the phosphate and borate buffer mixture used to prepare mTAT/Tyrosine/KGA reaction mixtures, mTAT displayed the highest activity at pH 7 (Figure. 3.2b). Sixteen α-keto acids (listed in Materials and Methods section) were tested for their potential as an amino group acceptor for mTAT with 5 mM tyrosine (5 mM glutamate for pHPP) as the amino group donor. The enzyme only showed detectable activity towards KGA, pHPP, phenylpyruvate, and α-ketocaproic acid. The enzyme kinetic study determined the enzyme kinetic parameters towards these four keto-acids (Table 3.1). mTAT does not have detectable activity towards glycine, alanine, and aspartate. Since hTAT showed transamination activity towards glutamate, phenylalanine as well as tyrosine (*42*), kinetic parameters of mTAT towards these three amino acids were also tested and calculated (Table 3.1).

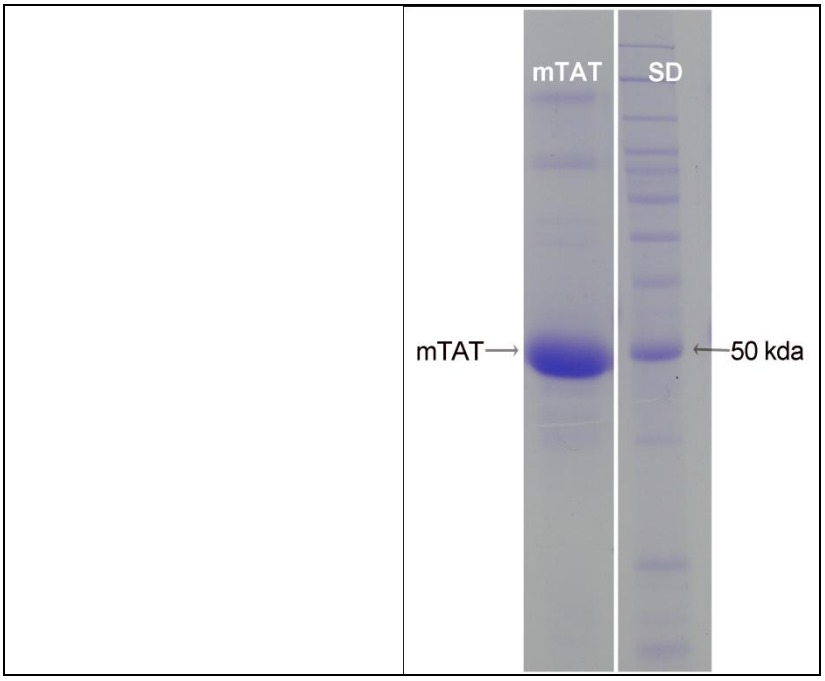


**Figure 3.1 Purified recombinant mTAT on SDS-polyacrylamide gel.**
The purified recombinant mTAT protein and protein standards were run in 10% SDS-polyacrylamide gel. After electrophoresis, the gel was stained with Coomassie blue. SD, protein standards; kDa, kilodalton

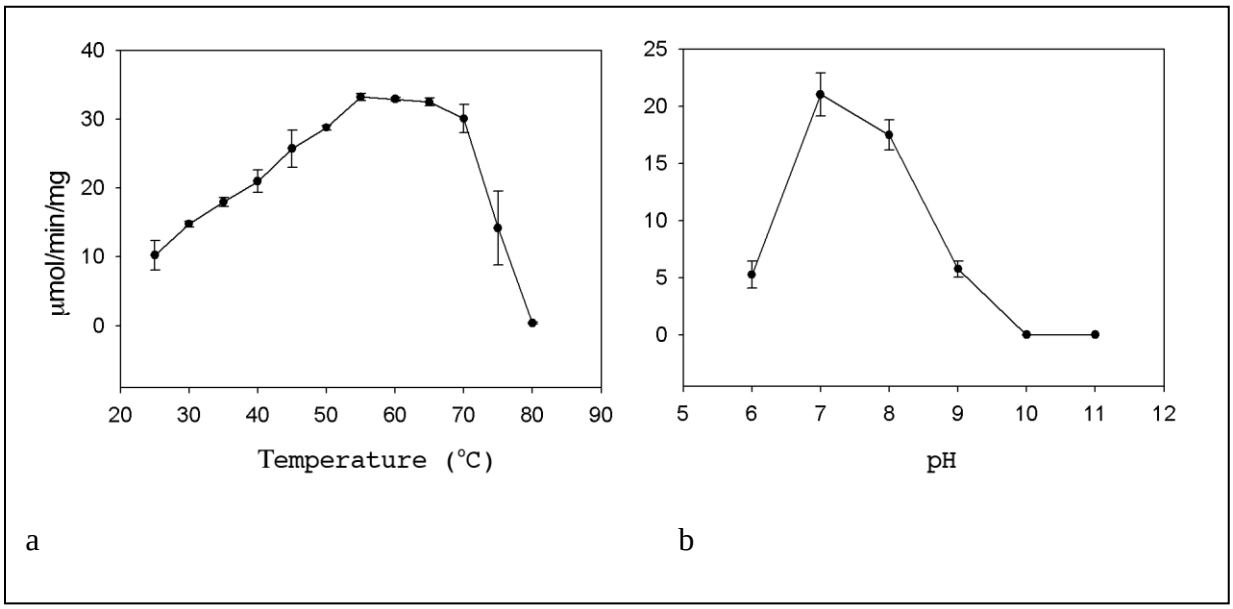


**Figure 3.2 Effect of temperature and pH on enzyme activity.**
The activities of recombinant mTAT (a) at different temperatures and (b) at different pH values.

**Table 3.1 Kinetic parameters of mTAT towards α-keto acids.** The activities were measured as described in the Materials and Methods section. The Km and kcat for α-keto acids were derived by using varying concentrations (0.2 to 10 mM) of individual α-keto acids in the presence of 5 mM of tyrosine (10 mM glutamate for pHPP). The Km and kcat for amino acids were derived by using varying concentrations (0.2 to 5 mM) of individual amino acids in the presence of 10 mM of KGA (or 2 mM pHPP for glutamate). The parameters were calculated by fitting the Michaelis–Menten equation to the experimental data using the enzyme kinetics module. Results are means ± SE.

| | $K_m$ mM | $k_{cat}$ $min^{-1}$ | $k_{cat}/K_m$ $min^{-1}mM^{-1}$ |
|---|---|---|---|
| Amino acid substrates | | | |
| tyrosine | 1.8 ± 0.5 | 1160 ± 240 | 640 |
| glutamate | 4.9 ± 0.8 | 560 ± 40 | 120 |
| phenylalanine | 11.4 ± 4.1 | 920 ± 210 | 80 |
| Keto acid substrates | | | |
| pHPP | 0.7 ± 0.4 | 950 ± 260 | 1360 |
| KGA | 1.8 ± 0.2 | 1540 ± 80 | 850 |
| phenylpyruvate | 0.9 ± 0.1 | 160 ± 10 | 180 |
| α-ketocaproic acid | 7.3 ± 3.1 | 110 ± 30 | 20 |

***Overall Structure***

The crystal structure of mTAT was determined by molecular replacement and refined to 2.9 Å resolution (Figure 3.3). The final model contains 378 amino acid residues and yields a crystallographic R value of 26.3% and an R-free value of 29.5% (Table 3.2). The first 23 residues at the N-terminal end are disordered, and missing in the structure. All residues in the structure are in allowed regions of the Ramachandran plot as defined with PROCHECK (*45*). The structure has a large domain and a small domain. The large domain (residues 86-334) contains an eight-stranded beta sheet, and the small domain comprises the C-terminal part (residues 335-442) and a small fragment in the N-terminal part (residues 64-85), which folds into a 2-stranded beta sheet covered with helices (Figure 3.4). The residue Asp247 interacts with the pyridine nitrogen of the cofactor (Figure 3.5) which is structurally and functionally conserved within fold-type I. A DALI-based search (*51*) revealed significant structural homology of mTAT with hTAT (PDB code 3dyd; root-mean-square deviation (RMSD), 0.6 Å, number of aligned positions, 388) and tcTAT (PDB code 1bw0; RMSD, 1.2 Å; number of aligned positions, 413) (*16*) in the Protein Data Bank. All these TATs, together with most of kynurenine aminotransferases I and III, belong to the aminotransferase subfamily Iγ (*52-54*).

***Active site of mTAT***

Residual electron density clearly revealed the presence of covalently bound PLP in the active center (Figure 3.5A). The C4A atom of PLP is covalently attached to the NZ atom of Lys280 through the formation of an internal Schiff base, and the internal aldimine gives rise to residue LLP280, represented as sticks in Figure 3.5. The PLP pyridoxal ring is stacked between residues Ile249 and Phe169 by hydrophobic interactions, and the C2A atom of PLP exhibits a hydrophobic interaction with the Asn215 side chain. The side chain of Asn219 is hydrogen bonded to the O3 of the pyridoxal. The phosphate moiety of PLP is anchored by polar interactions with the peptide amide group of residue Cys144 as well as with the side chains of Ser145 and Arg288.

**Table 3.2 Data collection and refinement statistics of mTAT crystals.**

| Crystal Data | |
|---|---|
| Space Group | $C222_1$ |
| Unit Cell | |
| α = (Å) | 69.3 |
| β = (Å) | 84.8 |
| γ = (Å) | 158.0 |
| α = β = γ (°) | 90 |
| **Data collection** | |
| X-ray source | BNL[a]-X29 |
| Wavelength (Å) | 1.0809 |
| Resolution (Å)[b] | 2.9 (3.0-2.9) |
| Total number of reflections | 55966 |
| Number of unique reflections | 10641 |
| R-merge [b] | 8.6 (38.8) |
| *I*/s [b] | 24.4 (2.3) |
| Redundancy [b] | 6.0 (4.1) |
| Completeness (%)[b] | 87.7 (43.6) |
| **Refinement statistics** | |
| R-work (%) | 26.3 |
| R-free (%) | 29.5 |
| RMS Bond lengths (Å) | 0.017 |
| RMS Bond angles (°) | 1.718 |
| No. of ligand or cofactor molecules [c] | 1 LLP |
| No. of water molecules | 38 |
| Average B overall ($Å^2$) | 107.8 |
| **Statistics on Ramachandran plot (%)** | |
| Most favored regions | 83.5 |
| Additional allowed regions | 15.9 |
| Generously allowed regions | 0.6 |
| Disallowed regions | 0 |

[a] Brookhaven National Laboratory
[b] The values in parentheses are for the highest resolution shell
[c] LLP,lysine-pyridoxal-5'-phosphate

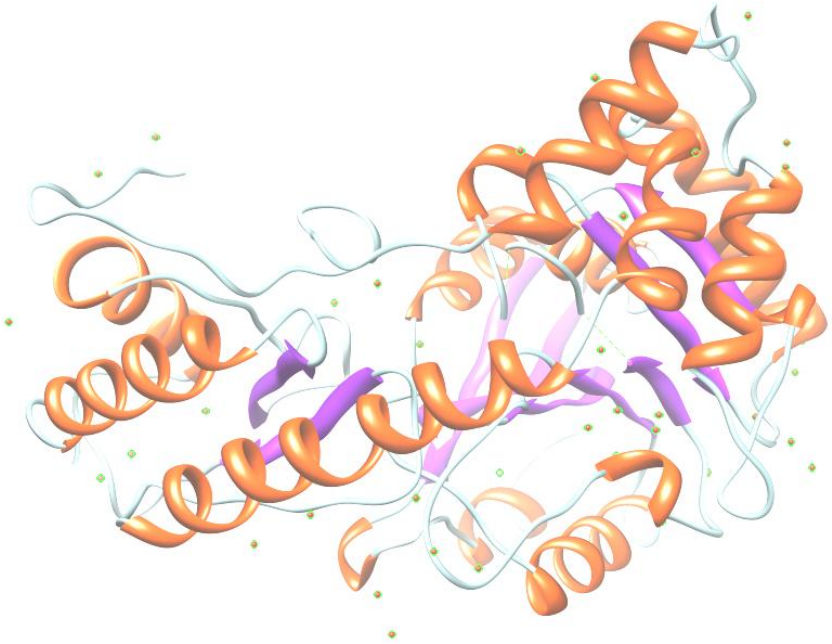

**Figure 3.3 Three dimensional structure of mTAT showing the eight antiparallel β-pleated sheets in purple color.**
(The α-helices have been shown in orange color and water molecules have been shown in green color)

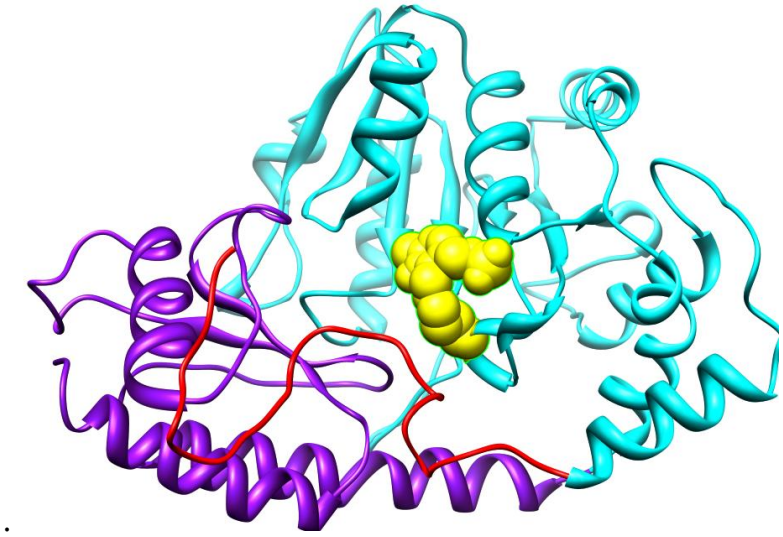

**Figure 3.4 Three dimensional ribbon structure of mTAT showing the small domain (Purple), large domain (Cyan), N-terminus (Red), and LLP (Yellow).**

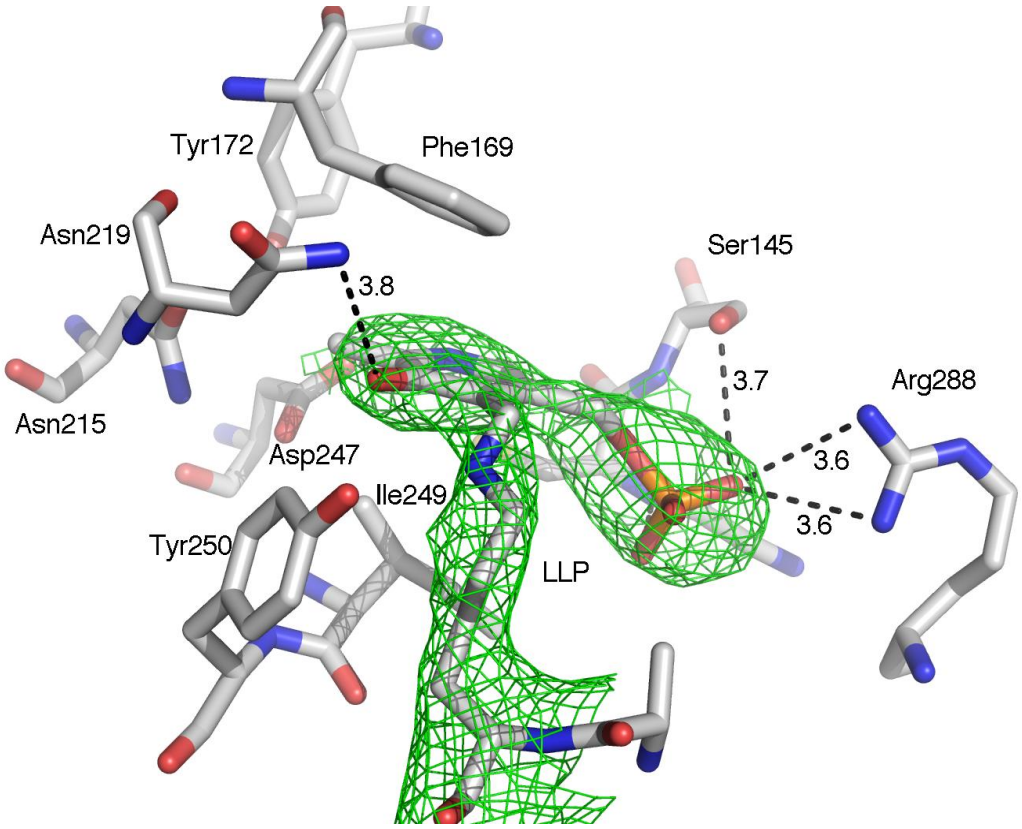


**Figure 3.5 Active center of mTAT structure.**
LLP (PLP bonded with Lys280) and residues within 4 Å distance from PLP are shown in sticks. The 2*Fo*–*Fc* electron density map covering LLP is shown contoured at the 1.1 sigma level.

***Disulfide bond formation***

One disulfide bond is observed in the mTAT structure between Cys144 and Cys275 residues (Figure 3.6a). Via superposition of hTAT and mTAT (RMSD, 0.6 Å) we identified the residues within a 6 Å range of PLP in both structures, and those residues having significant conformational difference are shown in Figure 3.6b. Cys144 is shown to be in the active site, forming hydrogen bonds with the O3, O1, and N1 atoms of PLP. The hydrogen bonding interaction with the N1 atom of the PLP pyridine ring may interfere with the interaction between the PLP N1 atom and Asp247, which is critical to the transamination reaction. Therefore, the formation of this disulfide bond could be involved in the regulation of enzyme catalysis. The formation of an intra or inter TAT disulfide was long ago proposed as being involved in the inactivation of the enzyme (*55-57*). An important feature of the observed inactivation was its reversibility by thiol compounds (*55, 56*). Our findings of a disulfide bond formation between Cys144 and Cys275 residues support this previous suggestion. The thiol groups of Cys144 and Cys275 are on an enzyme active center cleft surface (Figure 3.6c).

***Substrate specificity of TATs revealed by molecular docking and dynamics simulation***

Molecular docking and molecular dynamics (MD) simulations were conducted in an attempt to identify structural features that contribute to substrate specificity. Free energy and clusters used of the docked complexes are shown in Table 3.3. Following MD simulations, principal components analysis was conducted on each of the systems in this study to explore the fundamental, low-frequency vibrations of the protein structure that contribute to catalysis. No differences were observed in the vibrational modes of uncomplexed and complexed TAT enzymes, indicating that binding of tyrosine and alanine did not affect the structural stability of either hTAT or tcTAT. Figure 3.7 illustrates the structures of the complexes in this study after 5 ns of MD simulation. In each case, a representative TAT structure was chosen to illustrate the protein, and the final positions of the ligands in each of the three simulations are superimposed onto this structure following rotational and translational fitting of the system to the reference structure.

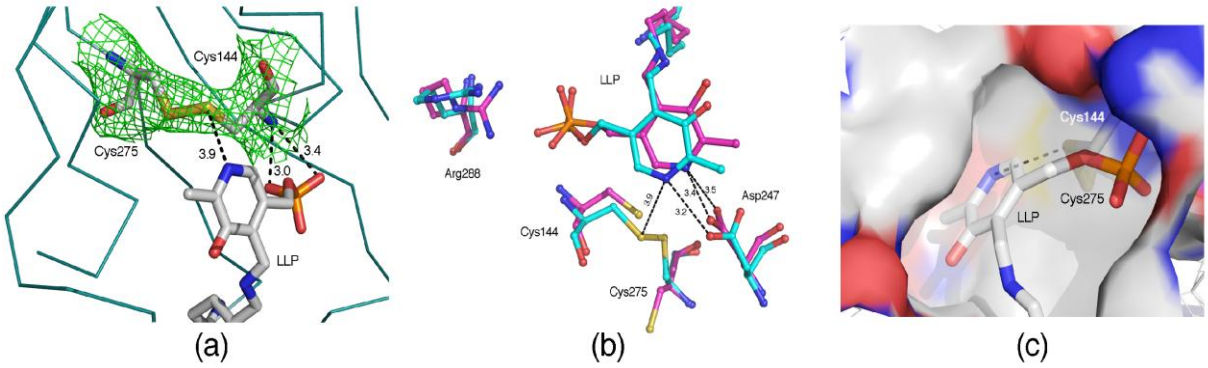


**Figure 3.6 Formation of disulfide bond in mTAT.**
(a) LLP and the disulfide bond formed between Cys144 and Cys275 residues are shown in sticks. The 2*F*o–*F*c electron density map covering residues Cys144 and Cys275 is shown contoured at the 1.1 sigma level. (b) The mTAT structure is superimposed onto the hTAT structure. Residues having significant conformational difference within 6 Å of PLP in the mTAT structure compared with the hTAT structure are shown. mTAT is colored in teal, and hTAT is in pink. (c) The enzyme active center cleft surface is colored by element (c) light gray, N: blue, O: red, S: yellow, P: orange); LLP and side chains of Cys144 and Cys275 are shown in sticks.

**Table 3.3 Docking results showing the lowest predicted free energy of binding and population size of the lowest-energy cluster for docked complexes.**
**(**Total population for each complex was 500 poses (members)).

| Docked complex | Free energy of binding (Kcal/mol) | Members in the first cluster |
|---|---|---|
| **tcTAT-Tyr** | -5.5 | 250 |
| **hTAT-Tyr** | -4.5 | 200 |
| **tcTAT-Ala** | -3.3 | 250 |
| **hTAT-Ala** | -3.1 | 450 |

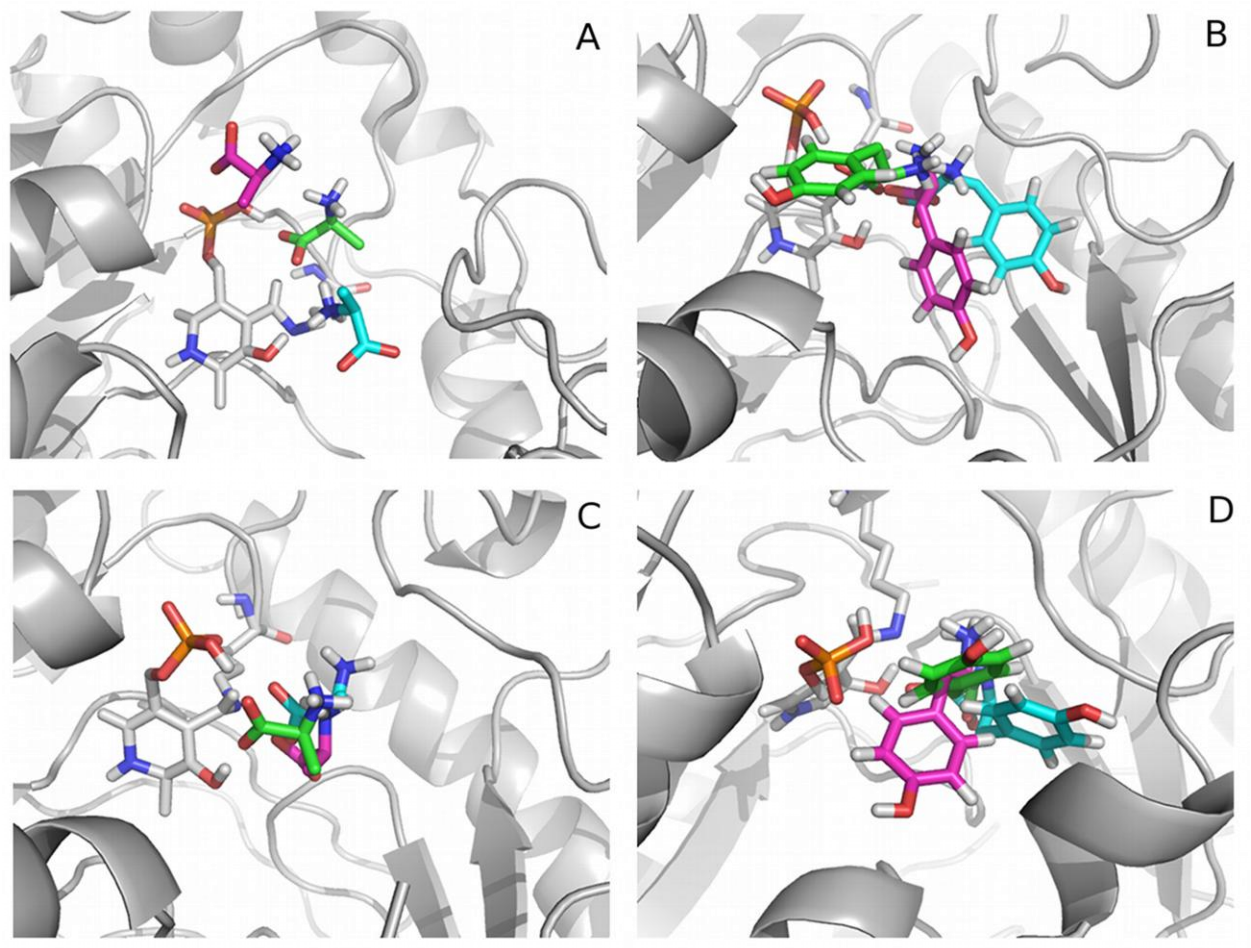


**Figure 3.7 Structures of substrate bound TAT.**
Structures of (a) hTAT-Ala, (b) hTAT-Tyr, (c) tcTAT-Ala, and (d) tcTAT-Tyr complexes at the end of 5 ns of MD simulation. The TAT protein in each case is shown as a gray cartoon, with bound ligands shown as sticks and colored by element, with carbon atoms tinted green, cyan, and magenta to indicate the results of the different simulations. PLP and the covalently attached lysine are shown as sticks and colored by element, with gray-tinted carbon atoms.

In the case of the hTAT-Ala complex (Figure 3.7A), it is clear that the position of the ligand (alanine) is more variable than in the case of the tcTAT-Ala complex (Figure 3.7C). The RMSD of the alanine ligand in hTAT is 0.75 ± 0.16 nm, averaged across all three replicate simulations, while in the case of the tcTAT-Ala complex; the RMSD of alanine is only 0.28 ± 0.05 nm. The RMSD indicates the level of deviation from the original docked pose, and another meaningful analysis is the root-mean-square fluctuation (RMSF) of the ligand, the magnitude of fluctuation about a mean position. Again, in the case of the hTAT-Ala complex, the bound alanine was more variable, with an average RMSF of 0.27 ±0.14 nm, while that of the tcTAT-Ala ligand was 0.11 ± 0.03 nm. From these results, it can be seen that the bound alanine in the hTAT-Ala complex fluctuates within the active site substantially over the course of the MD simulations, such that it is not consistently positioned to interact with LLP in a way that is amenable to catalysis, while in the case of tcTAT the bound pose is more stable and positioned for catalysis.

The position of the bound tyrosine in the hTAT-Tyr complex deviated substantially from the initial docked pose (Figure 3.7B), while that of tcTAT-Tyr remained more consistent (Figure 3.7D). The RMSD of tyrosine in the hTAT-Tyr complex was 0.53 ± 0.09 nm, averaged over all three simulations, but the RMSF was very low, 0.11 ± 0.03 nm. These results indicate that docking tyrosine to hTAT resulted in the tyrosine ligand being placed in a local, rather than global, energy minimum, leading to large movements of tyrosine (as indicated by the RMSD), but that the final positions achieved in the MD simulations were stable (as indicated by the RMSF). In the tcTAT-Tyr complex, the bound tyrosine was moved very little, with an average RMSD of 0.25 ± 0.09 nm and an average RMSF of 0.09 ± 0.04.

In both the hTAT-Tyr and tcTAT-Tyr complexes, the α-amino group remained proximal to the imine functional group of the LLP cofactor, oriented in such a way that catalysis could be carried out. In the case of hTAT-Tyr, the average distance between the LLP imine and α-amino group on tyrosine was 0.73 ± 0.01 nm, while that of tcTAT-Tyr was 0.64 ± 0.10 nm. In the hTAT-Ala complex, the distance between the LLP imine and the α-amino group of alanine was, on average, 0.75 ± 0.24 nm, nearing 1.0 nm in one simulation. For tcTAT-Ala, this average distance was 0.68 ±0.04 nm.

Careful inspection of nearby residues in the TAT active site reveals the reason for the more consistent binding pose of alanine in tcTAT relative to hTAT. In tcTAT, two hydrophobic

residues, Ile19 and Val40, provide a hydrophobic platform with which the β-carbon of alanine (as well as tyrosine) can interact favorably (Figure 3.8). These residues are not present in the hTAT enzyme, allowing the alanine ligand greater mobility in the active site. This mobility is very likely the reason that hTAT cannot carry out catalysis on alanine as it does not bind stably in the proper orientation. In contrast, the binding of tyrosine to both tcTAT and hTAT is very stable. The position and orientation of tyrosine in the active site of both hTAT and tcTAT is largely unchanged in each simulation (Figure 3.7). In the case of tcTAT, tyrosine forms hydrogen bonds with Arg20 while simultaneously interacting with Ile19 and Val40 through hydrophobic interactions (Figure 3.8).

In the hTAT-Tyr complex, the bound tyrosine ligand is principally stabilized by interactions with Arg419 (both cation-π and hydrogen bonding) and Phe410 (aromatic stacking), as shown in Figure 3.9. These interactions were observed in all three simulations, but persisted in only two of the simulations. In the third simulation of the hTAT-Tyr complex, the tyrosine ligand oriented itself towards Phe169, a residue that is more distant from the active site. Tyrosine, by virtue of its size, is able to interact with Arg419 and Phe410, which are somewhat distant from the PLP cofactor. The distance of Phe410 from the active site prevents smaller ligands, like alanine, from forming stabilizing hydrophobic interactions while simultaneously remaining in position near the PLP cofactor.

In summary, the interaction of alanine and tyrosine ligands with tcTAT is stabilized by hydrophobic interactions involving Ile19 and Val40. In tcTAT-Tyr, the tyrosine ligand is further stabilized by hydrogen bonding with Arg20. In the case of hTAT-Tyr, the tyrosine ligand forms favorable contacts with Phe410 and Arg419 at the periphery of the active site. Binding of alanine to hTAT, however, is not stable; as the smaller ligand cannot form stabilizing contacts with the more distant phenylalanines, and, unlike tyrosine, alanine cannot interact favorably with the guanidinium group of arginine.

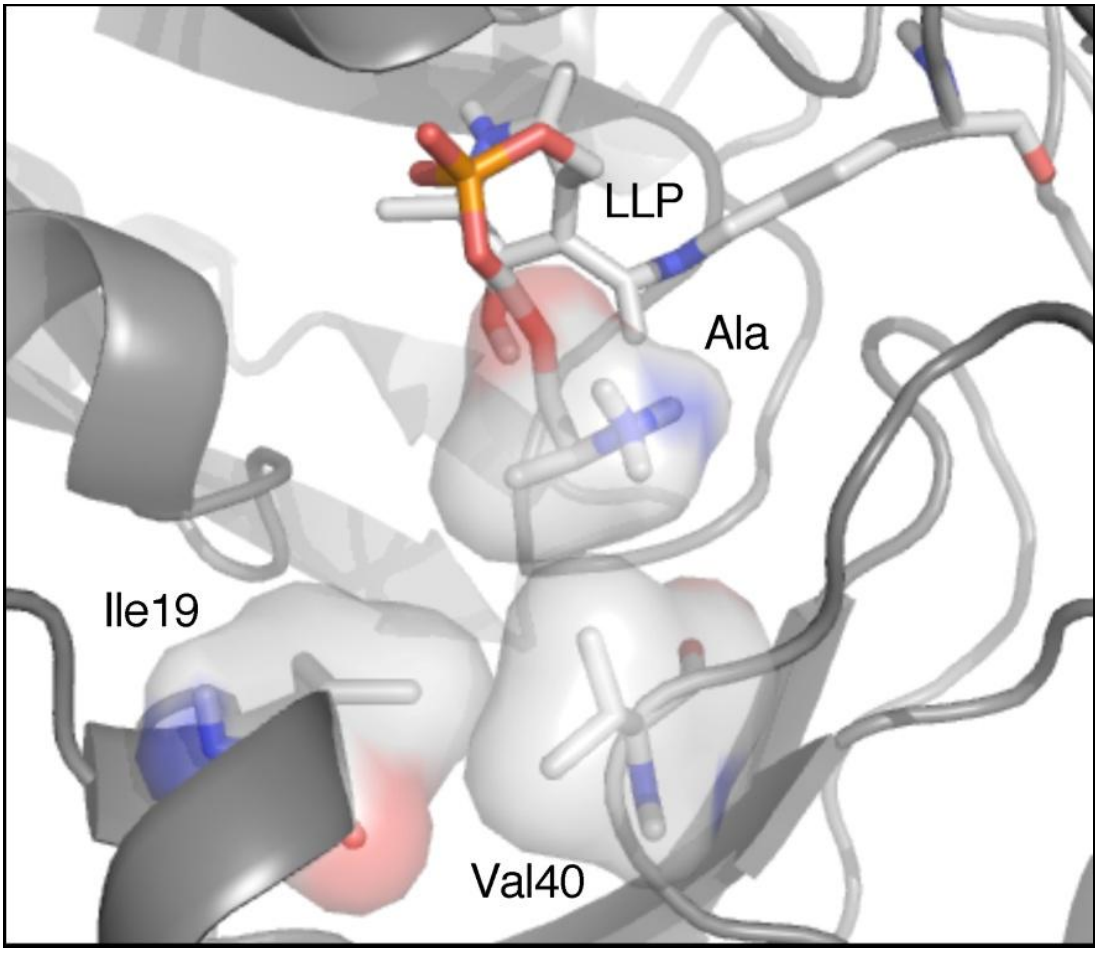


**Figure 3.8 Details of the tcTAT-Ala complex.**
The alanine ligand, Ile19, and Val40 are shown as sticks with overlaid surfaces, and are colored by element. The pyridoxal 5'-phosphate and covalently attached lysine are shown as sticks and colored by element.

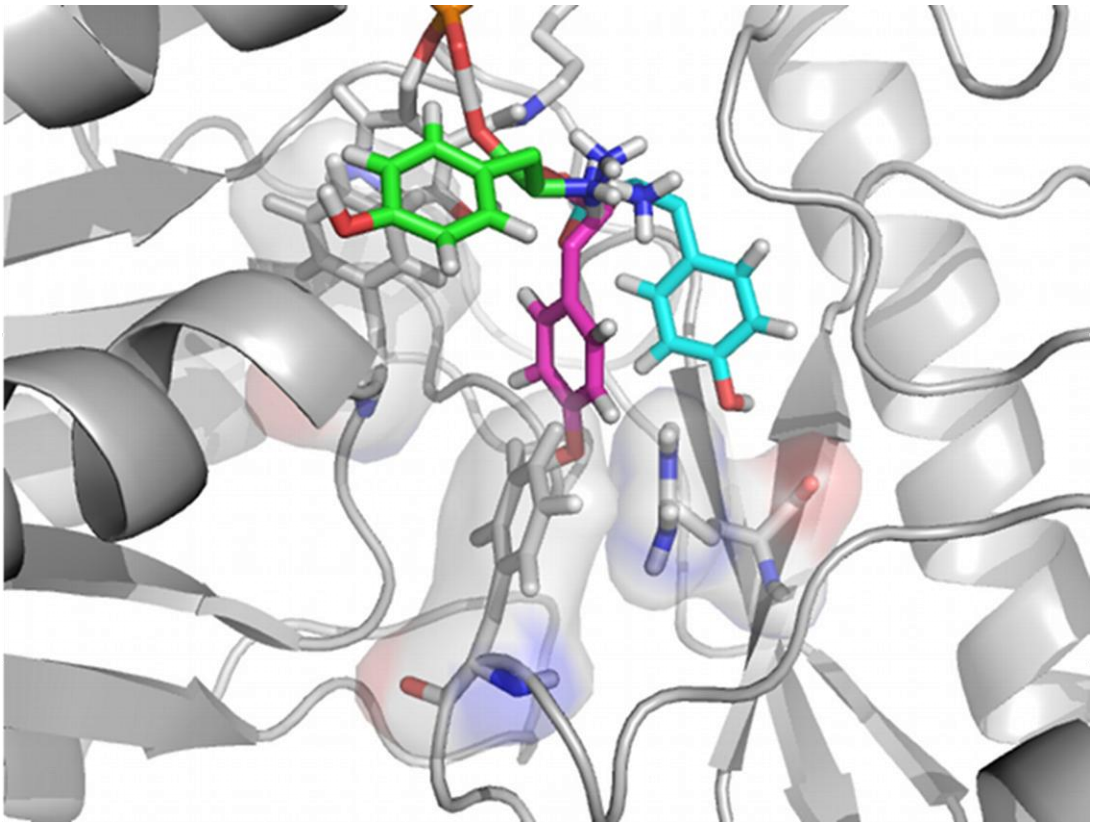

**Figure 3.9 Interactions between tyrosine and the hTAT active site.**
Residues Phe169, Phe410, and Arg419 are shown as sticks and colored by element, with van der Waals surfaces overlaid to illustrate packing. The TAT enzyme and bound tyrosine residues are depicted as in Figure 3.7.

## 3.5 Discussion

It is generally accepted that mammalian TATs play important roles in tyrosine degradation metabolism. Mutations in this enzyme lead to disease like tyrosinemia type II. In this study attempts have been made to fulfill several gaps in the literature regarding structural and biochemical studies of TATs. The kinetic analysis mTAT showed highest affinity and catalytic efficiency toward the amino acid tyrosine and keto acid p-hydroxyphenylpyruvate, suggesting tyrosine is a best amino acid donor and p-hydroxyphenylpyruvate is a best amino acid acceptor for mTAT. Based on the mTAT substrate specificity, mTAT behaves in a manner similar to hTAT, in that it has a narrow substrate specificity compared to tcTAT (*18, 42-44*). TcTAT, on the other hand, has broad substrate specificity; in particular, it has an affinity to alanine, which differs considerably from tyrosine, the primary substrate of mTAT and hTAT (*44*).

Critical residues for catalysis in mTAT and hTAT are conserved. For example, the residue Asp247 interacts with the pyridine nitrogen of the cofactor (Figure 3.5) which is structurally and functionally conserved within fold-type I of the PLP-dependent enzyme family, indicating its importance for catalysis in mTAT and hTAT. Based upon the above feature of the structure, mTAT is a fold-type I PLP-dependent enzyme (*46-50*). Interaction of PLP with other active site residues suggests that active site is stabilized by hydrophilic, hydrophobic, and electrostatic interactions.

One of important findings of this manuscript is formation of intra-molecular disulfide bond which is present on the surface of mTAT structure. Therefore, it may be ready to be targeted by an oxidant or a reducing agent. Forming a disulfide bond can lead to a conformational change in Cys144, causing it to interact with the N1 atom of the PLP ring, which is probably the mechanism of TAT inactivation. Reducing agents may reduce the disulfide bond and change the Cys144 conformation back to an active form, which is the most likely explanation for the reversibility feature of the TAT inactivation. Site-directed mutagenesis of these two residues in future studies will shed light on their roles in protein inactivation.

A superposition of hTAT (PDB code 3dyd) and mTAT shows that the two proteins have the same architecture and that all residues around the PLP molecule (within 6 Å) are identical in the two enzymes. This suggests that hTAT and mTAT share the same PLP binding sites.

MD simulations predicted that there are hydrophobic interactions in tcTAT that can be utilized by both alanine and tyrosine in binding to the enzyme, and that tyrosine is further stabilized by hydrogen bonding to a nearby arginine residue. In the case of hTAT, probably in mTAT as well, additional hydrophobic and hydrogen bonding interactions also promote the binding of tyrosine, but are too distant from the active site to be utilized by alanine.

Although the mTAT-tyrosine interactions have been suggested in this report using MD, the low resolution crystal structure of mTAT-tyrosine complex will confirm the interactions of tyrosine with mTAT. MD studies suggested several interactions between tyrosine and mTAT. Mutation and further kinetic characterization of those residues will shed light on whether or not these residues stabilize the mTAT- tyrosine complex. Mutation of cysteine residues involved in disulfide bond formation is recommended in order to understand the role of disulfide bond in the stability mTAT**.**

**Acknowledgements**

This work was supported in part by a research grant from NINDS (NS062836) and carried out in part at the National Synchrotron Light Source, Brookhaven National Laboratory. We are grateful to Stephanie N. Lewis for her help with molecular docking.

## References

1. al-Hemidan, A. I., and al-Hazzaa, S. A. (1995) Richner-Hanhart syndrome (tyrosinemia type II). Case report and literature review, *Ophthalmic Genet 16*, 21-26.

2. Natt, E., Westphal, E. M., Toth-Fejel, S. E., Magenis, R. E., Buist, N. R., Rettenmeier, R., and Scherer, G. (1987) Inherited and de novo deletion of the tyrosine aminotransferase gene locus at 16q22.1----q22.3 in a patient with tyrosinemia type II, *Hum Genet 77*, 352-358.

3. Minami-Hori, M., Ishida-Yamamoto, A., Katoh, N., Takahashi, H., and Iizuka, H. (2006) Richner-Hanhart syndrome: report of a case with a novel mutation of tyrosine aminotransferase, *J Dermatol Sci 41*, 82-84.

4. Maydan, G., Andresen, B. S., Madsen, P. P., Zeigler, M., Raas-Rothschild, A., Zlotogorski, A., Gutman, A., and Korman, S. H. (2006) TAT gene mutation analysis in three Palestinian kindreds with oculocutaneous tyrosinaemia type II; characterization of a

silent exonic transversion that causes complete missplicing by exon 11 skipping, *J Inherit Metab Dis 29*, 620-626.

5. Meissner, T., Betz, R. C., Pasternack, S. M., Eigelshoven, S., Ruzicka, T., Kruse, R., Laitenberger, G., and Mayatepek, E. (2008) Richner-Hanhart syndrome detected by expanded newborn screening, *Pediatr Dermatol 25*, 378-380.

6. Pasternack, S. M., Betz, R. C., Brandrup, F., Gade, E. F., Clemmensen, O., Lund, A. M., Christensen, E., and Bygum, A. (2009) Identification of two new mutations in the TAT gene in a Danish family with tyrosinaemia type II, *Br J Dermatol 160*, 704-706.

7. Charfeddine, C., Monastiri, K., Mokni, M., Laadjimi, A., Kaabachi, N., Perin, O., Nilges, M., Kassar, S., Keirallah, M., Guediche, M. N., Kamoun, M. R., Tebib, N., Ben Dridi, M. F., Boubaker, S., Ben Osman, A., and Abdelhak, S. (2006) Clinical and mutational investigations of tyrosinemia type II in Northern Tunisia: identification and structural characterization of two novel TAT mutations, *Mol Genet Metab 88*, 184-191.

8. Endo, F. (1998) [Hereditary tyrosinemia type II], *Ryoikibetsu Shokogun Shirizu*, 134-136.

9. Natt, E., Kida, K., Odievre, M., Di Rocco, M., and Scherer, G. (1992) Point mutations in the tyrosine aminotransferase gene in tyrosinemia type II, *Proc Natl Acad Sci U S A 89*, 9297-9301.

10. Macsai, M. S., Schwartz, T. L., Hinkle, D., Hummel, M. B., Mulhern, M. G., and Rootman, D. (2001) Tyrosinemia type II: nine cases of ocular signs and symptoms, *Am J Ophthalmol 132*, 522-527.

11. Bein, N. N., and Goldsmith, H. S. (1977) Recurrent massive haemorrhage from benign hepatic tumours secondary to oral contraceptives, *Br J Surg 64*, 433-435.

12. Cavelier-Balloy, B., Venencie, P. Y., Lemonnier, V., Verola, O., Servant, J. M., Puissant, A., and Civatte, J. (1985) [Histiocytoid hemangioma of the scalp], *Ann Dermatol Venereol 112*, 965-972.

13. Rego, J. V., Murta, S. M., Nirde, P., Nogueira, F. B., de Andrade, H. M., and Romanha, A. J. (2008) *Trypanosoma cruzi*: characterisation of the gene encoding tyrosine aminotransferase in benznidazole-resistant and susceptible populations, *Exp Parasitol 118*, 111-117.

14. Touboul, T., Hannan, N. R., Corbineau, S., Martinez, A., Martinet, C., Branchereau, S., Mainot, S., Strick-Marchand, H., Pedersen, R., Di Santo, J., Weber, A., and Vallier, L. (2010) Generation of functional hepatocytes from human embryonic stem cells under chemically defined conditions that recapitulate liver development, *Hepatology 51*, 1754-1765.

15. Fu, L., Dong, S. S., Xie, Y. W., Tai, L. S., Chen, L., Kong, K. L., Man, K., Xie, D., Li, Y., Cheng, Y., Tao, Q., and Guan, X. Y. (2010) Down-regulation of tyrosine aminotransferase at a frequently deleted region 16q22 contributes to the pathogenesis of hepatocellular carcinoma, *Hepatology 51*, 1624-1634.

16. Blankenfeldt, W., Nowicki, C., Montemartini-Kalisz, M., Kalisz, H. M., and Hecht, H. J. (1999) Crystal structure of *Trypanosoma cruzi* tyrosine aminotransferase: substrate specificity is influenced by cofactor binding mode, *Protein Sci 8*, 2406-2417.

17. Hargrove, J. L., and Mackin, R. B. (1984) Organ specificity of glucocorticoid-sensitive tyrosine aminotransferase. Separation from aspartate aminotransferase isoenzymes, *J Biol Chem 259*, 386-393.

18. Sobrado, V. R., Montemartini-Kalisz, M., Kalisz, H. M., De La Fuente, M. C., Hecht, H. J., and Nowicki, C. (2003) Involvement of conserved asparagine and arginine residues from the N-terminal region in the catalytic mechanism of rat liver and *Trypanosoma cruzi* tyrosine aminotransferases, *Protein Sci 12*, 1039-1050.

19. Gross-Mesilaty, S., Hargrove, J. L., and Ciechanover, A. (1997) Degradation of tyrosine aminotransferase (TAT) via the ubiquitin-proteasome pathway, *FEBS Lett 405*, 175-180.

20. Ciechanover, A., Orian, A., and Schwartz, A. L. (2000) Ubiquitin-mediated proteolysis: biological regulation via destruction, *Bioessays 22*, 442-451.

21. Ko, T. P., Wu, S. P., Yang, W. Z., Tsai, H., and Yuan, H. S. (1999) Crystallization and preliminary crystallographic analysis of the *Escherichia coli* tyrosine aminotransferase, *Acta Crystallogr D Biol Crystallogr 55*, 1474-1477.

22. Han, Q., Fang, J., and Li, J. (2001) Kynurenine aminotransferase and glutamine transaminase K of *Escherichia coli*: identity with aspartate aminotransferase, *The Biochemical journal 360*, 617-623.

23. Otwinowski, Z., and Minor, W. (1997) Processing of X-ray Diffraction Data Collected in Oscillation Mode, *Methods in Enzymology 276*, 307-326.

24. Vagin, A., and Teplyakov, A. (1997) MOLREP: an automated program for molecular replacement., *J Appl Cryst 30*, 1022-1025.

25. Murshudov, G. N., Vagin, A. A., and Dodson, E. J. (1997) Refinement of macromolecular structures by the maximum-likelihood method, *Acta Crystallogr D Biol Crystallogr 53*, 240-255.

26. Krissinel, E., and Henrick, K. (2004) Secondary-structure matching (SSM), a new tool for fast protein structure alignment in three dimensions *Acta Crystallogr D60*, 2256-2268.

27. DeLano, W. L. (2002) The PyMOL Molecular Graphics System In *The PyMOL Molecular Graphics System*, Delano Scientifc, San Carlos, CA, USA. .

28. Huey, R., Morris Garrett, M., Olson Arthur, J., and Goodsell David, S. (2007) A semiempirical free energy force field with charge-based desolvation, *Journal of Computational Chemistry 28*, 1145-1152.

29. Morris, G. M., Goodsell, D. S., Halliday, R. S., Huey, R., Hart, W. E., Belew, R. K., and Olson, A. J. (1998) Automated docking using a Lamarckian genetic algorithm and an empirical binding free energy function, *Journal of Computational Chemistry 19*, 1639-1662.

30. Pettersen, E. F., Goddard, T. D., Huang, C. C., Couch, G. S., Greenblatt, D. M., Meng, E. C., and Ferrin, T. E. (2004) UCSF Chimera--a visualization system for exploratory research and analysis, *J Comput Chem 25*, 1605-1612.

31. Hess, B., Kutzner, C., van der Spoel, D., and Lindahl, E. (2008) GROMACS 4: Algorithms for Highly Efficient, Load-Balanced, and Scalable Molecular Simulation, *Journal of Chemical Theory and Computation 4*, 435-447.

32. Berendsen, H. J. C., Postma, J. P. M., Van Gunsteren, W. F., and Hermans, J. (1981) Interaction models for water in relation to protein hydration, *Jerusalem Symposia on Quantum Chemistry and Biochemistry 14*, 331-342.

33. Oostenbrink, C., Villa, A., Mark Alan, E., and van Gunsteren Wilfred, F. (2004) A biomolecular force field based on the free enthalpy of hydration and solvation: the GROMOS force-field parameter sets 53A5 and 53A6, *Journal of Computational Chemistry 25*, 1656-1676.

34. Berendsen, H. J. C., Postma, J. P. M., Van Gunsteren, W. F., DiNola, A., and Haak, J. R. (1984) Molecular dynamics with coupling to an external bath, *Journal of Chemical Physics 81*, 3684-3690.

35. Hoover, W. G. (1985) Canonical dynamics: Equilibrium phase-space distributions, *Phys. Rev. A: At. Mol. Opt. Phys. A31*, 1695-1697.

36. Nose, S. (1984) A unified formulation of the constant-temperature molecular-dynamics methods, *Journal of Chemical Physics 81*, 511-519.

37. Parrinello, M., and Rahman, A. (1981) Polymorphic transitions in single crystals: A new molecular dynamics method, *Journal of Applied Physics 52*, 7182-7190.

38. Nose, S., and Klein, M. L. (1983) Constant pressure molecular dynamics for molecular systems, *Molecular Physics 50*, 1055-1076.

39. Essmann, U., Perera, L., Berkowitz, M. L., Darden, T., Lee, H., and Pedersen, L. G. (1995) A smooth particle mesh Ewald method, *Journal of Chemical Physics 103*, 8577-8593.

40. Darden, T., York, D., and Pedersen, L. (1993) Particle mesh Ewald: an N.log(N) method for Ewald sums in large systems, *Journal of Chemical Physics 98*, 10089-10092.

41. Hess, B., Bekker, H., Berendsen, H. J. C., and Fraaije, J. G. E. M. (1997) LINCS: a linear constraint solver for molecular simulations, *Journal of Computational Chemistry 18*, 1463-1472.

42. Sivaraman, S., and Kirsch, J. F. (2006) The narrow substrate specificity of human tyrosine aminotransferase--the enzyme deficient in tyrosinemia type II, *FEBS J 273*, 1920-1929.

43. Donini, S., Ferrari, M., Fedeli, C., Faini, M., Lamberto, I., Marletta, A. S., Mellini, L., Panini, M., Percudani, R., Pollegioni, L., Caldinelli, L., Petrucco, S., and Peracchi, A. (2009) Recombinant production of eight human cytosolic aminotransferases and assessment of their potential involvement in glyoxylate metabolism, *The Biochemical journal 422*, 265-272.

44. Nowicki, C., Hunter, G. R., Montemartini-Kalisz, M., Blankenfeldt, W., Hecht, H., and Kalisz, H. M. (2001) Recombinant tyrosine aminotransferase from *Trypanosoma cruzi*: structural characterization and site directed mutagenesis of a broad substrate specificity enzyme, *Biochim Biophys Acta 1546*, 268-281.

45. Laskowski, R. A., Macarthur, M. W., Moss, D. S., and Thornton, J. M. (1993) Procheck - a Program to Check the Stereochemical Quality of Protein Structures, *J of Appl Crystallogr 26*, 283-291.

46. Jansonius, J. N. (1998) Structure, evolution and action of vitamin B6-dependent enzymes, *Curr Opin Struct Biol 8*, 759-769.

47. Grishin, N. V., Phillips, M. A., and Goldsmith, E. J. (1995) Modeling of the spatial structure of eukaryotic ornithine decarboxylases, *Protein Sci 4*, 1291-1304.

48. Kack, H., Sandmark, J., Gibson, K., Schneider, G., and Lindqvist, Y. (1999) Crystal structure of diaminopelargonic acid synthase: evolutionary relationships between pyridoxal-5'-phosphate-dependent enzymes, *J Mol Biol 291*, 857-876.

49. Schneider, G., Kack, H., and Lindqvist, Y. (2000) The manifold of vitamin B6 dependent enzymes, *Structure 8*, R1-6.

50. Mehta, P. K., Hale, T. I., and Christen, P. (1993) Aminotransferases: demonstration of homology and division into evolutionary subgroups, *Eur J Biochem 214*, 549-561.

51. Holm, L., and Sander, C. (1993) Protein Structure Comparison by Alignment of Distance Matrices, *J. Mol. Biol. 233*, 123-138.

52. Han, Q., Cai, T., Tagle, D. A., and Li, J. (2010) Structure, expression, and function of kynurenine aminotransferases in human and rodent brains, *Cell Mol Life Sci 67*, 353-368.

53. Han, Q., Robinson, H., Cai, T., Tagle, D. A., and Li, J. (2009) Biochemical and structural properties of mouse kynurenine aminotransferase III, *Mol Cell Biol 29*, 784-793.

54. Rossi, F., Han, Q., Li, J., Li, J., and Rizzi, M. (2004) Crystal structure of human kynurenine aminotransferase I, *J Biol Chem 279*, 50214-50220.

55. Beneking, M., Schmidt, H., and Weiss, G. (1978) Subcellular distribution of a factor inactivating tyrosine aminotransferase. Study of its mechanism and relationship to different forms of the enzyme, *Eur J Biochem 82*, 235-243.

56. Federici, G., Di Cola, D., Sacchetta, P., Di Ilio, C., Del Boccio, G., and Polidoro, G. (1978) Reversible inactivation of tyrosine aminotransferase from guinea pig liver by thiol and disulfide compounds, *Biochem Biophys Res Commun 81*, 650-655.

57. Buckley, W. T., and Milligan, L. P. (1978) Participation of cysteine and cystine in inactivation of tyrosine aminotransferase in rat liver homogenates, *Biochem J 176*, 449-454.

# Chapter 4. Review of Literature on *N*-acetyltransferases

Amino acid metabolism is an important physiological process. One of the mechanisms by which the general control of amino acids takes place is via certain enzymes (*1*). The focus of this literature review is general control of amino acids (GCN-5-related *N*)-acetyltransferases (GNAT) family members. GNAT superfamily members use acetyl coenzyme A (AcCoA) as acetyl group donor and proteins and small molecules as acetyl group acceptor (*1*). GNATs play important roles in gene regulation, antibiotic resistance, and hormonal regulation of circadian rhythms (*1*). A major portion of this literature review sheds light on various biochemical and physiological aspects of *N*-acetyltransferases.

## 4.1 Structural features of GNAT superfamily

The first members of the GNAT superfamily were identified in 1980 and consisted of the aminoglycoside *N*-acetyltransferases in bacteria (*2, 3*). The GNAT family has four conserved sequence motifs termed, C, D, A, and B in N- to C-terminal order (*4*). These regions are involved in AcCoA binding and substrate bindings (*1, 5*). The GNAT superfamily is also defined by a common fold core that includes, α-helices on both sides of six-stranded mixed β-sheets (*6*). Despite retaining a common core around which a more inconsistent stock of structures is built, GNAT superfamily members display limited sequence similarity and retain few invariant residues (*1*). The four conserved motifs contribute to protein stability, in the case of C and D, and to AcCoA binding, in the case of A and B, with Motif A exhibiting the greatest conservation across the GNAT superfamily members. The remaining motifs are frequently interrupted by acceptor substrate specificity determinants, which are not discernable by sequence comparison alone, making homology detection a challenge (*1, 7*). Although the primary sequences among the GNAT superfamily do not share high level of homology, their characteristic GNAT fold is well conserved (*3*). This fold commonly binds the AcCoA by its pantetheine region and forms a hydrogen bond with the carbonyl of the thioester (*3*). The process of binding the pantetheine arm of AcCoA often initiates essential conformational changes in the "P loop" which coordinates the pyrophosphate moiety of the α1/α2 and the adjoining loop of the fold region (*1, 3*).

## 4.2 Functional diversity in GNAT superfamily/ Classification of GNAT superfamily

GNATs catalyze a diverse arrays of substrates, such as, *N*-acetylation of lysine residues of proteins, (histones and transcription factors), and small molecules, including polyamines, aminoglycosides, or arylalkylamines (*5*). Acetylation of the arylalkylamine is catalyzed by arylalkylamine *N*-acetyltransferase (AANAT) (*8*). *N*-acetyltransferase can be classified based on their affinity towards substrates, which include biogenic amines (e.g., dopamine), aminoglycosides (e.g., glucosamine), and hydrazines. Different *N*-acetyltransferases have been widely investigated, including those involved in the physiological processes (*7, 9*) of humans , several unicellular green algae non-metazoans (*10*), bacteria (*11*), and several insects species (*12, 13*). A number of these acetyltransferases are reviewed as follows:

**I) Histone *N*-acetyltransferase**

Acetylation of the histone amino-terminal tail has been associated with the transcriptional activation of chromatin and gene activation (*14*). Of the known structures from the GCN-5 acetyltransferase, seven correspond to histone *N*-acetyltransferase (*1*). Acetylation of the amino terminal histone "tails" removes a positive charge, and it is possible that this results in weaker binding of the nucleosome core particles, composed of histones (*1*). These loci are then free to interact with the complex transcriptional machinery, resulting in improved transcription and translation of protein products (*15*).

**II) Aminoglycosides *N*-acetyltransferases**

Aminoglycoside *N*-acetyltransferase is antibiotic resistant protein, which was first identified in *Enterococcus faecium* by Courvalin and coworkers (*1, 16*), and the gene for the protein was subsequently cloned and over-expressed in *Escherichia coli (17)*. This work led to detailed studies on the specific mechanisms associated with the behavior of aminoglycosides 6'-*N*-acetyltransferase (AAC (6')-Ii) (*17*). As a result, the kinetic parameters for the acetylation of numerous aminoglycosides have been determined (*17*). In addition, the conformation of two aminoglycosides bound to enzyme has been studied by NMR (*18*). The structure of AAC (6')-Ii suggests that the aminoglycoside *N*-acetyltransferase belongs to GNAT superfamily (*1*).

**III) Arylalkylamine *N*-acetyltransferase (AANAT)**

AANAT represents the third class of GNAT enzymes that have been structurally characterized (*3*). AANAT is the penultimate enzyme in melatonin synthesis (Figure 4.1) and controls the night/day rhythm of melatonin production in the vertebrate pineal gland (*8*). The structure of ovine AANAT has been solved both in its native in its the complex form with a bisubstrate analog (*19*).

**Melatonin**

Melatonin which influences sleep patterns is also essential for seasonal reproduction in many species. In mammals pinealocytes are involved in the rhythmic synthesis and release of the melatonin hormone (*20*). The other cells which produce melatonin are retinal photoreceptors and skin (*21, 22*). Melatonin is synthesized in a four-step enzymatic process from dietary tryptophan. Tryptophan is converted in two steps to serotonin, which is then acetylated by AANAT and methylated by hydroxyindole-*O*-methyltransferase (HIOMT) to melatonin (Figure 4.1). The rhythm of AANAT activity correlates strongly with the rhythm of melatonin synthesis (*9*). Melatonin is not only involved in the seasonal timing of reproduction (*23, 24*) but also in the circadian regulation of many physiological functions such as heart rate (*23*). Even though the rhythm in melatonin synthesis reflects the circadian oscillator in pineal cells, a number of changes can affect melatonin output independently of the oscillator. For example, AANAT activation decreases rapidly when animals are exposed to light at night (*8*, *25*).

Literature correlates involvement of AANAT in multifactorial genetic diseases such as distorted behavior in sleep/wake cycle (e.g delayed sleep phase syndrome (*26*)). AANAT may also contribute to arthus reaction, asthama, ganglionic cysts, and melanoma (*27-30*).

In general AANATs not only act on tryptophan metabolites but also on tyrosine metabolites such as dopamine and tyramine. Klein reviewed that the GNAT superfamily also includes an additional AANAT family member, represented by dopamine *N*-acetyltransferase (*Dat*), which is expressed in *Drosophila melanogaster (9)*. Klein, reported that *Dat* may contribute in cuticle sclerotization and neurotransmission rather than melatonin synthesis (*9*). He further stated that *Dat* and AANAT family members have not been found in the same genome (*9*).

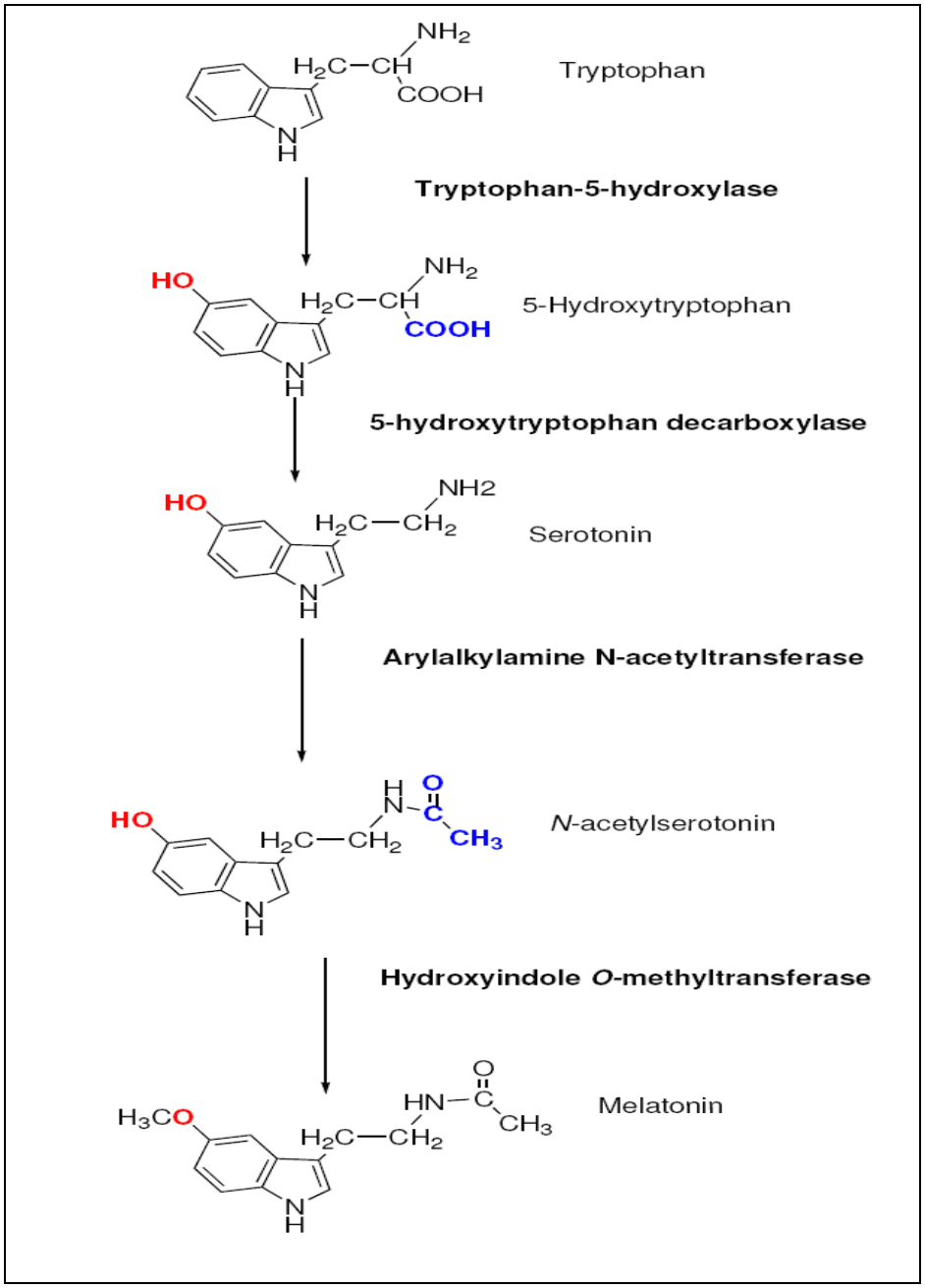


**Figure 4.1 General melatonin synthesis pathway** (*9*)**.**

## 4.3 Evolution of AANATs in eukaryotes

Eukaryotic AANATs and their homologs form a family inside the GNAT superfamily (*1*, *3*). As mentioned in the previous section, the members of the GNAT superfamily possess a conserved AcCoA binding domain and share a common mechanism of acetyl transfer. However,

each family prefers different substrates, ranging from histones to arylamines (*3, 20*). Mammals, avian, and anuran genomes possess a single copy of AANAT gene (*20*). In these species, arylalkylamines are the preferred as substrates over the arylamine preferred as substrates in vertebrates (*31*). Recently seven AANAT genes have been found in cephalochordates, and all of them have non-vertebrate features (*32*). It has been indicted that the nonexistence of AANATs from the genome of Hemichordates and Urochordates may represent an important event in the evolution of the AANATs, possibly occurring at the beginning of vertebrate evolution (*32*). In fish two isoforms, AANAT1 and AANAT2, have been found in the retina and pineal gland, respectively (*33, 34*). AANAT plays several roles in eukaryotes including detoxification and synthesis of compounds such as melatonin and *N*-acetyldopamine which is the precursor for cuticle formation (*35, 36*). AANAT acetylates of serotonin to *N*-acetylserotonin, and the later is subsequently converted to melatonin by hydroxyindole *O*-methyltransferase (HIOMT) (*37*). Circulating melatonin levels are higher at night, providing a hormonal signal of circadian and seasonal time (*38*).

In mammals circadian oscillator controls the output of AANATs (*9*). But in lower vertebrates, AANAT is under the control of the circadian clock located in the pinealocytes (*37, 39*).

## 4.4 Regulation of AANATs

It has been established that changes in melatonin synthesis and secretion essentially follow changes in the enzymatic activity of AANAT (*38*). AANAT activity is dynamic and highly regulated (*9*). Moreover, it responds to all the factors that have power over melatonin output, including light and the presence of norepinephrine (*40*). Finely tuned changes in melatonin output and any phase shifts in melatonin regularity are consequently reflected by acute changes in AANAT activity, as well as phase shifts in the rhythm of AANAT enzyme activity (*9*). The activity and mRNA levels of HIOMT, the enzyme that completes the synthesis of melatonin, also change under some conditions (*9*). However, whether this enzyme contributes significantly to the dynamic regulation of melatonin output is still uncertain in insects (*41*). Transcription of AANAT is subject to both positive and negative control (*9*). Expression of AANAT can be regulated either directly by a circadian oscillator, via transcription factors such

as BMAL/CLOCK and OTX5 (*9*, *23*, *42*), or indirectly via a neuronal pathway which is typical for mammals (*9*). Regulation of AANATs in insects has not been established.

## 4.5 Roles of AANAT in biogenic amines *N*-acetylation in insects

AANAT activity was first detected in the nervous system of insects almost four decades ago (*36*). Specifically, AANATs were thought to play roles in the sclerotization, neurotransmitter inactivation, detoxification of xenobiotics, and melatonin synthesis in some insects (*43*) of some insects. It has been reported that dopamine *N*-acetyltransferase is involved in the sclerotization of the adult cuticle of *Bombyx mori (44, 45).*

**I) Sclerotization**

In insects, their cuticular sclerotization, cuticles are stabilized by the inclusion of phenolic compounds (*46*, *47*). Insect cuticles are diverse, differing in thickness, stiffness, strength, elasticity, and color (*47*, *48*). In the review by Anderson, it has been stated that, despite the variances mentioned, insect cuticles have a general basic structure consisting of a procuticle and epicuticle (*47*, *48*). Much of the cuticular diversity is due to differences in molecular architecture in protein composition (*48*). However, certain aspects of the sclerotization process itself can also play an important role, such as the relative amounts of sclerotizing enzymes and precursors (*48*). However, a detailed understanding of the regional differences and knowledge of how the process is controlled is still very poor. What we do know is that during cuticular sclerotization, acyldopamine (*N*-acetyldopamine (NADA)), (*49*) and *N*-β-alanyldopamine (NBAD) (*50*) are oxidatively incorporated into the cuticular matrix (*47*). The first step in the cuticular sclerotization sequence involves the hydroxylation of the tyrosine to dopa, followed by the decarboxylation of dopa to dopamine, leading to the synthesis of NADA (Refer Figure 1.1. Chapter 1). NADA is the product formed via the acetylation of dopamine in the presence of AANAT and *N*-β-alanyldopamine in the presence of ebony protein (*51*). The possibility of catechols other than NADA and NBAD (such as *N*-acetylnorepinephrine) functioning as sclerotization precursors has also been mentioned in the literature (*52*). It has been suggested that NADA may have a role not only in sclerotization, but also in coloration (*44*). Specifically, it has been suggested that the brown colors of insect cuticles are related to NBAD-sclerotization (*44*). Most brown cuticles are probably sclerotized by a mixture of NADA and NBAD, and the ratio between these two sclerotization precursors may determine shade intensity (*46*)**.**

**II) Neurotransmitter inactivation**

Normal synaptic function requires the removal or inactivation of neurotransmitter molecules from the synaptic cleft following signal transmission. Wu et al. suggest that neurotransmitter inactivation has the additional significance of being a more likely facilitator of synaptic evolution than removal or reuptake (*53*). One of the mechanisms by which the neurotransmitters undergo inactivation uses enzymes. In mammals, monoamine oxidase A (MAO-A) and monoamine oxidase B (MAO-B) both play roles in neurotransmitters inactivation (*54*). But as little to no activity has been found for MAO-A and MAO-B in insects, it is possible, that for them, AANATs may fill this role in the inactivation of neurotransmitters (*13*). This view is supported by the suggestion that *N*-acetylation of dopamine, norepinephrine, octopamine, tryptamine, and serotonin can lead to inactivation of these neurotransmitters (*43*). Although *N*-acetyldopamine may be a substrate for tyrosinase in mushrooms (*55*), the fate of these *N*-acetylated compounds, such as *N*-acetyldopamine and *N*-acetyloctopamine in insects and the mammalian brain remains unclear.

**III) Significance of melatonin in insects**.

Melatonin is a hormone that is involved in the regulation of the circadian rhythms of several biological functions (*13*). Although one study using radioimmunoassay revealed that melatonin levels in *Drosophila* were more than double during the night as compared to the day time levels (*13, 56*), very little data have been reported on the role of AANAT in the biosynthesis of melatonin and its role in circadian rhythm regulation in insects (Figure 4.1). Only one insect suggests the presence of the enzyme which converts *N*-acetylserotonin to melatonin (*57*). Therefore, although it is possible that melatonin is involved in the circadian rhythm regulation of insects, its role in mosquito development and physiology still needs to be determined. There are several contrasting views with respect to the presence of melatonin in insects and its role in the biological rhythm of insects. The presence of biological rhythm in insects is an intriguing phenomenon and could be pursued by testing them for the presence of a self sustaining biological clock.

## 4.6 Biological rhythm in insects

Biological rhythm is characterized by well-defined periodicities in eukaryotic physiology and behavior. Further, these rhythmic cycles are controlled by an internal biological or circadian clock. The literature suggests that biological rhythms are typically synchronized to environmental signals. However, even in the absence of these markers, organisms still exhibit rhythmic activities regulated by the presence of a self sustaining endogenous biological clock (*58*). Biological rhythms provide several adaptive advantages to an organism by allowing it to anticipate certain cyclic environmental conditions as well as the changes in these cyclic events such as minute daily changes in the duration of seasonal daylight (*59*). Many mosquitoes conform to a daily biological rhythm according to their physiological and behavioral status. It has been reported that each species of mosquitoes has evolved diverse patterns of daily rhythms coupled to their behavioral activities *(60)*. For example *Ae. aegypti* is a diurnal species; which displays sharp flight activity early and late in photophase (*60*). Contrarily, in nocturnal species such as *Anopheles* and *Culex* species, the host-seeking and blood-feeding activities are restricted to the scotophase period. Both external and internal factors can modify the periodicities exhibited by mosquitoes (*61*). Mosquito's feeding behavior is also affected by long and short light pulses (*62*). In addition, the literature suggests that, neurochemicals and endogenous factors present in the central nervous system (CNS) may also contribute to the circadian rhythm activities of mosquitoes (*63, 64*). An increased understanding of the activity patterns of each mosquito species will promote our knowledge of disease transmission dynamics and information about the role of AANATs in the periodicity of these insects could contribute to that understanding.

## 4.7 *Aedes aegypti, an* important mosquito species

Mosquito-borne diseases are devastating to humans in areas where this vector is present. Yellow fever, also known as dengue, is a threat to millions of people (*65*). An estimated 200,000 cases of yellow fever, resulting in 30,000 deaths, occur worldwide each year (http://www.who.int/mediacentre/factsheets/fs100/en/index.html). The high rate of mosquito-borne diseases is a result of unavailability of effective vaccines, insecticides, and emergence drug resistant by vectors and pathogens, respectively (*65*). Therefore, there is an urgent need to

develop novel strategies to control the mosquito, *Ae. aegypti*, the primary worldwide arthropod vector for the yellow fever and dengue viruses.

*Ae. aegypti* is found throughout most tropical to subtropical world regions having a cosmotropical distribution between 40 °N and 40 °S (*66, 67*). Its survival is poor in hot, dry climates. Figure 4.2 represent the worldwide distribution of *Ae. aegypti*. However, the *Ae. aegypti* population is the highest in Gulf Coastal states (*66*). *Ae. aegypti* is considered to be the most docile mosquito species for laboratory culture, so it has been used for thorough laboratory investigations of genetics, vector competence, and mosquito biology (*68*). Determining the complete genome sequence of the *Ae. aegypti* represents a major breakthrough in learning about various proteins and their functions, since such proteins represent medically important protein subfamilies in mosquitoes (*69*). In general these proteins (or their products) affect the physiological behaviors in insects and vice versa. Some of these physiological behaviors in mosquitoes will be discussed in the following sections.

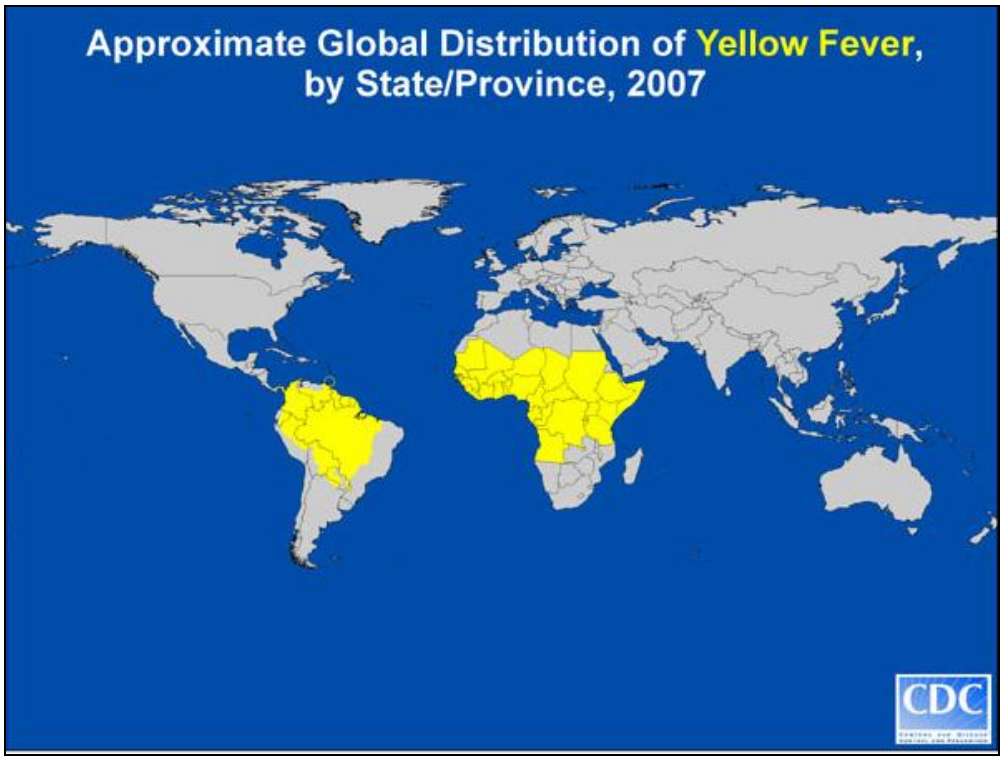


**Figure 4.2 Yellow Fever Global Map showing the approximate global distribution of Yellow fever, by State/province, 2007.**
(Used under fair use). (http://www.cdc.gov/ncidod/dvbid/yellowfever/YF_GlobalMap.html)

## 4.8 Important physiological behaviors in mosquitoes

**I) Sugar feeding behavior**

Mosquitoes feed on plant sugars from different parts of the plants (for example from flowers) for their survival (*64, 70*). These sugars are utilized as a source of energy by male and female mosquitoes during flight and fight mechanisms (*64, 70*). These energy sources also used when female mosquitoes needs to fly towards the host species to acquire their blood meal (*71*). Although male mosquitoes prefer plant sugars as their energy source, female mosquitoes prefer plant nectar as their energy source. Besides fight and flight mechanism sugars and blood is primarily utilized in the process of reproduction and survival. Sugar feeding is characteristic feature of young female (*71*). Some female mosquitoes in the early emerging stage (e. g *An. gambiae*) depend on the plant nectar for their early development because the signals for obtaining the blood meal only starts developing 24 hours after of adult emergence in female mosquitoes (*64*). In some female mosquitoes where blood meal may not be available plant sugar acts as a primary source for physiological functions such as egg maturation (*64*).

**II) Blood feeding in mosquitoes**

Blood feeding is a vital physiological behavior in mosquitoes. For most mosquito species it is essential for egg maturation and egg laying (*64, 72*). Typically, mosquitoes start blood feeding three days after adult emergence. This behavior is associated with certain detection mechanisms that take about 30 hours after adult emergence to develop, which enable the mosquito to respond to host odors (*64, 73*). In some species, however, the signaling mechanism that triggers blood feeding does not develop until 14 days after adult emergence (*64, 73*). Regardless of when it develops, this maturation milestone enables mosquitoes to respond to different substances released by blood hosts (*74-76*). Several studies have been conducted in which researchers have sought to isolate specific host chemicals that might explain how mosquitoes respond to these chemicals (*77-79*). In particular, L-lactic acid, ammonia, and $CO_2$ have been the focus of this research (*64, 78, 79*). Although these chemicals may function in isolation, researchers have also found that in order to initiate blood feeding behaviors among mosquitoes, these chemicals sometimes work in combination. For example, it has been reported that a mixture of L-lactic acid with acetone and dimethyl disulfide serves as a better attractant for the *Aedes* mosquitoes rather than using just L-lactic acid with acetone (*64, 78, 79*).

**III) Pre-oviposition and oviposition actions and factors affecting oviposition in mosquitoes**

Oviposition and pre-oviposition behaviors are very important in mosquitoes (*64*, *79*). As part of the pre-oviposition behavior, mosquitoes search for places where progeny can be raised and protected, and these places are typically aquatic environments (*64*, *79*). Many visual and chemical signals play an important role, such as signals from locations where other mosquitoes have already laid eggs (*64*, *79*). Different mosquito species can have the same signaling mechanism and therefore share nesting space (*64*). Some of these visual and chemical signals come from decomposition of bacterial or fungal deposits or from chemicals released by eggs, larva or pupa (*64*, *79*). Oviposition behavior is affected by different factors, including temperature, lighting, and availability of blood (*80*). Several studies have suggested biogenic amines are important internal factors in oviposition behaviors (*81*), a role which is further discussed here.

**IV) Importance of Biogenic amines in insects**

Biogenic amines play an important role in regulating insect behavior and physiology (*81*). For example, octopamine, tyramine, and serotonin are known to control egg-laying and reproductive behaviors in *D. melanogaster* (*82*). Dopamine and tyramine are involved in increasing ovarian growth in reproductive worker wasps (*83*). Biogenic amines are also important for regulating female mating receptivity in insects (*84*). Details regarding biogenic amines and their degradation products still need to be understood.

## 4.9 Gene duplication

Gene duplication can be defined as any duplication of a DNA region. Gene duplication can lead to species-specific gene functions, which might then facilitate species-specific adaptation (*85*). Gene duplication occurs in a large proportion of genes in eukaryotic genomes including mosquitoes (*86*). Gene duplication is also evolutionary in that some duplication of genes is more useful than others. Gene duplication that is not useful to eukaryotes eventually become pseudogenes (*87*).

**I) Evolutionary fate of duplicated genes**

**Pseudogenization and Subfunctionalization**

According to the literature, if there are two copies of one gene and one gene becomes functionless, that gene is known as a pseudogene (*88*, *89*). In contrast, when the presence of

additional genomic material is useful to an organism, both copies are retained—which is a process known as subfunctionalization. The process of subfunctionalization can occur at the mRNA level as well as at the protein level (*90*).

Homologous sequences are considered paralogous if they are separated by a gene duplication event and are typically present in the same species. In such a scenario, they may or may not have the same or even a similar function. There have been several studies investigating whether or not paralogs lead to subfunctionalization (*90, 91*). For example, it has been suggested that two isoforms of AANATs in fish and eight isoforms of AANATs in chordates may have arisen as a result of gene duplication events (*9, 92*). Moreover, there are a number of reports suggesting that several isoforms of AANATs may have arisen as a result of gene duplication events in insects. For example, in *Drosophila,* two AANAT isoforms were studied. Although they shared a similar substrate profile, it was concluded (based on their expression profile) that they may have different functions depending on their expression patterns (*13, 36*).

## 4.10 Summary

Although the last several decades have seen rapid growth in understanding the *N*-acetyltransferases in many species, their roles in mosquitoes is still not clear. Specifically, it will be important to understand the function of those AANATs which seem to have more physiological significance in insects than in mammals. Although *Drosophila* shares a close evolutionary relationship with *Ae. aegypti (93),* it is difficult to deduce the function of AANATs in *Ae. aegypti* based on the identified function in *Drosophila* (*13*). Our recent analysis of the *Ae. aegypti* genome database suggested the presence of nine paralogs of hypothetical *N*-acetyltransferases which were assumed to be the AANATs based on their conserved domains. Thus far, there is no study which sheds light on the functions of AANATs in *Ae. aegypti.* A major portion of this dissertation should provide the basis for predicting the functions of AANATs in *Ae. aegypti* as sequence analysis shows that each AANAT gene in *Ae. aegypti* studied in this dissertation forms a close relationship with AANATs in *Culex* and *Anopheles* mosquitoes, this study may also help to provide the basis for predicting functions in the other mosquito species.

## References


1. Dyda, F., Klein, D. C., and Hickman, A. B. (2000) GCN5-related *N*-acetyltransferases: a structural overview, *Annu Rev Biophys Biomol Struct 29*, 81-103.

2. Davies, J., and Wright, G. D. (1997) Bacterial resistance to aminoglycoside antibiotics, *Trends Microbiol 5*, 234-240.

3. Vetting, M. W., LP, S. d. C., Yu, M., Hegde, S. S., Magnet, S., Roderick, S. L., and Blanchard, J. S. (2005) Structure and functions of the GNAT superfamily of acetyltransferases, *Arch Biochem Biophys 433*, 212-226.

4. Angus-Hill, M. L., Dutnall, R. N., Tafrov, S. T., Sternglanz, R., and Ramakrishnan, V. (1999) Crystal structure of the histone acetyltransferase Hpa2: A tetrameric member of the GCN5-related *N*-acetyltransferase superfamily, *J Mol Biol 294*, 1311-1325.

5. Abo-Dalo, B., Ndjonka, D., Pinnen, F., Liebau, E., and Luersen, K. *(2004) A novel member of the GCN5-related N-acetyltransferase superfamily from Caenorhabditis elegans* preferentially catalyses the N-acetylation of thialysine [S-(2-aminoethyl)-L-cysteine], *Biochem J 384*, 129-137.

6. Wybenga-Groot, L. E., Draker, K., Wright, G. D., and Berghuis, A. M. (1999) Crystal structure of an aminoglycoside 6'-*N*-acetyltransferase: defining the GCN5-related *N*-acetyltransferase superfamily fold, *Structure 7*, 497-507.

7. Leslie, A. G., Moody, P. C., and Shaw, W. V. (1988) Structure of chloramphenicol acetyltransferase at 1.75-A resolution, *Proc Natl Acad Sci U S A 85*, 4133-4137.

8. Coon, S. L., Mazuruk, K., Bernard, M., Roseboom, P. H., Klein, D. C., and Rodriguez, I. R. (1996) The human serotonin *N*-acetyltransferase (EC 2.3.1.87) gene (AANAT): structure, chromosomal localization, and tissue expression, *Genomics 34*, 76-84.

9. Klein, D. C. (2007) Arylalkylamine *N*-acetyltransferase: "the Timezyme", *J Biol Chem 282*, 4233-4237.

10. Hardeland, R. (1999) Melatonin and 5-methoxytryptamine in non-metazoans, *Reprod Nutr Dev 39*, 399-408.

11. Tilden, A. R., Becker, M. A., Amma, L. L., Arciniega, J., and McGaw, A. K. (1997) Melatonin production in an aerobic photosynthetic bacterium: an evolutionarily early association with darkness, *J Pineal Res 22*, 102-106.

12. Vivien-Roels, B., Pevet, P., Beck, O., and Fevre-Montange, M. (1984) Identification of melatonin in the compound eyes of an insect, the locust (*Locusta migratoria*), by radioimmunoassay and gas chromatography-mass spectrometry, *Neurosci Lett 49*, 153-157.

13. Brodbeck, D., Amherd, R., Callaerts, P., Hintermann, E., Meyer, U. A., and Affolter, M. (1998) Molecular and biochemical characterization of the aaNAT1 (Dat) locus in *Drosophila melanogaster*: differential expression of two gene products, *DNA Cell Biol 17*, 621-633.

14. Brownell, J. E., Zhou, J., Ranalli, T., Kobayashi, R., Edmondson, D. G., Roth, S. Y., and Allis, C. D. (1996) Tetrahymena histone acetyltransferase A: a homolog to yeast Gcn5p linking histone acetylation to gene activation, *Cell 84*, 843-851.

15. Brownell, J. E., and Allis, C. D. (1996) Special HATs for special occasions: linking histone acetylation to chromatin assembly and gene activation, *Curr Opin Genet Dev 6*, 176-184.

16. Costa, Y., Galimand, M., Leclercq, R., Duval, J., and Courvalin, P. (1993) Characterization of the chromosomal aac(6')-Ii gene specific for *Enterococcus faecium*, *Antimicrob Agents Chemother 37*, 1896-1903.

17. Wright, G. D., and Ladak, P. (1997) Overexpression and characterization of the chromosomal aminoglycoside 6'-*N*-acetyltransferase from *Enterococcus faecium*, *Antimicrob Agents Chemother 41*, 956-960.

18. DiGiammarino, E. L., Draker, K. A., Wright, G. D., and Serpersu, E. H. (1998) Solution studies of isepamicin and conformational comparisons between isepamicin and butirosin A when bound to an aminoglycoside 6'-*N*-acetyltransferase determined by NMR spectroscopy, *Biochemistry 37*, 3638-3644.

19. Hickman, A. B., Namboodiri, M. A., Klein, D. C., and Dyda, F. (1999) The structural basis of ordered substrate binding by serotonin *N*-acetyltransferase: enzyme complex at 1.8 A resolution with a bisubstrate analog, *Cell 97*, 361-369.

20. Coon, S. L., and Klein, D. C. (2006) Evolution of arylalkylamine *N*-acetyltransferase: emergence and divergence, *Mol Cell Endocrinol 252*, 2-10.

21. Slominski, A., Fischer, T. W., Zmijewski, M. A., Wortsman, J., Semak, I., Zbytek, B., Slominski, R. M., and Tobin, D. J. (2005) On the role of melatonin in skin physiology and pathology, *Endocrine 27*, 137-148.

22. Bolliet, V., Begay, V., Taragnat, C., Ravault, J. P., Collin, J. P., and Falcon, J. (1997) Photoreceptor cells of the pike pineal organ as cellular circadian oscillators, *Eur J Neurosci 9*, 643-653.

23. Natesan, A., Geetha, L., and Zatz, M. (2002) Rhythm and soul in the avian pineal, *Cell Tissue Res 309*, 35-45.

24. Goldman, B. D. (2001) Mammalian photoperiodic system: formal properties and neuroendocrine mechanisms of photoperiodic time measurement, *J Biol Rhythms 16*, 283-301.

25. Coon, S. L., Roseboom, P. H., Baler, R., Weller, J. L., Namboodiri, M. A., Koonin, E. V., and Klein, D. C. (1995) Pineal serotonin *N*-acetyltransferase: expression cloning and molecular analysis, *Science 270*, 1681-1683.

26. Hohjoh, H., Takasu, M., Shishikura, K., Takahashi, Y., Honda, Y., and Tokunaga, K. (2003) Significant association of the arylalkylamine *N*-acetyltransferase ( AA-NAT) gene with delayed sleep phase syndrome, *Neurogenetics 4*, 151-153.

27. Slominski, A., Pisarchik, A., Semak, I., Sweatman, T., Wortsman, J., Szczesniewski, A., Slugocki, G., McNulty, J., Kauser, S., Tobin, D. J., Jing, C., and Johansson, O. (2002) Serotoninergic and melatoninergic systems are fully expressed in human skin, *FASEB J 16*, 896-898.

28. Liu, C., Fukuhara, C., Wessel, J. H., 3rd, Iuvone, P. M., and Tosini, G. (2004) Localization of Aa-nat mRNA in the rat retina by fluorescence in situ hybridization and laser capture microdissection, *Cell Tissue Res 315*, 197-201.

29. Tachibana, T., Taniguchi, S., Furukawa, F., Miwa, S., and Imamura, S. (1990) Serotonin metabolism in the arthus reaction, *J Invest Dermatol 94*, 120-125.

30. Wolf, E., De Angelis, J., Khalil, E. M., Cole, P. A., and Burley, S. K. (2002) X-ray crystallographic studies of serotonin *N*-acetyltransferase catalysis and inhibition, *J Mol Biol 317*, 215-224.

31. Namboodiri, M. A., Dubbels, R., and Klein, D. C. (1987) Arylalkylamine *N*-acetyltransferase from mammalian pineal gland, *Methods Enzymol 142*, 583-590.

32. Pavlicek, J., Sauzet, S., Besseau, L., Coon, S. L., Weller, J. L., Boeuf, G., Gaildrat, P., Omelchenko, M. V., Koonin, E. V., Falcon, J., and Klein, D. C. (2010) Evolution of AANAT: expansion of the gene family in the cephalochordate amphioxus, *BMC Evol Biol 10*, 154.

33. Begay, V., Falcon, J., Cahill, G. M., Klein, D. C., and Coon, S. L. (1998) Transcripts encoding two melatonin synthesis enzymes in the teleost pineal organ: circadian regulation in pike and zebrafish, but not in trout, *Endocrinology 139*, 905-912.

34. Coon, S. L., Begay, V., Deurloo, D., Falcon, J., and Klein, D. C. (1999) Two arylalkylamine *N*-acetyltransferase genes mediate melatonin synthesis in fish, *J Biol Chem 274*, 9076-9082.

35. Zilberman-Peled, B., Ron, B., Gross, A., Finberg, J. P., and Gothilf, Y. (2006) A possible new role for fish retinal serotonin-*N*-acetyltransferase-1 (AANAT1): Dopamine metabolism, *Brain Res 1073-1074*, 220-228.

36. Amherd, R., Hintermann, E., Walz, D., Affolter, M., and Meyer, U. A. (2000) Purification, cloning, and characterization of a second arylalkylamine *N*-acetyltransferase from *Drosophila melanogaster*, *DNA Cell Biol 19*, 697-705.

37. Klein, D. C., Coon, S. L., Roseboom, P. H., Weller, J. L., Bernard, M., Gastel, J. A., Zatz, M., Iuvone, P. M., Rodriguez, I. R., Begay, V., Falcon, J., Cahill, G. M., Cassone, V. M., and Baler, R. (1997) The melatonin rhythm-generating enzyme: molecular regulation of serotonin *N*-acetyltransferase in the pineal gland, *Recent Prog Horm Res 52*, 307-357; discussion 357-308.

38. Klein, D. C. (1985) Photoneural regulation of the mammalian pineal gland, *Ciba Found Symp 117*, 38-56.

39. Iuvone, P. M., Tosini, G., Pozdeyev, N., Haque, R., Klein, D. C., and Chaurasia, S. S. (2005) Circadian clocks, clock networks, arylalkylamine *N*-acetyltransferase, and melatonin in the retina, *Prog Retin Eye Res 24*, 433-456.

40. Kennaway, D. J., Voultsios, A., Varcoe, T. J., and Moyer, R. W. (2003) Melatonin and activity rhythm responses to light pulses in mice with the Clock mutation, *Am J Physiol Regul Integr Comp Physiol 284*, R1231-1240.

41. Ribelayga, C., Pevet, P., and Simonneaux, V. (2000) HIOMT drives the photoperiodic changes in the amplitude of the melatonin peak of the Siberian hamster, *Am J Physiol Regul Integr Comp Physiol 278*, R1339-1345.

42. Natesan, A. K., and Cassone, V. M. (2002) Melatonin receptor mRNA localization and rhythmicity in the retina of the domestic chick, *Gallus domesticus*, *Vis Neurosci 19*, 265-274.

43. Smith, T. J. (1990) Phylogenetic distribution and function of arylalkylamine *N*-acetyltransferase, *Bioessays 12*, 30-33.

44. Dai, F. Y., Qiao, L., Tong, X. L., Cao, C., Chen, P., Chen, J., Lu, C., and Xiang, Z. H. (2010) Mutations of an arylalkylamine-n-acetyl transferase, BM-IAANAT, are responsible for the silkworm melanism mutant, *J Biol Chem*.

45. Zhan, S., Guo, Q., Li, M., Li, J., Miao, X., and Huang, Y. (2010) Disruption of an *N*-acetyltransferase gene in the silkworm reveals a novel role in pigmentation, *Development 137*, 4083-4090.

46. Dennell, R. (1958) The amino acid metabolism of a developing insect cuticle: the larval cuticle and puparium of *Calliphora vomitoria*. III. The formation of the puparium, *Proc R Soc Lond B Biol Sci 149*, 176-183.

47. Andersen, S. O., Hojrup, P., and Roepstorff, P. (1995) Insect cuticular proteins, *Insect Biochem Mol Biol 25*, 153-176.

48. Andersen, S. O. (2010) Insect cuticular sclerotization: a review, *Insect Biochem Mol Biol 40*, 166-178.

49. Sekeris, C. E., and Karlson, P. (1962) [on tyrosine metabolism by insects. VII. The catabolic decomposition of tyrosine and the biogenesis of the sclerotizing substance, *N*-acetyldopamine.], *Biochim Biophys Acta 62*, 103-113.

50. Hopkins, T. L., Morgan, T. D., Aso, Y., and Kramer, K. J. (1982) *N*-beta-Alanyldopamine: Major Role in Insect Cuticle Tanning, *Science 217*, 364-366.

51. Suderman, R. J., Dittmer, N. T., Kanost, M. R., and Kramer, K. J. (2006) Model reactions for insect cuticle sclerotization: cross-linking of recombinant cuticular proteins upon their laccase-catalyzed oxidative conjugation with catechols, *Insect Biochem Mol Biol 36*, 353-365.

52. Perez, M., Wappner, P., and Quesada-Allue, L. A. (2002) Catecholamine-beta-alanyl ligase in the medfly Ceratitis capitata, *Insect Biochem Mol Biol 32*, 617-625.

53. Wu, Q., Gu, X., Wang, Y., Li, N., Liu, X., Wu, C., and Yu, L. (2006) Neurotransmitter inactivation is important for the origin of nerve system in animal early evolution: a suggestion from genomic comparison, *Prog Neurobiol 78*, 390-395.

54. Meyer, J. H., Ginovart, N., Boovariwala, A., Sagrati, S., Hussey, D., Garcia, A., Young, T., Praschak-Rieder, N., Wilson, A. A., and Houle, S. (2006) Elevated monoamine oxidase a levels in the brain: an explanation for the monoamine imbalance of major depression, *Arch Gen Psychiatry 63*, 1209-1216.

55. Saul, S. J., and Sugumaran, M. (1989) *N*-acetyldopamine quinone methide/1,2-dehydro-*N*-acetyldopamine tautomerase. A new enzyme involved in sclerotization of insect cuticle, *FEBS Lett 255*, 340-344.

56. Hintermann, E., Grieder, N. C., Amherd, R., Brodbeck, D., and Meyer, U. A. (1996) Cloning of an arylalkylamine *N*-acetyltransferase (aaNAT1) from *Drosophila melanogaster* expressed in the nervous system and the gut, *Proc Natl Acad Sci U S A 93*, 12315-12320.

57. Itoh, M. T., Nomura, T., and Sumi, Y. (1997) Hydroxyindole-*O*-methyltransferase activity in the silkworm (*Bombyx mori*), *Brain Res 765*, 61-66.

58. Saunders, D. S. (1997) Insect circadian rhythms and photoperiodism, *Invert Neurosci 3*, 155-164.

59. Wikelski, M., Martin, L. B., Scheuerlein, A., Robinson, M. T., Robinson, N. D., Helm, B., Hau, M., and Gwinner, E. (2008) Avian circannual clocks: adaptive significance and possible involvement of energy turnover in their proximate control, *Philos Trans R Soc Lond B Biol Sci 363*, 411-423.

60. Cabrera, M., and Jaffe, K. (2007) An aggregation pheromone modulates lekking behavior in the vector mosquito *Aedes aegypti* (Diptera: Culicidae), *J Am Mosq Control Assoc 23*, 1-10.

61. Saunders, D. S. (2010) Controversial aspects of photoperiodism in insects and mites, *J Insect Physiol 56*, 1491-1502.

62. Das, S., and Dimopoulos, G. (2008) Molecular analysis of photic inhibition of blood-feeding in *Anopheles gambiae*, *BMC Physiol 8*, 23.

63. Siju, K. P., Hansson, B. S., and Ignell, R. (2008) Immunocytochemical localization of serotonin in the central and peripheral chemosensory system of mosquitoes, *Arthropod Struct Dev 37*, 248-259.

64. Siju, K. P. (2009) Neuromodulation in the chemosensory system of mosquitoes - neuroanatomy and physiology, In *Dept. Plant Protection Biology*, pp 1-68.

65. Kokoza, V., Ahmed, A., Cho, W. L., Jasinskiene, N., James, A. A., and Raikhel, A. (2000) Engineering blood meal-activated systemic immunity in the yellow fever mosquito, *Aedes aegypti*, *Proc Natl Acad Sci U S A 97*, 9144-9149.

66. Womack, M. L. (1993) Distribution, abundance and bionomics of *Aedes albopictus* in southern Texas, *J Am Mosq Control Assoc 9*, 367-369.

67. Clemons, A., Haugen, M., Flannery, E., Tomchaney, M., Kast, K., Jacowski, C., Le, C., Mori, A., Simanton Holland, W., Sarro, J., Severson, D. W., and Duman-Scheel, M. (2010) *Aedes aegypti:* an emerging model for vector mosquito development, *Cold Spring Harb Protoc 2010*, pdb emo141.

68. Severson, D. W., Brown, S. E., and Knudson, D. L. (2001) Genetic and physical mapping in mosquitoes: molecular approaches, *Annu Rev Entomol 46*, 183-219.

69. Severson, D. W., Knudson, D. L., Soares, M. B., and Loftus, B. J. (2004) *Aedes aegypti* genomics, *Insect Biochem Mol Biol 34*, 715-721.

70. Foster, W. A. (1995) Mosquito sugar feeding and reproductive energetics, *Annu Rev Entomol 40*, 443-474.

71. Takken, W., and Knols, B. G. (1999) Odor-mediated behavior of Afrotropical malaria mosquitoes, *Annu Rev Entomol 44*, 131-157.

72. Brown, M. R., Clark, K. D., Gulia, M., Zhao, Z., Garczynski, S. F., Crim, J. W., Suderman, R. J., and Strand, M. R. (2008) An insulin-like peptide regulates egg maturation and metabolism in the mosquito *Aedes aegypti*, *Proc Natl Acad Sci U S A 105*, 5716-5721.

73. Bowen, M. F., and Davis, E. E. (1989) The effects of allatectomy and juvenile hormone replacement on the development of host-seeking behaviour and lactic acid receptor sensitivity in the mosquito *Aedes aegypt*i, *Med Vet Entomol 3*, 53-60.

74. Bosch, O. J., Geier, M., and Boeckh, J. (2000) Contribution of fatty acids to olfactory host finding of female *Aedes aegypti*, *Chem Senses 25*, 323-330.

75. Steib, B. M., Geier, M., and Boeckh, J. (2001) The effect of lactic acid on odour-related host preference of yellow fever mosquitoes, *Chem Senses 26*, 523-528.

76. Ponlawat, A., and Harrington, L. C. (2005) Blood feeding patterns of *Aedes aegypti* and *Aedes albopictus* in Thailand, *J Med Entomol 42*, 844-849.

77. Ghaninia, M., Larsson, M., Hansson, B. S., and Ignell, R. (2008) Natural odor ligands for olfactory receptor neurons of the female mosquito *Aedes aegypti*: use of gas chromatography-linked single sensillum recordings, *J Exp Biol 211*, 3020-3027.

78. Bernier, U. R., Kline, D. L., Allan, S. A., and Barnard, D. R. (2007) Laboratory comparison of *Aedes aegypti* attraction to human odors and to synthetic human odor compounds and blends, *J Am Mosq Control Assoc 23*, 288-293.

79. Geier, M., Bosch, O. J., and Boeckh, J. (1999) Ammonia as an attractive component of host odour for the yellow fever mosquito, *Aedes aegypti*, *Chem Senses 24*, 647-653.

80. McCrae, A. W. (1983) Oviposition by African malaria vector mosquitoes. I. Temporal activity patterns of caged, wild-caught, freshwater *Anopheles gambiae* Giles sensu lato, *Ann Trop Med Parasitol 77*, 615-625.

81. Fahrbach, S. E., and Mesce, K. A. (2005) "Neuroethoendocrinology": integration of field and laboratory studies in insect neuroendocrinology, *Horm Behav 48*, 352-359.

82. Monastirioti, M. (1999) Biogenic amine systems in the fruit fly *Drosophila melanogaster*, *Microsc Res Tech 45*, 106-121.

83. Sasaki, K., Yamasaki, K., and Nagao, T. (2007) Neuro-endocrine correlates of ovarian development and egg-laying behaviors in the primitively eusocial wasp (*Polistes chinensis*), *J Insect Physiol 53*, 940-949.

84. Yamane, T., and Miyatake, T. (2010) Reduced female mating receptivity and activation of oviposition in two Callosobruchus species due to injection of biogenic amines, *J Insect Physiol 56*, 271-276.

85. Carbone, I., Ramirez-Prado, J. H., Jakobek, J. L., and Horn, B. W. (2007) Gene duplication, modularity and adaptation in the evolution of the aflatoxin gene cluster, *BMC Evol Biol 7*, 111.

86. Sankoff, D. (2001) Gene and genome duplication, *Curr Opin Genet Dev 11*, 681-684.

87. Kondrashov, F. A., Rogozin, I. B., Wolf, Y. I., and Koonin, E. V. (2002) Selection in the evolution of gene duplications, *Genome Biol 3*, RESEARCH0008.

88. Lynch, M., O'Hely, M., Walsh, B., and Force, A. (2001) The probability of preservation of a newly arisen gene duplicate, *Genetics 159*, 1789-1804.

89. Harrison, P. M., Hegyi, H., Balasubramanian, S., Luscombe, N. M., Bertone, P., Echols, N., Johnson, T., and Gerstein, M. (2002) Molecular fossils in the human genome: identification and analysis of the pseudogenes in chromosomes 21 and 22, *Genome Res 12*, 272-280.

90. MacCarthy, T., and Bergman, A. (2007) The limits of subfunctionalization, *BMC Evol Biol 7*, 213.

91. Fleisch, V. C., Schonthaler, H. B., von Lintig, J., and Neuhauss, S. C. (2008) Subfunctionalization of a retinoid-binding protein provides evidence for two parallel visual cycles in the cone-dominant zebrafish retina, *J Neurosci 28*, 8208-8216.

92. Innan, H., and Kondrashov, F. (2010) The evolution of gene duplications: classifying and distinguishing between models, *Nat Rev Genet 11*, 97-108.

93. Severson, D. W., DeBruyn, B., Lovin, D. D., Brown, S. E., Knudson, D. L., and Morlais, I. (2004) Comparative genome analysis of the yellow fever mosquito *Aedes aegypti* with *Drosophila melanogaster* and the malaria vector mosquito *Anopheles gambiae*, *J Hered 95*, 103-113.

# Chapter 5. Same Name, Different Game: an Insight into the Hypothetical *N*-Acetyltransferases in *Aedes aegypti*

Prajwalini Mehere, Haizhen Ding, Jianyong Li

As first author I designed and performed experiments and prepared the figures and the manuscript. Haizhen Ding did all cloning and protein expression

.

## 5.1 Abstract

This study involved the molecular and biochemical characterizations of the *Aedes aegypti* arylalkylamine *N*-acetyltransferase (AANAT) family. A BLAST search of the *Ae. aegypti* genome using an activity-verified *Drosophila* AANAT enlisted nine putative AANAT sequences sharing 13-52% sequence identity with the *Drosophila* enzyme. Although these *Ae. aegypti* sequences contain recognizable similarities with the *Drosophila* enzyme, they share very low sequence similarity with AANAT sequences from non-insect species. Moreover, for most of these mosquito sequences, the level of their sequence identity to the activity-verified *Drosophila* enzyme was inadequate for predicting them as AANAT. mRNA amplification confirmed that eight of the nine putative AANATs are transcribed in *Ae. aegypti*. Their corresponding recombinant proteins were expressed using a bacterial expression system. Screening of purified recombinant proteins against dopamine, octopamine, tyramine, tryptophan, 5-hydroxytryptamine, and methoxytryptamine established that five of the eight recombinant proteins are active at least to one of the tested arylalkylamines (with two of them active to all tested arylalkylamines). Analysis of the transcriptional profiles of both the five confirmed AANATs and the three unconfirmed AANATs revealed that some are expressed during larval and pupae stages, and some are expressed in adult stages (especially in the adult head). Some are either up- or down-regulated in the adult female tissues after blood feeding. Based on their substrate specificity and expression profiles during development, we suggest that AANATs play diverse roles in the *Ae. aegypti*, including sclerotization, neurotransmitter inactivation, and regulation of the reproductive cycle. In conclusion, our data provide an important base towards achieving a comprehensive understanding of the biochemistry and physiology of AANAT from the *Ae. aegypti* species, as well as a useful reference for studying the AANAT family of proteins from other species.

## 5.2 Introduction

Proteins that catalyze the transacetylation of acetyl coenzyme A (AcCoA) to arylamines and arylalkylamines are commonly referred to as arylamine *N*-acetyltransferases (ANAT) and arylalkylamine *N*-acetyltransferases (AANAT), respectively (*1*). In mammals, AANAT is primarily involved in the synthesis of *N*-acetylserotonin. The *N*-acetylation of serotonin (5-hydroxytryptamine) is a rate-limiting step for the synthesis of melatonin in the pineal gland. Additionally, in the pineal gland AANAT is transcriptionally regulated in a manner that reflects daily physiological requirements for the release of melatonin (*2, 3*). Because the concentrations of melatonin coincide with internal biological clock, mammalian AANAT ultimately regulates circadian rhythm and is considered one of the circadian proteins (*2, 3*). Although the function of mammalian AANAT is well established, the roles of AANAT proteins in many other species remains unclear.

It has been indicated that invertebrate AANATs play a role in the inactivation of arylalkylamines (*4, 5*). Arylalkylamines, such as octopamine, dopamine, and serotonin function as key neurotransmitters, and the levels of these compounds need to be regulated in order to prevent neurotoxicity and prolonged signaling. In mammals, excessive dopamine or other aromatic amines are inactivated by monoamine oxidases (MAO) (*6*). This may be true in other vertebrate species. A database search of currently available invertebrate genome sequences indicates that MAO homologs are absent from invertebrates (*7*). This provides a basis for the argument that invertebrate AANATs may play a role in preventing the over-accumulation of some neurotransmitters.

According to a review by Smith, AANATs are involved in cuticle sclerotization, aromatic neurotransmitter inactivation, and melatonin synthesis in insects (*8*). Based on the physiological requirements of insects, all proposed physiological functions regarding insect AANATs are reasonable predictions. AANAT proteins have been studied in *Drosophila melanogaster* (*5, 9*) and *Periplaneta americana* (*10, 11*), but the precise functions of these insect AANAT sequences remain to be substantiated. However, a recent study dealing with an AANAT from *Bombyx mori* clearly established its function in adult cuticle sclerotization through the production of *N*-acetyldopamine (NADA), a key cuticle protein crosslinking precursor (*12*).

The available genome sequences for a number of insect species make it possible to predict AANAT sequences via a bioinfomatical approach. A genome-wide search using the Basic Local Alignment Search Tool (BLAST) with the activity-verified *Drosophila melanogaster* AANAT against individual available insect genome sequences (including *Drosophila melanogaster*, *Aedes aegypti*, *Anopheles gambiae*, *Culex pipience*, and *Tribolium castaneum*) revealed from each species 4-10 sequences showing recognizable similarity, suggesting the presence of an AANAT family in insects. Sequence comparison also revealed that most of the putative AANAT sequences from the same species often share recognizable, but limited sequence identity (10-30%) in a given species. Moreover, most of the individual AANATs from one species also share limited sequence identity with orthologues in other species For example, most of the predicted *Ae. aegypti* AANATs share about 20% sequence identity with *Drosophila* AANATs. Given the low sequence identity between the insect AANATs it is difficult to predict the function of given AANAT sequences in one species based on a functionally verified AANAT protein from a distant insect species. Consequently, it is necessary to study the AANAT family from a number of individual insect species that are evolutionarily distant before reaching some general conclusions regarding the overall physiological functions of insect AANATs.

Although it is difficult to predict the counterpart AANATs across evolutionarily distinct species, the same type of AANAT enzymes can be determined through sequence alignment in evolutionarily close species. For example, among the putative AANAT sequences from different mosquito species, counterpart enzymes can be identified through sequence alignment (Figure 5.1). As a result, substrate specificity and biochemical function, identified for a given AANAT from one mosquito species, can be applied to the counterpart enzyme from other mosquito species.

Using *Ae. aegypti* as a model species in this study, we evaluated the expression profiles of the putative *Ae. aegypti* AANAT (AeAANAT) sequences, expressed their recombinant proteins in a bacterial protein expression system, and screened the substrate specificity for each of the expressed recombinant proteins. We achieved the over-expression of eight recombinant proteins out of the nine putative AeAANATs and substrate screening resulted in the verification of true AeAANAT identity for five of nine predicted AANAT proteins. Our data offer some basis to suggest the possible functions for several AANAT proteins and provide a foundation for

elucidating the specific function for each AeAANAT protein. Our data also provide a useful reference for studying AANAT proteins from other mosquito species and comparing AANAT families from other insect species.

## 5.3 Materials and Methods

**Identification of the hypothetical *N*-acetyltransferase in *Aedes aegypti***

A protein–specific BLAST search combined with a Position-Specific Iterated BLAST (PSI BLAST) search (*13*) using *Drosophila* AANAT (NP_995934) revealed nine GCN (General control of amino acids)-5-*N*-acetyltransferase family members from *Ae. aegypti* mosquito (Figure 5.1 and Table 5.1). These proteins were listed as hypothetical proteins in the database. Based on the peculiar conserved domains present in these proteins, we were able to predict them as putative AANATs. Table 5.1 lists essential information for the putative AeAANATs studied herein including GeneBank accession numbers, description, chromosomal location, strand direction, start and end in the genome, amount of exons, transcript length, and translation length (*13*).

**Sequence similarity search and phylogenetic analysis of AANAT homologs in different species**

In order to identify AANAT homologs from different species a search of the non-redundant database of protein sequences using the BLAST and PSI-BLAST search features (National Center for Biotechnology Information [NCBI] http://www.ncbi.nlm.nih.gov) was conducted. Representatives from various groups including insects, bacteria, fungi, and animals were selected and a multiple sequence alignment of the respective protein sequences was constructed using the MEGA4-ClustalW alignment program (*14*). A maximum likelihood phylogenetic tree was constructed using the neighbor joining method and bootstrap analysis (*14*).

**Expression and purification of hypothetical recombinant *N*-acetyltransferase members**

Amplification of cDNA for hypothetical AeAANATs was achieved using the forward and reverse primers corresponding to 5'- and 3'- regions of the coding sequences of AeAANATs (Table 5.2). Their amplified cDNA sequences were cloned into an Impact™-CN plasmid (pTBY12 vector) (New England Biolabs) for expression of fusion proteins containing a chitin binding domain. The AeAANATs were produced as recombinant fusion proteins using the N-terminal tag. This tag enabled purification of the AeAANATs by chitin binding affinity

purification. Transformed *E. coli* cells were cultured at 37 °C. After induction with 0.1 mM isopropyl-1-thio-β-D-galactopyranoside (IPTG), the cells were cultured at 15 °C for 48 hours. Four to 20 liters (depending upon the level of the expressed recombinant protein) of cell cultures were harvested as the starting material for affinity purification. The cells were lysed by sonication on ice in a lysis buffer containing 50 mM Tris-HCl [pH 8.0], 500 mM NaCl, and 1 mM EDTA. The resulting mixture was first incubated for an hour at 4 ºC and then centrifuged for 30 minutes at 37,500 x *g*. The supernatant was applied to a chitin bead column that had been equilibrated using the lysis buffer. The column was washed extensively with the lysis buffer (at least 10 volumes of the bed volume). The column with associated recombinant protein was equilibrated with the hydrolysis buffer containing 50 mM tris (pH 8.0) and 50 mM β-mercaptoethanol and incubated for 24 hours at 4 $^{o}$C. The protein was eluted using 20 mM 4-(2-hydroxyethyl)-1-piperazineethanesulfonate (HEPES) buffer (pH 7.5) and concentrated using a membrane concentrator with a molecular weight cutoff at 10,000 kDa (Millipore Corp). The concentrated protein samples were further purified by ion exchange (Mono-Q column, GE Health) and gel-filtration (Superose 12 column, GE Health) chromatographies. Protein concentration was determined by Bradford assay (Bradford 1976) using bovine serum albumine as a standard, and the purity of the AeAANATs was ascertained and assessed by the presence of a single band between 25 kDa and 30 kDa on an SDS-PAGE gel.

**Table 5.1 Conserved hypothetical proteins found in *Ae. aegypti* genome as a result of a BLAST search using the *Drosophila* NP_995934 sequence**.

| Gene | Gene ID | Chromosomal (supercontig) Location | Start | End | Exons | Transcript Length (bp) | Translation Length (a.a) |
|---|---|---|---|---|---|---|---|
| AeAANAT1 | AaeL_AAEL011088 | Supercont1.540 contig_20023 | 459,031 | 509,488 | 5 | 1821 | 288 |
| AeAANAT2 | AaeL_AAEL012952 | Supercont1.766 contig_24253 | 154,320 | 167,075 | 4 | 1246 | 222 |
| AeAANAT3 | AaeL_AAEL004847 | Supercont1.132 contig_7562 | 1,935,510 | 1,936,184. | 1 | 675 | 224 |
| AeAANAT4 | AaeL_AAEL002255 | Supercont1.52 contig_3460. | 1,754,718 | 1,755380 | 1 | 663 | 220 |
| AeAANAT5 | AaeL_AAEL004827 | Supercont1.132 contig_7562 | 1,997,239 | 1,998,124 | 1 | 886 | 217 |
| AeAANAT6 | AaeL_AAEL012866 | Supercont1.752 contig_24066 | 209,570- | 210,139 | 1 | 558 | 168 |
| AeAANAT7 | AaeL_AAEL012870 | Supercont1.752 contig_24070. | 362,533 | 363,312. | 2 | 717 | 238 |
| AeAANAT8 | AaeL_AAEL012864 | Supercont1.752 contig_24072. | 384,934 | 386,013 | 3 | 943 | 240 |
| AeAANAT9 | AaeL_AAEL012860 | Supercont1.752 Contig_24066. | 227,851 | 247,030 | 3 | 1008 | 238 |

**Assay of hypothetical *N*-acetyltransferase (AANAT activity assay) and substrate profile**

To determine the activity and substrate specificity of various exogenous substrates *in vitro*, each of the purified recombinant proteins (10 μg) was mixed with acetyl-CoA (AcCoA at a final concentration of 1 mM) and each of the selected arylalkylamines (dopamine, octopamine, tyramine, tryptamine, methoxytryptamine, or 5-hydroxytryptamine at a final concentration of 5 mM) in a total volume of 100 μL prepared in 50 mM HEPES buffer (pH 7.5). All the substrates were prepared fresh to avoid oxidation of the monoamines. The reaction mixtures were incubated for 10 minutes at 37 °C and the reaction was stopped by addition of an equal volume of 800 mM formic acid. The acidified reaction mixtures were centrifuged for 10 minutes at 15,000 x g at 4 $^{o}$C. Supernatants were chromatographed by HPLC with a reverse-phase column (C18 of 5 μm particles, 4.6 X 1100 mm) and resolved substrate and product by reverse-phase HPLC with electrochemical detection.

**Kinetic analysis of AANAT1 and AANAT2 to dopamine and 5-hydroxytryptamine (serotonin)**

An initial analysis indicated that AANAT1 and AANAT2 were highly active to dopamine and 5-hydroxytryptamine. To have a linear range for a five min period of incubation, both enzymes had to be diluted to no more than 2 μg per ml in the final reaction mixture. To stabilize AANAT1 and AANAT2, they were diluted to 5 μg per ml enzyme stock using 1 mg BSA prepared in 50 mM phosphate buffer. An initial evaluation of AcCoA on enzyme activity also indicated that when AcCoA was at 0.8 mM or above, no further increase in activity rate was observed. To test the affinity of AANAT1 and AANAT2 to dopamine and 5-hydroxytryptamine, the rate of enzyme activity was determined at 1 mM final concentration of AcCoA in the presence of varying concentration of dopamine and 5-hydroxytryptamine. Briefly, reaction mixtures of 100 μl, containing 20 μL of enzyme stock (or 0.1 μg enzyme), 1 mM AcCoA and varying concentrations of dopamine or 5-hydroxytryptamine (25 μM to 6.4 mM), were incubated for 4 min at 25 $^{o}$C and the reaction was stopped by adding an equal volume of 0.8 M formic acid into the reaction mixture. The acidified reaction mixtures were centrifuged for 10 min at 4 $^{o}$C and supernatants were analyzed by reverse phase HPLC with electrochemical detection (HPLC-ED). The amounts of acetyldopamine or acetylated 5-hydroxytryptamine formed in the reaction mixtures were quantitated based on a standard curve of authentic acetyldopamine or acetylated 5-hydroxytryptamine generated under identical assay conditions. The data were fitted to

Michaelis–Menten equation. Estimation of apparent $K_m$ values was obtained by e SigmaPlot Enzyme Kinetics Module (SPSS, San Jose, CA).

**Expression profiling of AeAANATs based on real-time PCR**

**Rearing of mosquitoes and tissue collection**

*Ae*. *aegypti* mosquitoes were reared at 27 °C with 75% relative humidity and maintained in the insectary of the Department of Biochemistry at Virginia Tech. Generation time was about 2-3 weeks under these conditions. Larvae and pupae were collected and processed on the same day. Adults used were dissected after 5-6 days of post-emergence. These tissues were dissected on ice from live mosquitoes that were kept at 4 °C for 10 minutes. Female mosquitoes were blood-fed for approximately 20 minutes and ovaries were dissected 12, 24, 36, 48, 60, and 72 hours after blood-feeding. The tissues such as head, abdomen (rest of the body besides head, thorax and ovaries) and thorax were collected 48 hours before and after blood feeding.

**RNA extraction and cDNA synthesis of AeAANATs**

Total RNA extraction was carried out following the manufacturer's protocol using mirVana kit (Ambion). Tissue samples in microcentrifuge tubes were disrupted in a lysis/binding buffer at 10 to 1 ratio between lysis buffer and tissue mass (for example, 1 ml lysis binding buffer was used for 0.1 g of tissue) and were placed into a homogenization vessel on ice. Homogenization of tissues was conducted using digital benchtop homogenizers (PRO Scientific Inc). One-tenth volume of miRNA homogenate additive (Ambion. Inc) was added to the lysate, and the mixture was incubated on ice for 10-30 min (For example, a lysate volume of 270 µL was added to 30 µL of homogenate additive). The samples were extracted with acidifies-phenol: chloroform equal to the initial lysate volume. Samples were then centrifuged for 10 minutes at 14000 g in an Eppendorf centrifuge (Beckman coulter TM) at room temperature to separate the aqueous and organic phase. After centrifugation, the aqueous phase was removed without disturbing the lower organic phase and applied to the normal phase columns (Ambion. Inc). The columns were washed twice with approximately 70% ethanol and 30% gaunidinium thiocyanate. Further, RNA was eluted with nuclease free water, which was heated at 95 ºC prior to elution of RNA. The concentration of the RNA samples in water was evaluated using NanoDrop Spectrophotometer (Nanodrop Technology). The purity of the total RNA was assessed using the $A_{260/280}$ and $A_{260/230}$ ratios given by NanoDrop.

**cDNA synthesis**

The cDNA synthesis was done following the manufacturer's protocol (SuperScript® III First-Strand Synthesis System, Invitrogen) for all the samples. 1 µM of oligo(dT)20-mer, and 10 mM of dNTP mix were mixed with 5 µg of total RNA in nuclease free water. The mixture was incubated at 65 °C for 5 minutes and then immediately placed on ice. Following to that, 10 µl cDNA synthesis mix (Invitrogen) containing 25 mM $MgCl_2$, 0.1 M DTT, 40 U (1 µL) of RNAse OUT $^{TM}$, and 200 U (1 µL) of Superscript® III RT were added to the RNA sample and the volume was adjusted to a total volume of 20 µL with diethylpyrocarbonate (DEPC)-treated distilled water. The sample was incubated at 50 °C for 50 minutes and the temperature was increased at 85 °C to stop the reaction by denaturing reverse transcriptase. The RNA templates were digested by RNase H at 37 °C for 20 minutes. The cDNA was diluted (1: 5) before the real-time quantitative polymerase chain reaction (qRT)-PCR and stored at -20 ºC until used.

**Expression profiles of putative AeAANATs using quantitative real–time PCR**

QRT-PCR was performed in a Real-Time PCR Detection System (Applied biosystem (ABI) 7300, Foster city, CA, USA) using SYBR Green, QPCR master mix (Platinum SYBR Green qPCR master mix, Invitrogen) in a 96 well format. Each pair of PCR primer pairs for AeAANATs (Table 5. 3) were designed to span a cDNA exon-exon or intron-exon gene wherever possible and amplify 202 bp individual AeAANAT fragments from cDNA. Primer pair that amplifies a 202 bp fragment of *Ae. aegypti rpS7* gene, a relatively abundant constitutively expressed gene, was used to normalize the results of variable target genes and to correct for sample-to-sample variations. The thermocycler program was conducted using these sequence combinations: an initial phase of 50 ºC for 2 min, 95 °C for 10 min, followed by a 40 cycles, with each cycle consisting of DNA denaturation at 95 °C for 15 sec each, and annealing or extension at 52-54 ºC for 1 min. SYBR green assays were carried out in parallel for the control *rpS7* gene. All test samples and the controls were performed in triplicate. For every sample, an amplification plot was generated showing the reporter dye fluorescence (ΔRn) at each PCR cycle. A threshold cycle (CT) was determined for each amplification cycle, representing the cycle number at which the fluorescence passes the threshold. This was the method by which the CT values of AeAANAT1, AeAANAT2, AeAANAT3, AeAANAT4, AeAANAT7, AeAANAT8, and AeAANAT9, as well as for the control gene (*Ae-rpS7*), were determined. The

CT value of the control gene was then subtracted from the CT value of the AANAT genes. Finally, $2^{-\Delta\Delta CT}$ values were calculated to estimate the fold changes in the mRNA levels of AeAANATs in different samples. For comparison of initial developmental stages first instar larvae was used as calibrator and for developmental stages 48 hours non-blood fed ovaries were used as calibrator. The controls, without reverse transcriptase, showed CT values of 40, indicating no amplification of product. The interpretation of the results for expression pattern is based on two trials.

**Table 5.2 Primers for the recombinant protein expression.**
Restriction enzyme sites used for the cloning are underlined (CATATG= NdeI, GAATTC= EcoRI, CTCGAG= XhoI)

| **Genes** | **Cloning primers** |
|---|---|
| AeAANAT1 | F-5' CATATGGCTTCGAAGATGTCGACCGTT 3'<br>R-5' GAATTCAGGCCAGTCTTTTTGTTAGAATAC 3' |
| AeAANAT2 | F-5' CATATGTTGGACAGCAAGCTCAACAAC 3'<br>R-5' GAATTCAGTTGATCACTTTGCACATAATTTT 3' |
| AeAANAT3 | F-5' CATATGGAAGAGTCAACCTCTCGTAA 3'<br>R-5' GAATTCATACAATCAATAGTTTAACAA 3' |
| AeAANAT4 | F-5' CATATGGGAGCCACGCCGTTGA 3'<br>R-5' GAATTCATTGCAATATCTTAACCATCC 3' |
| AeAANAT5 | F-5'GAATTCTCAGCAGTTTAACACATGT 3'<br>R-5'CATATGGTCGCCCCCGAAAGCAT 3' |
| AeAANAT7 | F-5' CATATGAAATGGACAAGGTCGGTG 3'<br>R-5'GAATTCAATCAACTCTCAAGCTCATA 3' |
| AeAANAT8 | F- 5'CATATGGGTTGGCAAAGACCTTC 3'<br>R-5' GAATTCATTCGATTATCAGACTCATCA 3' |
| AeAANAT9 | F-5' CATATGGTTTGGACGCGACC 3'<br>R-5' CTCGAGTTATTCGACTTTCAAGCTCAT 3' |

**Table 5.3 Primers for the gene expression analysis.**

| Genes | Forward Primer | Reverse Primer | Product size of cDNA (bp) |
|---|---|---|---|
| AeAANAT1 | 5' AGGATGTCCTGAAATTGCTGA 3 | 5' TCAGTCTCTTTCGGCCTGTT 3' | 202 |
| AeAANAT2 | 5' CAACATCCGTTTCGAGACAA 3' | 5' GTCGCCATCGTTGGAAATAG 3' | 202 |
| AeAANAT3 | 5' CAAGGAATGGCGATAAAAGC 3' | 5' ACACGTTGTACCGTTGCAGA 3' | 203 |
| AeAANAT4 | 5' CGGACGAATCGTTGGACTAT 3' | 5' GAGAATCAACCGCCAAGAAG 3' | 200 |
| AeAANAT7 | 5' TGAGATCGTGGGAGTCAACA 3' | 5' GCCTCGTCCTCGATATTTTG 3' | 202 |
| AeAANAT8 | 5' GATTGCTGGCATCAACATGA 3' | 5' CAGTCCTCGACCACGGTACT 3' | 202 |
| AeAANAT9 | 5' TTTTCCAGCGCTACAATGTG 3' | 5' GATTGCTGGCATCAACATGA 3' | 202 |
| RPS7 | 5' ATCTGTACATCACCCGCGCT 3' | 5' GATCGTGGACGCTTCTGCTT 3' | 202 |

## 5.4 Results

### Hypothetical AeAANAT family

*D. melanogaster* AANAT (NP_995934), which is capable of catalyzing the acetylation of tyramine, octopamine, dopamine, and serotonin (*5*), was used as a query sequence to search the *Ae. aegypti* genomic sequence in the National Center of Biotechnology and Information (NCBI) database using the BLAST and PSI BLAST search programs (*13*). The programs returned nine individual sequences sharing 13–52% sequence identity with the *D. melanogaster* NP_995934 (Table 5.4). When a functionally verified *B.mori* AANAT (NP_001073122) (*12*) was used to search the *Ae. aegypti* database, the same set of sequences for AeAANATs was obtained with identity from 13% to 27% to the silk moth protein (Table 5.4). Analysis of these selected *Ae. aegypti* proteins determined that they contain two motifs (commonly named Motif A and Motif B), which are characteristic of the *N*-acetyltransferase superfamily. There is also a consensus fragment (R/QXXGXG/A) corresponding to the AcCoA binding region (Figure 5.1). Further evaluation suggests that they contain recognizable regions, commonly named C/c-1, D/c-1, and D/c-2, for which functions remain unclear, but are evolutionarily conserved in the AANAT subfamily (*15*). The presence of these conserved motifs and regions corresponding to the *N*-acetyltransferase superfamily, (AcCoA binding and AANAT subfamily, respectively), support their possible AANAT identity.

The nine predicted AeAANAT proteins share 9-69% sequence identity with each other (Table 5.5). For convenience, they are sequentially referred as AeAANAT1-AeAANAT9 based on their level of sequence identity to the *D. melanogaster* NP_995934 protein, which has been named as DmAANAT1 (Table 5.4) and which was used to search the *Ae. aegypti* database. AeAANATs can be further clustered into three subgroups based on the level of amino acid sequence identity (Figure 5.2). The high sequence identity of AeAANAT1 with the activity-verified DmAANAT may provide insight into its function, but the degree of sequence identity to DmAANAT1 (13-30%) for the rest of the putative AeAANATs is not sufficient for concluding AANAT identity without activity verification. AeAANATs share 13-27% sequence identity with the functionally verified *B. mori* AANAT (*12*), which also seems inadequate for concluding their true AANAT identity.

Further analysis of AANAT subfamily in insects using a BLAST and PSI –BLAST (*13*) search revealed that a similar AANAT family is present in other mosquito species and other insect species including fruit flies, honey bees, and cockroaches.

For example, there are ten putative AANAT sequences in *Culex quinquefasciatus*, and six AANAT sequences in *Anopheles. gambiae*. Phylogenetic inference (Figure 5.3) shows that ortholog for AeAANAT1, AeAANAT2, AeAANAT4, AeAANAT6, AeAANAT7, and AeAANAT8 were found in all three sequenced mosquito species, (*Ae. aegypti*, *An. gambiae*, and *C. quinquefasciatus*). Based on these results, *Aedes* was chosen as a representative genus in the mosquitoes.

To understand the phylogenetic relationship between insect AANATs and other vertebrates and invertebrates, a phylogenetic tree was constructed based on 37 amino acid sequences including representatives from human, mouse, rats, sheep, flies, mosquitoes, honey bees, chicken, fish, green algae, metazoan, and bacteria. A neighbor joining tree was constructed using the MEGA software (*14*) and bootstrap values were calculated using 5000 bootstrapped replicates(Figure 5.4). Phyletic distribution analysis confirmed a major distinction of the insect AANATs from those of bacteria, algae, metazoan, and other vertebrate species (*16*).

**Table 5.4 The amino acid percent identity between the conserved hypothetical proteins in *Ae. aegypti* against *Drosophila* AANAT and *Bombyx mori* AANAT.**

| GenBank Accession Numbers | AeAANAT | Percent identity with *Bombyx mori* AANAT | Percent identity with *Drosophila melanogaster* AANAT |
|---|---|---|---|
| AaeL_AAEL011088/ XP_001661400 | AeAANAT1 | 27 | 52 |
| AaeL_AAEL012952/ XP_001663122 | AeAANAT2 | 26 | 30 |
| AaeL_AAEL004847/ XP_001649915 | AeAANAT3 | 24 | 26 |
| AaeL_AAEL002255/ XP_001661173 | AeAANAT4 | 19 | 26 |
| AaeL_AAEL004827/ XP_001649916 | AeAANAT5 | 17 | 22 |
| AaeL_AAEL012866/ XP_001663012 | AeAANAT6 | 18 | 20 |
| AaeL_AAEL012870/ XP_001663019 | AeAANAT7 | 18 | 17 |
| AaeL_AAEL012864/ XP_001663020 | AeAANAT8 | 15 | 16 |
| AaeL_AAEL012860/ XP_001663014 | AeAANAT9 | 13 | 13 |

**Table 5.5 Sequence identity comparison among the AeAANATs**.
The values represent the mean percent identity of amino acids between each pairwise comparison of the AeAANAT proteins found in *Ae. aegypti*. The amino acid percent similarity ranges between 9-69% as determined by ClustalW.

| AeAANATs | AeAANAT1 | AeAANAT2 | AeAANAT3 | AeAANAT4 | AeAANAT5 | AeAANAT6 | AeAANAT7 | AeAANAT8 | AeAANAT9 |
|---|---|---|---|---|---|---|---|---|---|
| AeAANAT1 | - | | | | | | | | |
| AeAANAT2 | 33 | - | | | | | | | |
| AeAANAT3 | 20 | 18 | - | | | | | | |
| AeAANAT4 | 25 | 26 | 31 | - | | | | | |
| AeAANAT5 | 22 | 21 | 40 | 38 | - | | | | |
| AeAANAT6 | 22 | 15 | 15 | 15 | 22 | - | | | |
| AeAANAT7 | 21 | 19 | 9 | 17 | 12 | 69 | - | | |
| AeAANAT8 | 23 | 17 | 12 | 19 | 15 | 54 | 52 | - | |
| AeAANAT9 | 17 | 17 | 14 | 16 | 11 | 42 | 44 | 40 | - |

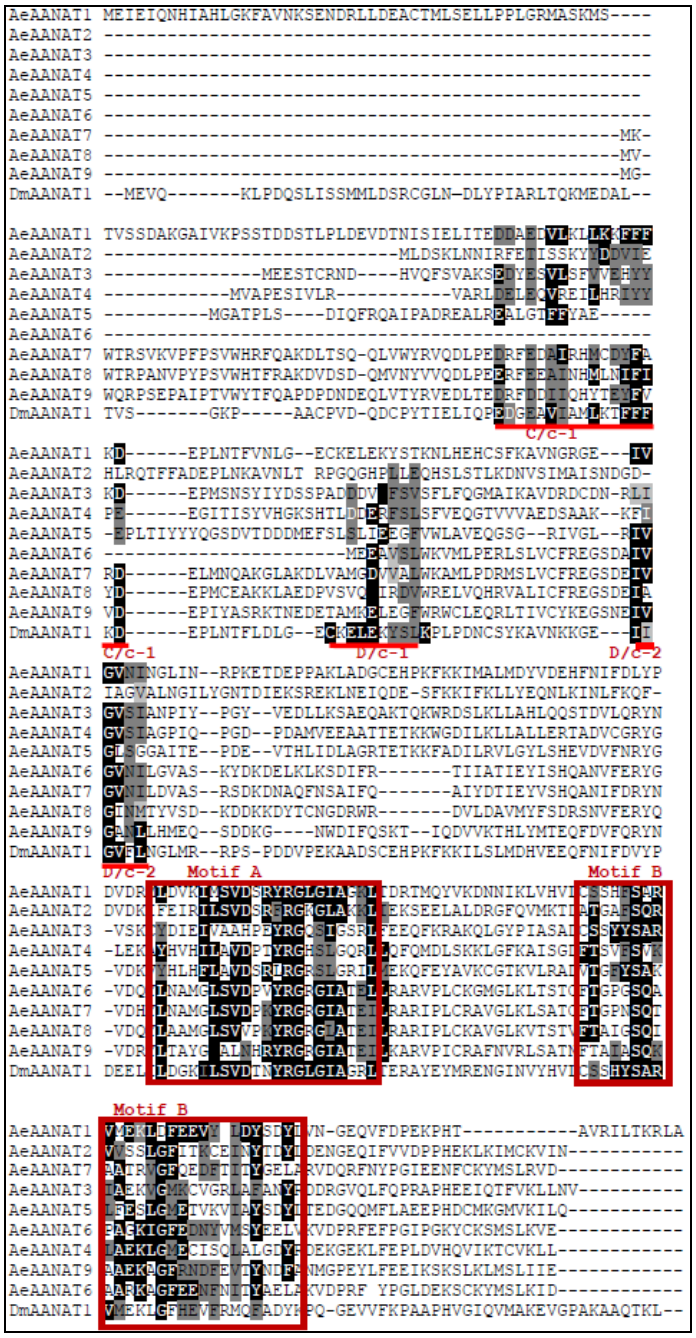


**Figure 5.1 Multiple sequence alignment of AANAT sequences**.
DmAANAT1 (*Drosophila* AANAT) has compared with the newly identified AeAANATs. Sequences were aligned using ClustalW, and then manually adjusted. Only the residues in the conserved domains are highlighted. In the conserved domains, residues highlighted in black are "identical" and residues highlighted in gray are "similar" among the compared sequences. Motifs (A and B) (Red boxes) and Conserved regions (C/c-1, D/c-1, D/c-2) (Red underlined) are discussed in the text.

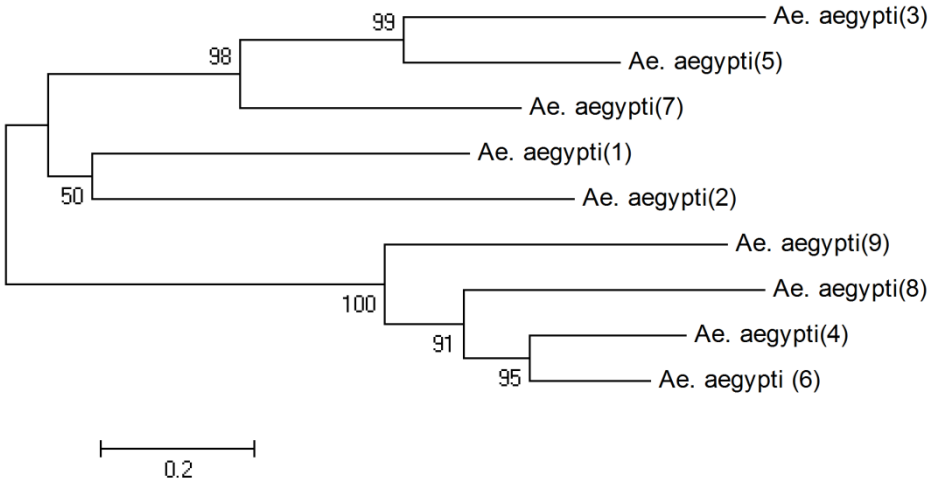


**Figure 5.2 Phylogenetic analyses of AeAANATs.**
Sequences were aligned using ClustalW and the dendrogram was generated using the neighbor joining method. The approach for the alignment is unbiased because truncation of sequences was not done. The number on the internal branches shows the bootstrap values (percentage) based on 5000 replicates. *Ae. aegypti*(1) (GenBank accession no. XP_001661400); *Ae. aegypti*(2) (GenBank accession no XP_001663122); *Ae. aegypti*(3) (GenBank accession no XP_001649915); *Ae. aegypti*(4) (GenBank accession no XP_001661173); *Ae. aegypti*(5) (GenBank accession no XP_001649916); *Ae. aegypti*(6) (GenBank accession no XP_001663012); *Ae. aegypti*(7) (GenBank accession no XP_001663019); *Ae.aegypti*(8) (GenBank accession no XP_001663020); *Ae. aegypti*(9) (GenBank accession no XP_001663014)

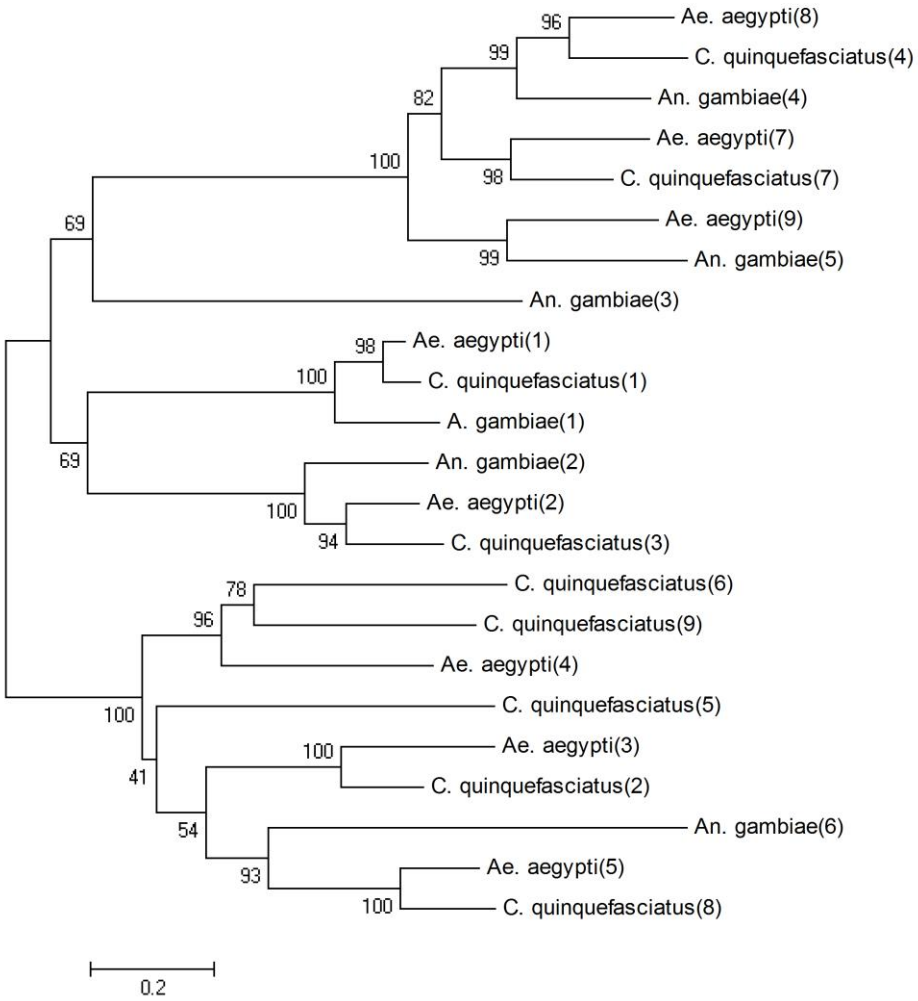


**Figure 5.3 Phylogenetic analysis of mosquito species.**
Sequences were aligned using ClustalW and the dendrogram was generated using the neighbor joining method. The numbers on the internal branches show the bootstrap values (percentage) based on 5000 replicates. *C. quinquefasciatus*(1) (GenBank accession no XP_001865527); *C. quinquefasciatus*(2) (GenBank accession no XP_001863217); *C. quinquefasciatus*(3) GenBank accession no XP_001863411*); C. quinquefasciatus*(4) (GenBank accession no XP_001842324); *C. quinquefasciatus*(5) (GenBank accession no XP_001863216); *C. quinquefasciatus*(6) (GenBank accession no XP_001866314); *C. quinquefasciatus*(7) (GenBank accession no XP_001842325); *C. quinquefasciatus*(8) (GenBank accession no XP_001863218); C. quinquefasciatus(9) (GenBank accession no XP_001866315); *An. gambiae*(1) (GenBank accession no XP319299); *An. gambiae*(2) (GenBank accession no XP_309481); *An. gambiae*(3) (GenBank accession no XP_321677); *An. gambiae*(4) (GenBank accession no XP_313828); *An. gambiae*(5) (GenBank accession no XP_309481); *An. gambiae*(6) (GenBank accession no XP_313828); .*Ae. aegypti*(1) (GenBank accession no. XP_001661400); *Ae. aegypti*(2) (GenBank accession no XP_001663122); *Ae. aegypti*(3) (GenBank accession no XP_001649915); *Ae. aegypti*(4) (GenBank accession no XP_001661173); *Ae. aegypti*(5) (GenBank accession no XP_001649916); *Ae. aegypti*(7) GenBank accession no XP_001663019); *Ae. aegypti*(8) (GenBank accession no XP_001663020); *Ae. aegypti*(9) (GenBank accession no XP_001663014).

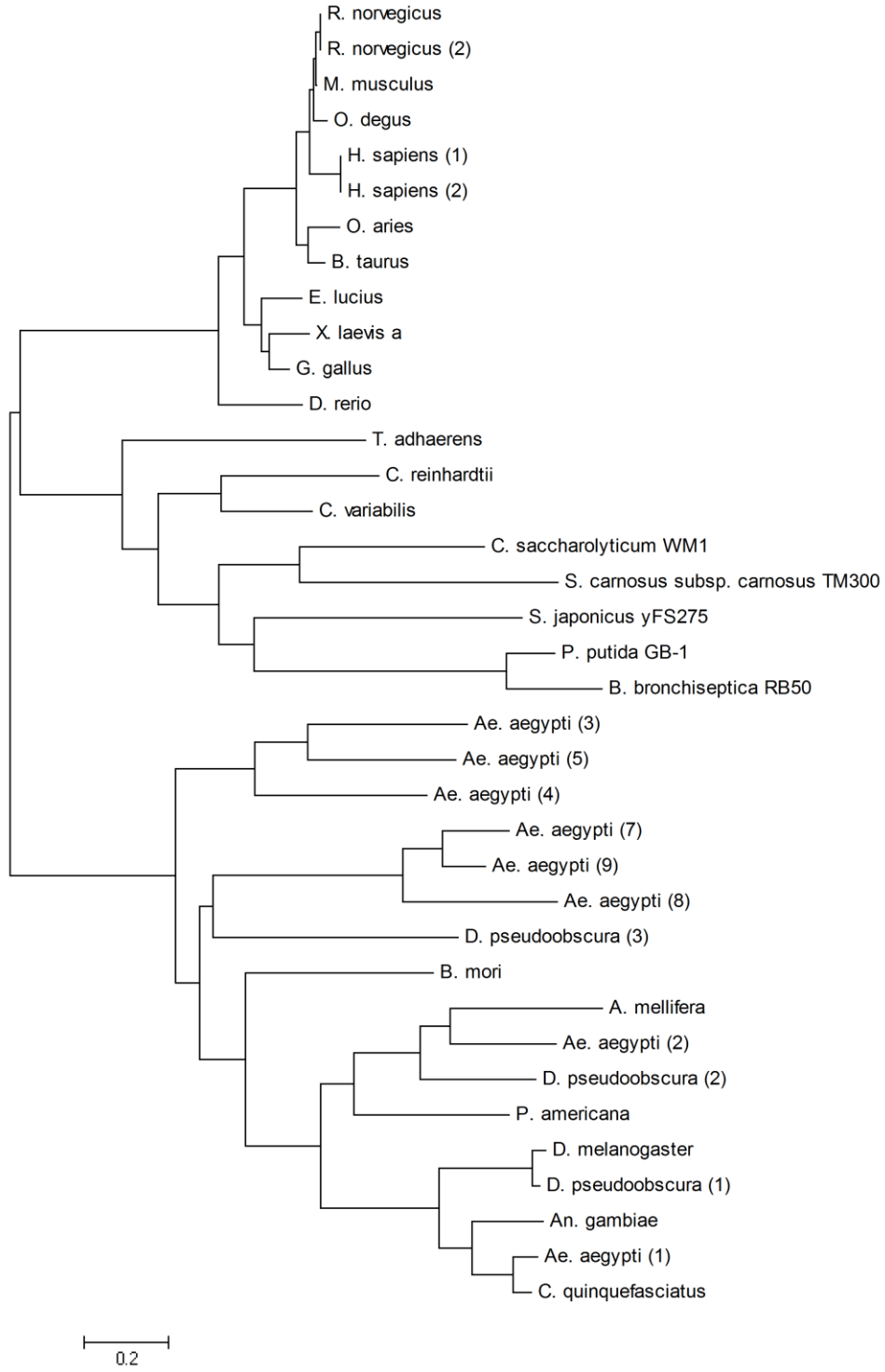


**Figure 5.4 Phylogenetic analysis based on AANAT sequences from different species.** (Details on next page) Sequences were aligned using ClustalW and the dendrogram was generated using neighbor joining method. The number on the internal branches shows the bootstrap values (percentage) based on 5000 replicates. Table 5. 6 represents Species, Gene Bank accession numbers, and Abbreviation in dendrogram.

**Table 5.6 List of species used in figure 5.4 for construction of phylogenic tree .**

| Species | Abbreviation in dendrogram | GeneBank accession No |
|---|---|---|
| *Bombyx mori* | *B. mori* | DQ256382 |
| *Periplaneta americana* | *P. americana* | AB106562 |
| *Drosophila melanogaster* | *D. melanogaster* | Y07964 |
| *Anopheles gambiae* | *An. gambiae* | XP_319299 |
| *Apis mellifera* | *A. mellifera* | XP394768 |
| *Drosophila pseudoscura* | *D. pseudoscura (1)* | EAL25482 |
| *Drosophila pseudoscura* | *D. pseudoscura (2)* | EAL31520 |
| *Drosophila pseudoscura* | *D. pseudoscura (3)* | EAL32377 |
| *Aedes aegypti* | *Ae. aegypti (1)* | XP_001661400 |
| *Aedes aegypti* | *Ae. aegypti (2)* | XP_001663122 |
| *Aedes aegypti* | *Ae. aegypti (3)* | XP_001649915 |
| *Aedes aegypti* | *Ae. aegypti (4)* | XP_001661173 |
| *Aedes aegypti* | *Ae. aegypti (5)* | XP_001649916 |
| *Aedes aegypti* | *Ae. aegypti (7)* | XP_001663019 |
| *Aedes aegypti* | *Ae. aegypti (8)* | XP_001663020 |
| *Aedes aegypti* | *Ae. aegypti (9)* | XP_001663014 |
| *Culex quinquefasciatus* | *C. quinquefasciatus* | XP_001865527 |
| *Homo sapiens 1* | *H. sapiens (1)* | NM 001088 |
| *Homo sapiens 2* | *H. sapiens (2)* | NP_001160051 |
| *Rattus norvegicus 1* | *R. norvegicus (1)* | U38306 |
| *Rattus norvegicus 2* | *R. norvegicus (2)* | NP_036950 |
| Esox lucius | *E. lucius* | AF034081 |
| *Gallus gallus* | *G. gallus* | U46502 |
| *Xenopus laevis* | *X. laevis* | AY316296 |
| *Danio rerio* | *D. rerio* | NP_571486 |
| Bos taurus | *B. taurus* | DAA18183 |
| *Octodon degus* | *O. degus* | ACO56120 |
| *Mus musculus* | *M. musculus* | NP_033721 |
| *Chlostridium saccharolyticum* | *C saccharolyticum* | YP_003823415 |
| *Pesudomonas peutida* | *P. peitida* | YP_001669494 |
| *Staphylococcus carnosussubspcarnosus* | *S. carnossubspcarnosus* | YP_002635499 |
| *Chorella veriabilis* | *C. verbialis* | EFN577355 |
| *Trichoplax adhaerance* | *T. adhaerance* | XP_002113075 |
| *Schizosaccharomyces* | *S._japonicus_yFS275* | XP_002173506 |
| *Chlamydomonas reinhardtii* | *C. reinhardtii* | BAH10512 |
| *Bordetella bronchiseptica* | *B. bronchaspetica* | NP_887628 |

**Determination of AANAT identity**

***Protein expression and purification***

To determine whether the selected *Ae. aegypti* sequences were true AANATs, their coding sequences were amplified from *Ae. aegypti* cDNA preparations and recombinant proteins were expressed using the bacterial protein expression system. Soluble recombinant proteins for eight individual putative AANATs were successfully expressed and purified sequentially by chitin affinity, ion exchange, and gel filtration chromatography techniques. The final preparation contained the single major band for all the AeAANATs between 20-30 kDa (Figure 5.5). No recombinant protein of putative AeAANAT6 was expressed. Further analysis indicated that the deduced amino acid sequence of the putative AeAANAT6 is much shorter than other putative AANATs, suggesting that possibly AeAANAT6 sequence might not be a functional protein and no further effort was made to express its protein.

***Substrate specificity***

Each recombinant protein was screened for AANAT activity using tyramine, dopamine, tryptamine, serotonin, norepinephrine, and methoxytrypamine as the acetyl group acceptor and AcCoA as acetyl group donor. Five recombinant proteins displayed activity to at least one of the tested acetyl group acceptors. Among them, AeAANAT1 and AeAANAT2 can use all the tested arylalkylamines as substrates. AeAANAT3 displayed activity toward dopamine, octopamine, and tyramine, while AeAANAT4 and AeAANAT7 were active to dopamine, tyramine, and serotonin. AeAANAT8 and AeAANAT9 showed essentially no activity to the tested arylalkylamine in this study (Table 5.7).

Substrate screening suggests that AeAANAT1 and AeAANAT2 have relatively broad substrate specificity. The AeAANAT3, AeAANAT4, and AeAANAT7 have narrow substrate specificity towards the tested arylalkylamines. As a result, it was difficult to specify or at least narrow down their physiological functions based on their substrate profile. Although all five of the above mentioned AeAANATs were active to dopamine, some of them shared relatively limited sequence identity (9-33%), indicating that substrate specificity of AeAANATs is somewhat poorly related to their sequence identity.

***Kinetic analysis of AeAANAT1 and AeAANAT2***

Although AeAANAT1 and AeAANAT2 showed broad substrate specificity, kinetic parameters for only dopamine and serotonin were tested. AeAANAT1 showed lower $K_m$ towards

dopamine (8.76 X 10 $^{-2}$ mM) than serotonin (0.397 mM) (Table 5.8). AeAANAT2 showed lower $K_m$ for serotonin (0.31 mM) than dopamine (0.55 mM). Both AeAANAT1 and AeAANAT2 showed substrate inhibition for the dopamine at 3.2 mM and for serotonin at 1.6 mM.

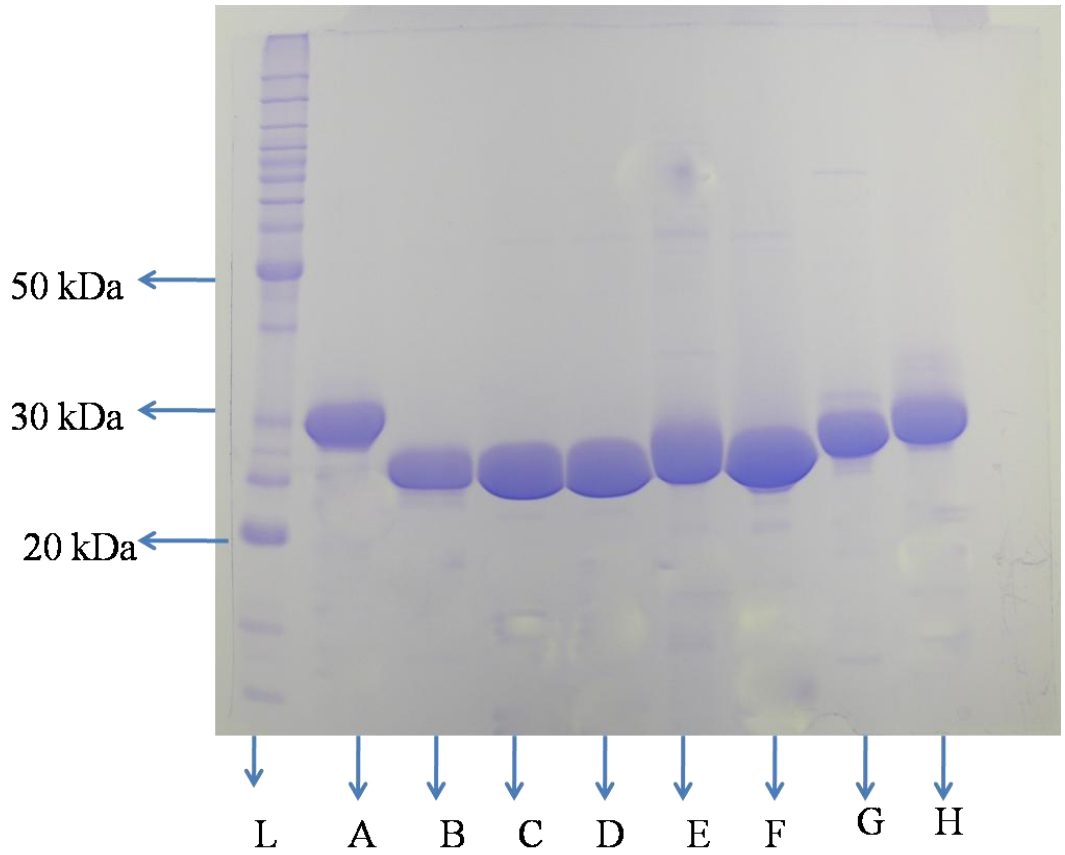


**Figure 5.5 Characterization of the recombinant AeAANAT proteins.**
SDS-PAGE analysis of purified (A) AeAANAT1, (B) AeAANAT2, (C) AeAANAT3, (D) AeAANAT4, (E) AeAANAT5, (F) AeAANAT7, (G) AeAANAT8, and (H) AeAANAT9 together with protein benchmark ladder (L).

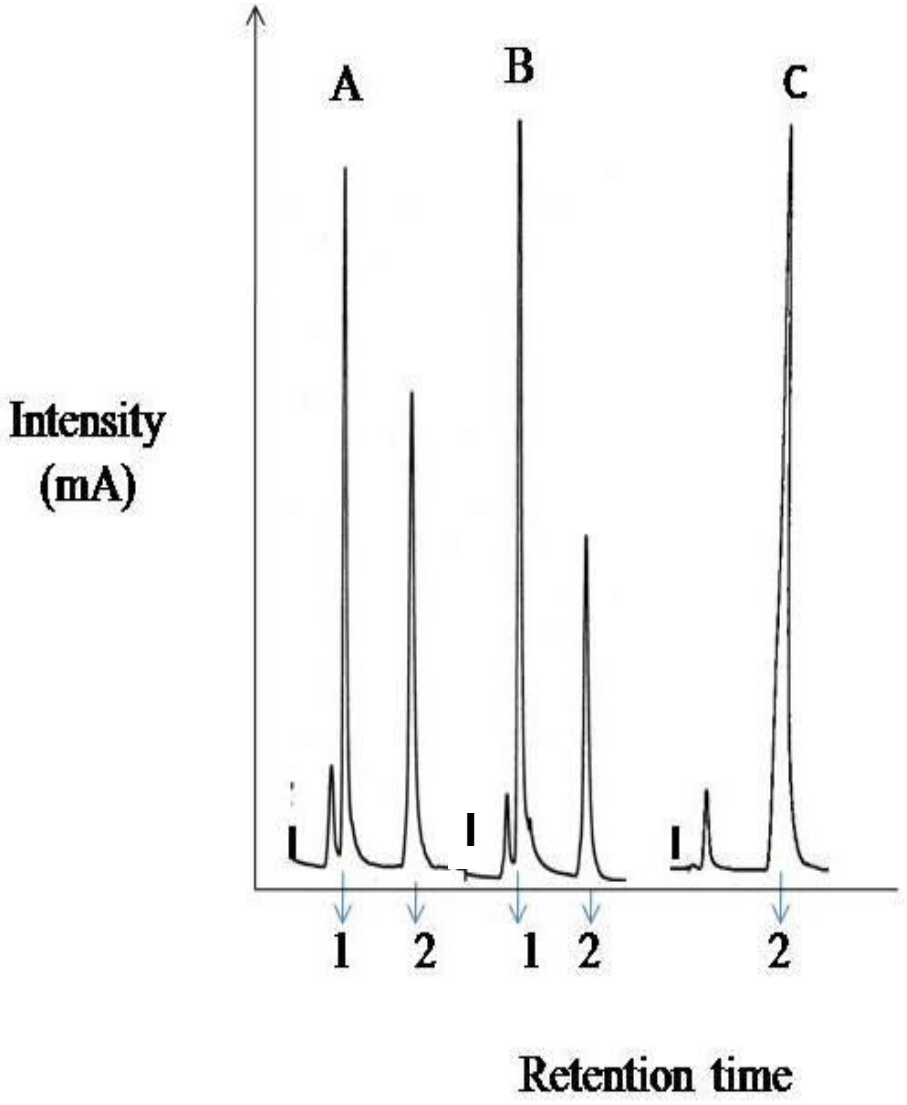


**Figure 5.6 Activity assay for (A) AeAANAT1 and (B) AeAANAT2**. (C) is a standard. I=Injection;1=tryptamine; 2=*N*-acetyl-tryptamine.

.

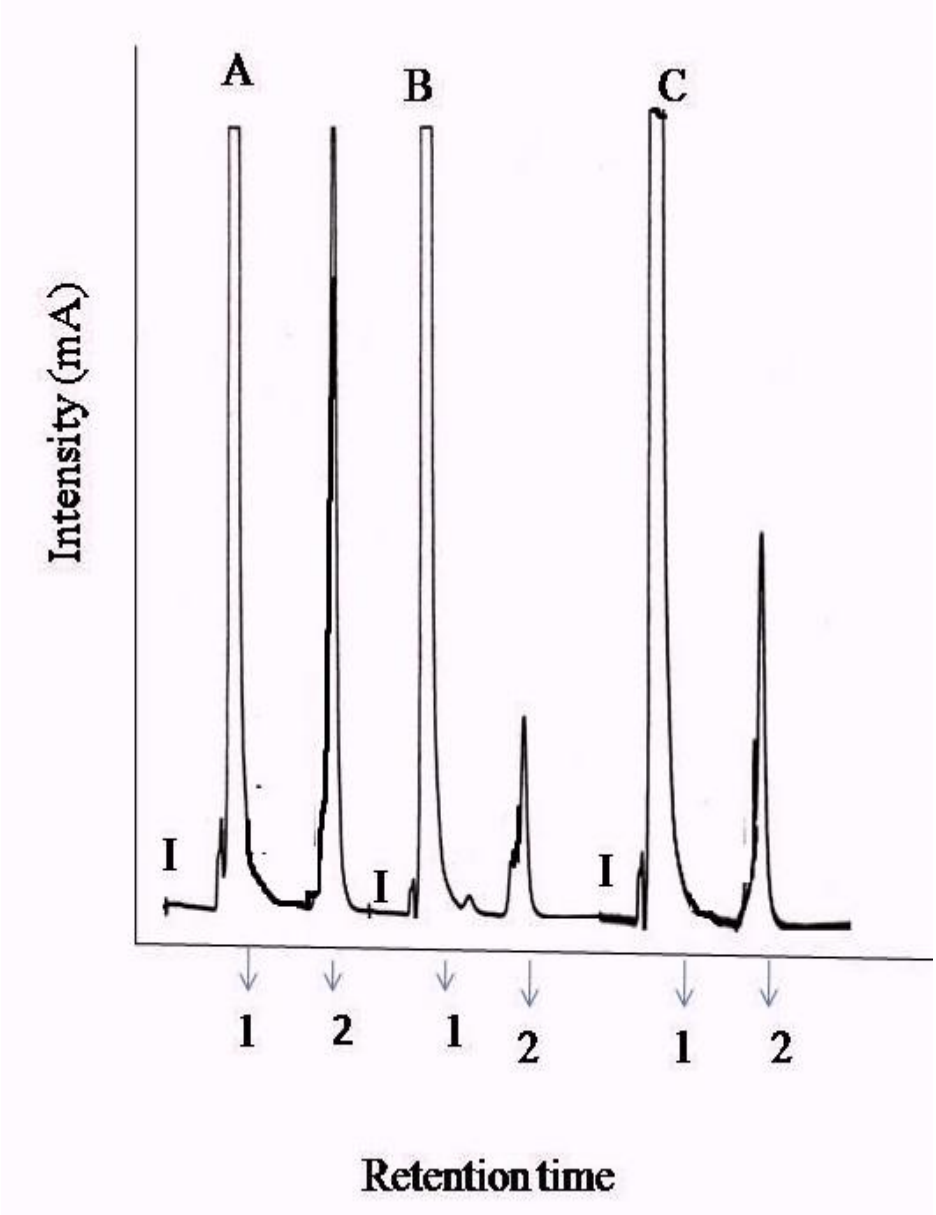


**Figure 5.7 Activity assays for (A) AeAANAT3, (B) AeAANAT4, and (C) AeAANAT7.** I=Injection; 1=Dopamine; 2=*N*-acetyldopamine.

**Table 5. 7 Comparison of substrate specificity for AeAANATs.**
Substrate selectivity of each AeAANAT was tested via HPLC-electrochemical detection using 5 mM of substrate, and 1 mMof AcCoA at pH 7.5 and temperature 37 ºC. (+) =Detected, (-) =Not detected, (X) = Negligible.

| Substrate | AeAANAT1 | AeAANAT2 | AeAANAT3 | AeAANAT4 | AeAANAT5 | AeAANAT7 | AeAANAT8 | AeAANAT9 |
|---|---|---|---|---|---|---|---|---|
| **Dopamine** | + | + | + | + | - | + | **X** | - |
| **Octopamine** | + | + | + | - | - | - | - | - |
| **Tyramine** | + | + | + | + | - | + | - | - |
| **Nor-epinephrine** | + | + | - | - | - | - | - | - |
| **Serotonin** | + | + | - | + | - | + | - | - |
| **Tryptamine** | + | + | - | - | - | - | - | - |
| **Methoxy-tryptamine** | + | + | - | - | - | - | - | - |

**Table 5. 8 Kinetic analysis of AeAANAT1 and AeAANAT2.**

| Enzymes | Dopamine | Serotonin |
|---|---|---|
| | Apparent $K_m$ (mM) | |
| **AeAANAT1** | 0.0876 | 0.397 |
| **AeAANAT2** | 0.55 | 0.31 |

**Temporal expression analysis of AeAANATs**

QPCR was performed to compare the transcription levels of AeAANATs from female mosquito tissues and larval molt cycles. Specifically, the transcript levels of AeAANAT1, AeAANAT2, AeAANAT3, AeAANAT4, AeAANAT7, AeAANAT8, and AeAANAT9 were analyzed. For developmental stages expression, levels of AeAANATs transcripts were compared to those of larvae stage day one. For the adult tissues expression, levels of AeAANAT transcripts were compared to those of non-blood-fed ovaries (After 48 hours of sugar feeding). Gene specific qPCR primers for AeAANAT5 could not be found towards this end. The expression profiles studied herein were the discontinuous expression profile because larvae and pupae were collected every 24 hours after hatching of mosquito eggs. Tissues, such as abdomen, thorax, and head were collected before and after 48 hours from sugar fed and blood fed mosquito groups, and ovaries were collected every 12 hours up to 72 hours after blood feeding. As described earlier, the cDNA for all tissues and developmental stages were synthesized from 5 µg of mRNA. The comparative $2^{-\Delta\Delta ct}$ method was used to quantify results obtained for AeAANATs transcripts by using qPCR. All the samples were normalized with respect to ribosomal binding protein (*rpS7*) of *Ae. aegypti*.

AeAANAT1 was expressed throughout the lifecycle and was the only gene that showed highest expression in the black pupae stage as compared to other AeAANATs. AeAANAT2 was and AeAANAT3 were also expressed in the larval stages. After laraval stages AeAANAT3 was down-regulated. In the larval molt cycle, expression of AeAANAT4 transcripts was highest during larvae stage (day 1), but then significantly decreased during the rest of the molt cycles. In the case of AeAANAT7, although it showed expression in the initial developmental stages, level of its transccript dropped after larval stage day three. In the larval molt cycle, expression of AeAANAT8 showed its highest expression in the larvae stage (day 5), but then decreased in the pupal stages (Figure 5.8).

The transcription of AeAANAT1, AeAANAT3, and AeAANAT8 were highest in day 5 as compared to the other larval stages. AeAANAT9 showed highest expression in day 3 larvae. The transcription level of AeAANAT1 and AeAANAT8 in the larvae stage (day 5) was approximately 3 to 10-fold higher than the other larval periods. Similarly, the transcription level of AeAANAT3 was approximately 10-fold higher than the other larval periods. The transcription

levels AeAANAT8 and AeAANAT9 were higher in the white pupae stage than in the black pupae stage (Figure 5.8).

The transcription levels of AeAANAT2, AeAANAT4, AeAANAT7, AeAANAT8, and AeAANAT9 in ovaries were the highest at 72 hours of blood feeding (Figure 5.9). AeAANAT1 and AeAANAT9 showed increased expression at 12 hours after blood feeding and 48 hours blood feeding as compared to other ovarian stages.

AeAANAT1 was up-regulated in the blood-fed abdomen compared to the non-blood-fed abdomen. It should also be noted that AeAANAT1 showed the highest level of expression in the blood-fed abdomen compared to the other AeAANATs. None of the genes were expressed in the non-blood-fed abdomen except AeAANAT9, while only three genes were expressed in the non-blood-fed thorax, namely, AeAANAT7, AeAANAT8, and AeAANAT9. AeAANAT1, AeAANAT2, AeAANAT4, AeAANAT7, AeAANAT8, and AeAANAT9 were expressed in the non-blood-fed head. However, their transcripts were reduced approximately 3-fold to 5-fold after blood feeding in the head. AeAANAT7 was expressed in non-blood-fed abdomen. Following blood feeding AeAANAT7 was down-regulated in the abdomen. AeAANAT4 and AeAANAT7 were expressed in the non-blood-fed thorax but following the blood feeding they were down-regulated in the thorax. Our results suggest that the genes may play diverse roles in these various adult tissues (Figure 5.10).

It should be noted that although the magnitudes of the changes in transcript abundances for all genes quantified in both trials differed between the trials, the changes in direction of expression remained consistent for a majority of the genes.

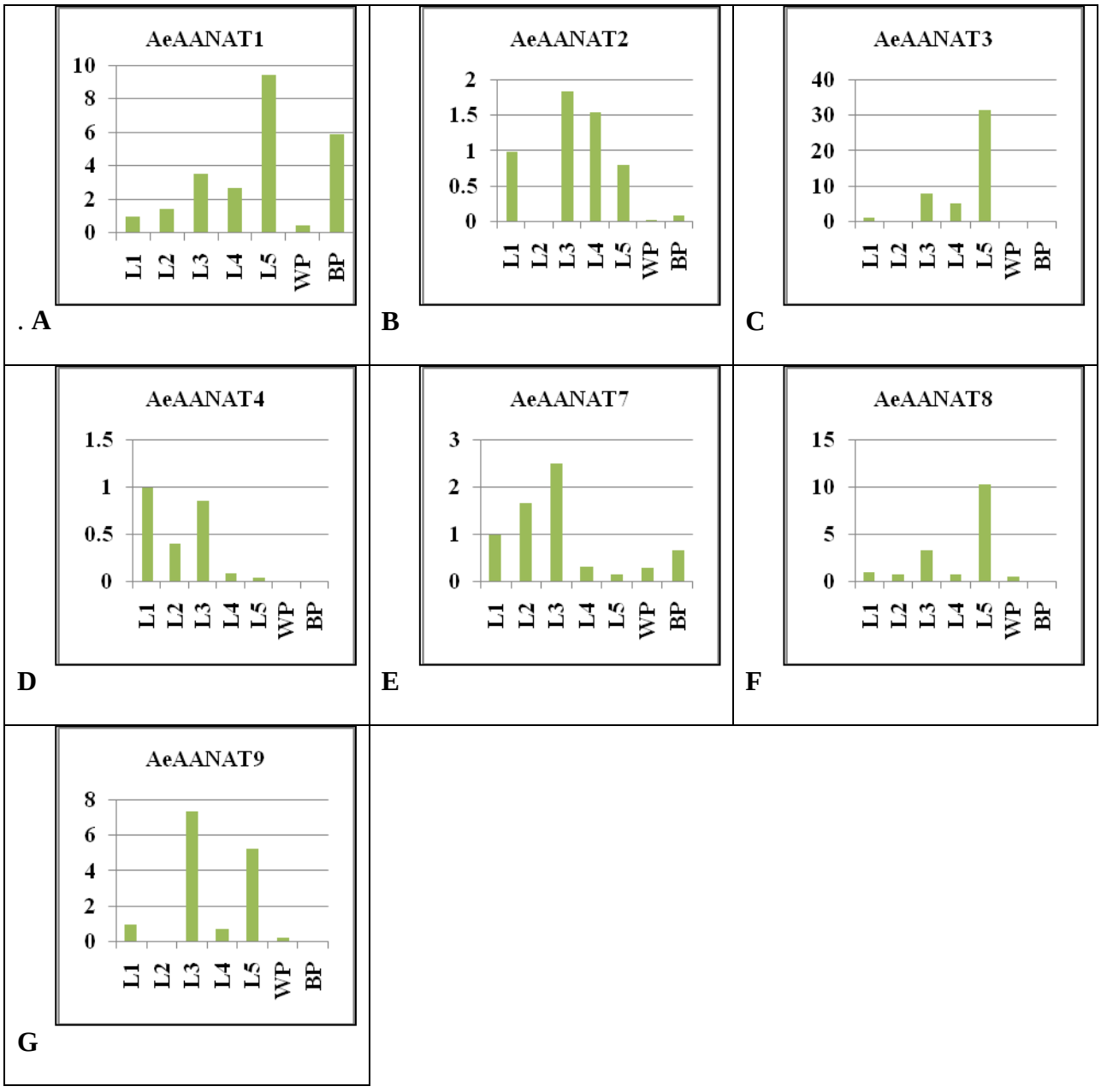


**Figure 5.8 Relative quantification of expression of *Ae. aegypti* AANATs transcription during larval and pupal development by real-time PCR**. X-axis shows developmental stages and y-axis shows the relative expression quantity, the expression of L1 was taken as the calibrator. L1: First-instar larvae (larvae day1), L2: second-instar larvae (larvae day2), L3: third-instar larvae (larvae day 3), L4: fourth-instar larvae (Larvae day 4), L5: fifth- instar larvae, WP: White pupae, BP: Black pupae. Panels (A-G) represent expression of AeAANATs. (A) AeAANAT1; (B) AeAANAT2; (C) AeAANAT3; (D) AeAANAT4; (E) AeAANAT7; (F) AeAANAT8; (G) AeAANAT9.

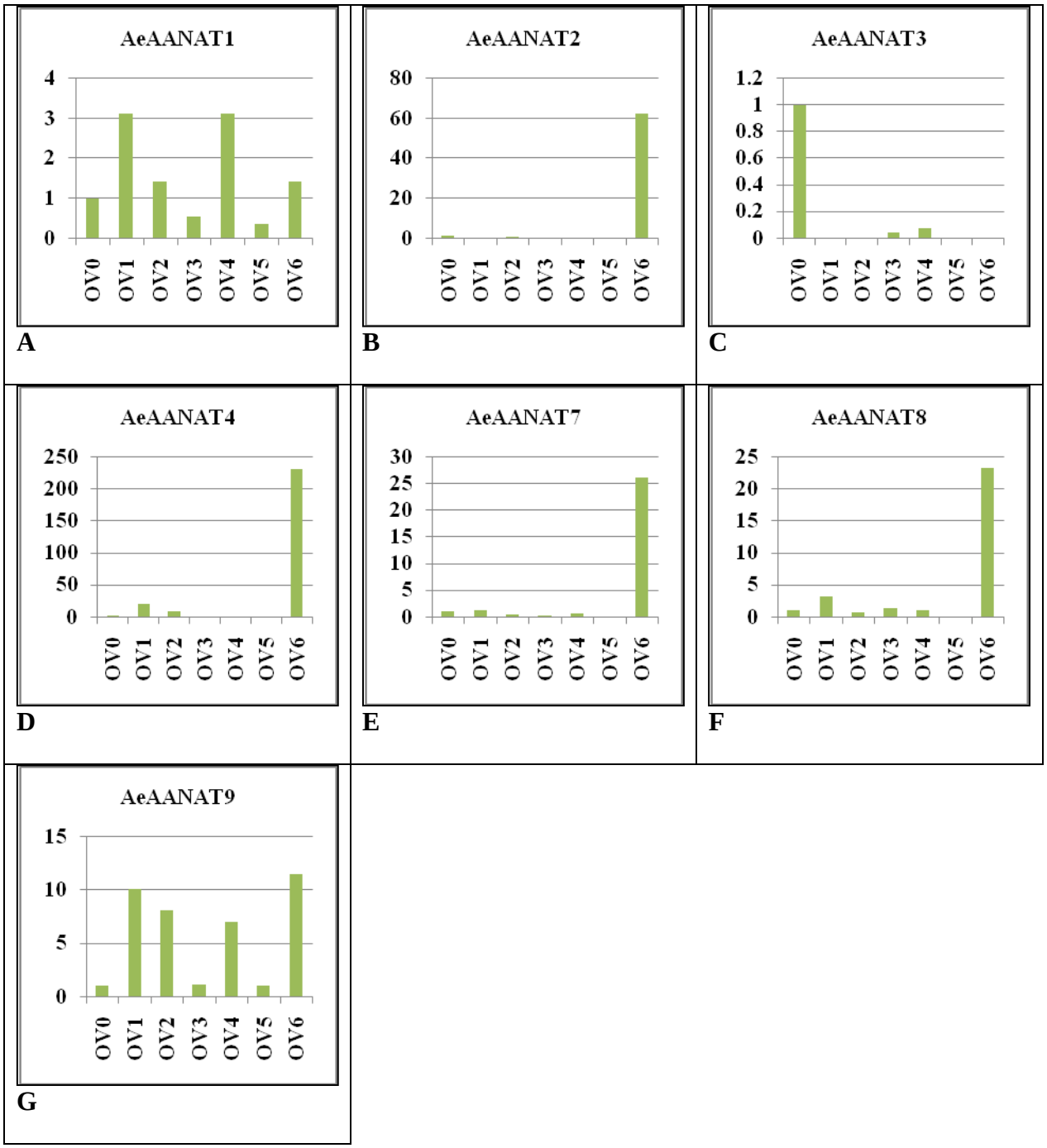


**Figure 5.9 Relative quantification of expression of *Ae. aegypti* AANATs transcription in developing ovaries by real-time PCR**. X-axis shows ovarian stages and y-axis shows the relative expression quantity, the expression of OV0 was taken as the calibrator. In these figures OV1-OV7 ovaries collected from 12-72 hours post blood-fed mosquitoes every 12 hours with the exception of OV0, which was collected from non-blood-fed mosquitoes. Panels (A-G) represent expression of AeAANATs. (A) AeAANAT1; (B) AeAANAT2; (C) AeAANAT3; (D) AeAANAT4; (E) AeAANAT7; (F) AeAANAT8; (G) AeAANAT9.

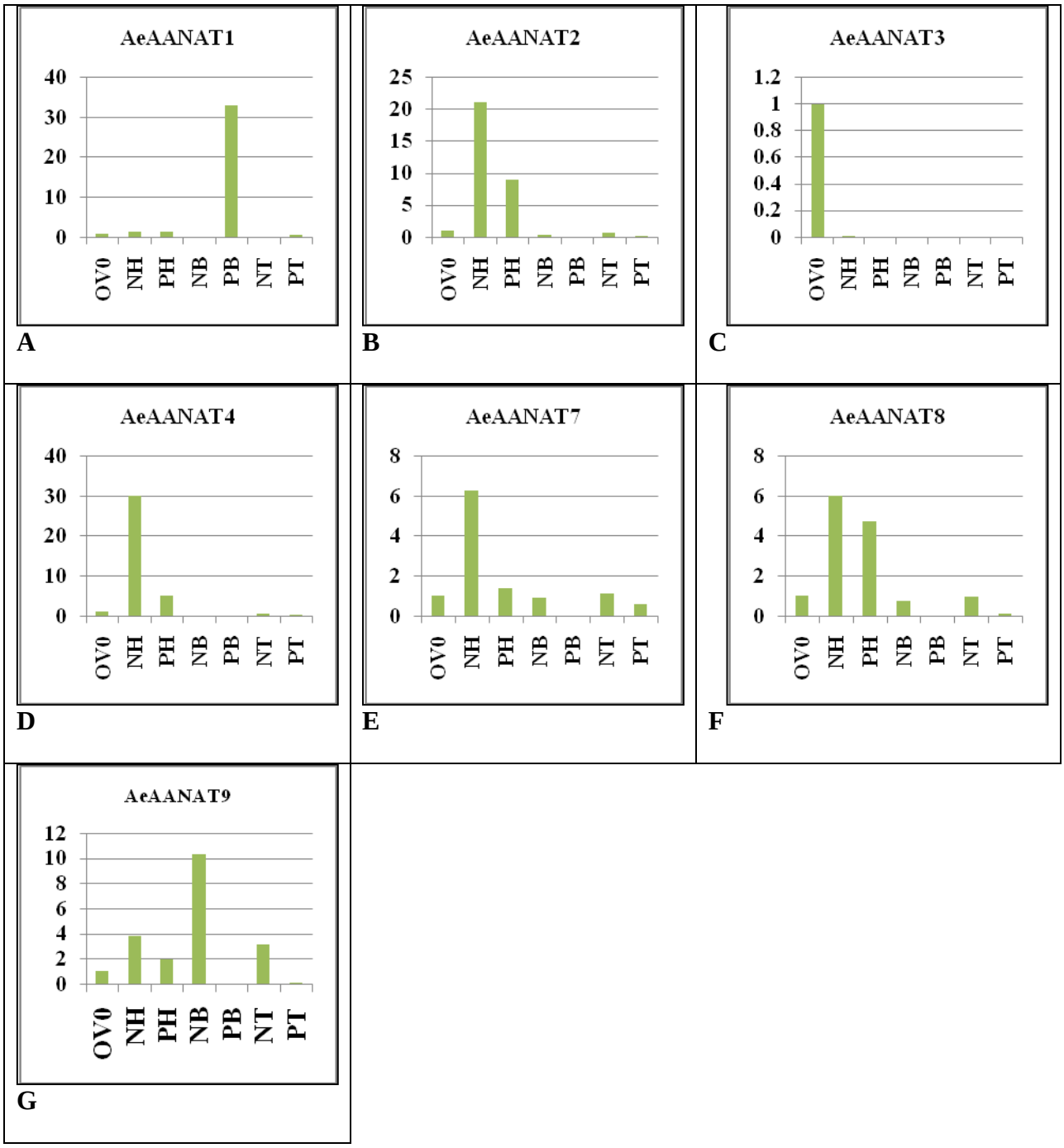


**Figure 5.10 Relative expression of AeAANATs in non-blood-fed and blood-fed tissues from female adult mosquitoe**. X-axis shows adult female blood-fed and non blood-fed tissues while y-axis shows the relative expression quantity, the expression of AeAANATs in the OV0 (48 hour non-blood-fed ovary) sample was taken as the calibrator. In these figures NH, NT, and NB refer to head, thorax, and abdomen from non-blood-fed mosquitoes respectively; PH, PT, and PB refer to head, thorax, and abdomen from blood-fed mosquitoes respectively. Panels (A-G) represent expression of AeAANATs. (A) AeAANAT1; (B) AeAANAT2; (C) AeAANAT3; (D) AeAANAT4 expression; (E) AeAANAT7; (F) AeAANAT8; (G) AeAANAT9.

## 5.5 Discussion

The genome sequence available of the *Ae. aegypti* mosquito served as a basis for this study (*17*). Examination of the AeAANAT sequences revealed that they lacks many of the features of vertebrate AANATs (*18*). However, the set of AeAANAT genes studied in this report is somewhat related to AANATs from *Drosophila,* which is similar to their protein architecture (Figure 5.1).

Sequence analysis suggested that multiple AANAT genes are present in insects. In mosquitoes, for example, six to nine putative AANAT genes were identified. Interestingly, however, vertebrate genomes contain a single AANAT gene. Some exceptions to this pattern are fish and cows, which possess three and two paralogs, respectively (*19*).

None of the AeAANATs mentioned in this study shares the features of vertebrate AANATs. Vertebrate AANATs possess the unique features that mediate rapid changes in enzyme activity; and facilitate catalysis (*20*). The bacterial and fungal AANATs also lack the defining physical characteristics of vertebrate AANATs (*18*). In phylogenetic analysis, insect AANATs form a separate clade from mammalian AANATs (vertebrate) and bacterial and fungal AANATs (Figure 5.4), suggesting that insect AANATs may have different functions as compared to AANATs from mammals and other prokaryotic organisms.

**Expression of AeAANATs**

AeAANAT1 and AeAANAT2 are expressed in all life stages and tissues tested, which is consistent with the patterns for *Drosophila* enzyme (*4, 21*). AeAANAT1 is highly up-regulated in the blood-fed abdomen compared to the other AeAANATs, suggesting that blood feeding has have a positive impact on AeAANAT1 in the abdomen. AeAANAT3 is expressed primarily in the larval stages. AeAANAT4 and AeAANAT2 are highly expressed in the mature ovaries. Because this is also the period when female mosquitoes can lay eggs, this suggests that AeAANAT may have a role in reproduction. AeAANAT2, AeAANAT4, AeAANAT7, AeAANAT8, and AeAANAT9 were down-regulated in the head following blood feeding suggesting that blood feeding has negative impact on these genes in the head. Conversely, it could be that these genes in mosquito head feature the regulatory elements that respond negatively to blood feeding. Differences in the expression pattern of AeAANATs suggest that they are under the control of different promoters.

**Biochemical Analysis of AeAANATs**

To determine the biochemical functions of AeAANATs, substrate specificity was investigated with a selection of the monoamines that have been used to characterize mammalian AANATs and other insect species (*4*). Broad substrate specificity of AeAANAT1 and AeAANAT2 suggests that they may have more than one function depending on the availability of the substrate and localization. Other insect AANATs such as *Drosophila* AANAT1, *P.americana* AANAT, and *B.mori* AANAT have shown broad substrate specificity like AeAANAT1 and AeAANAT2 (*4, 7, 10*). In constrast, AeAANAT3, AeAANAT4, and AeAANAT7 showed narrow substrate specificity to arylalkylamines, which suggests that their function may be limited to the availability of specific arylalkylamines (Table 5.7) and their localization. Differences in substrate specificities of the AeAANATs studied herein point to the differences in the active sites of proteins.

It has been reported that acidic AANAT acetylates norepinephrine but basic AANAT does not (*10, 11*). Although all of these proteins showed activity at pH 7.5, whether or not we can address these AeAANATs as acidic or basic is yet to be confirmed. Furthermore, we may be able to divide these AeAANATs based on catalysis of norepinephrine. For example, AeAANAT1 and AeAANAT2 are able to acetylate norepinephrine, while AeAANAT3, AeAANAT4, and AeAANAT7 does not.

Once we identified broad substrate specificity for AeAANAT1 and AeAANAT2, we conducted a kinetic analysis of both enzymes to determine the rank of specificity. Considering the physiological importance of dopamine and serotonin, the $K_m$ values for both enzyme substrates were evaluated. The affinity of AeAANAT1 to dopamine is 6.27 times higher than that of AeAANAT2 to dopamine. Further analysis indicated that AeAANAT1 and AeAANAT2 displayed substrate inhibition for dopamine at a level of 3.2 mM. The enzyme DmAANAT1, which is related to AeAANAT1 and shares 52% sequence identity with AeAANAT1, was shown to have a $K_m$ value of 1.15 mM to dopamin (*9*) an affinity that is 10 times lower than that of AeAANAT1 to dopamine. In comparison, the $K_m$ value for dopamine in cockroach (*Periplaneta americana*) was 25 µM (*11*), an affinity which is approximately 4 times higher than AeAANAT1 and approximately 15 times higher than AeAANAT2 to the same substrate (Refer to the Results section for the $K_m$ values of AeAANAT1 and AeAANAT2). In terms AANATs from other

species, AeAANAT2 showed a $K_m$ value that is closer to zebrafish (0.48 mM), seabream (0.33 mM), and sheep AANATs (1.76 mM) (*22*).

As indicated, we also evaluated affinity of AeAANAT1 and AeAANAT2 to serotonin. AeAANAT2 showed slightly higher affinity towards serotonin than AeAANAT1, which is comparable to $K_m$ value (1.62 mM) of *Drosophila* AANAT1 to serotonin but less than that reported for cockroach AANAT that has a $K_m$ value for serotonin at 50 µM (*11*). $K_m$ values for serotonin in rat, human, and sheep was reported at 1.7 mM, 1.3 mM, and 0.64 mM, respectively (*23*).

AeAANAT1 and AeAANAT2 displayed substrate inhibition by dopamine above 1.6 mM. Inhibition of AANAT by serotonin is reported in the seabream 1 mM, and in cockroach above 0.2 mM (*11, 24*). Inhibition behavior that was dependent on substrate concentration was not observed *Drosophila* AANAT1 or AANAT2 (*9, 11*), but was observed in *P. americana* AANAT beyond 0.2 mM (*11*).

**The possible functions of AeAANATs**

Data in this study indicate several possible functions of AeAANATs in *Ae. aegypti*. One possible role for the AeAANATs may be connected to neurotransmitter inactivation. As discussed above, this possibility is supported by the observation that AeAANAT1, AeAANAT2, AeAANAT3, AeAANAT4, and AeAANAT7 are able to acetylate at least one of the tested arylalkylamines/neurotransmitters, and these genes are also expressed in the head before and after blood feeding. Neurotransmitters, such as octopamine, dopamine, and serotonin are thought to play a role in neurotransmission in mosquitoes (*25, 26*). An accumulation of neurotransmitters such as dopamine can cause severe damage to insects since they do not have MAO-A and MAO-B that are major neurotransmitter inactivators (*27*). As a result, constant firing of the neurotransmitters may be fatal to mosquitoes as well as to other insects. Under these circumstances the presence of multiple AANATs that are capable of inactiving monoamines in the brain would be critical for the survival of these mosquitoes.

Another possible function of AeAANATs may be associated with the process of sclerotization. Sclerotization is an important event in the insect species, in which new cuticle forms in connection with each molt (*4, 28*). *N*-acetyldopamine and *N*-acetyloctopamine are the important precursors in the sclerotization process (*4, 28*). Our hypothesis that AeAANATs play a role in sclerotization is supported by the fact that five AeAANATs are able to acetylate

dopamine, three AeAANATs can acetylate octopamine and two AeAANATs can acetylate norepinephrine and form *N*-acetyldopamine, *N*-acetyloctopamine, and *N*-acetylnorepinephrine respectively. These *N*-acetylated compounds mentioned here are suggested to play role as sclerotization precursors.

Furthermore, AeAANAT1 and AeAANAT2 are able to acetylate serotonin, tyramine and octopamine, which suggests their involvement in the regulation of reproductive functions, as well as the fight-and-flight mechanism in insects (*29*). In particular, AeAANAT4 showed the highest expression in the mature ovarian stage. Given that after the maturation of ovaries female mosquitoes can lay eggs, it suggests that AeAANATs may have a role in reproduction. It should be emphasized that the gene expression profile for seven genes have been carried out and the substrate profiles for eight AeAANATs have been tested but only five were identified as true AANATs. In those five, kinetic analysis of AeAANAT1 and AeAANAT2 was carried out for substrate dopamine and serotonin.

**Conclusions and Future Implications**

This study investigated nine AeAANATs, which may have evolved as a result of evolutionary pressure for adaptation in mosquitoes. This is the first known study in which five of the eight predicted AeAANATs showed activity toward arylalkylamine, thereby verifying their true AANAT identity. Different expression patterns and difference in the substrate profiles suggest different functions for the AeAANATs studied in this report. This is also the first known mosquito-related research that provides a biochemical and molecular base for further analysis of AANATs in *Ae. aegypti* as well as in other mosquito species. The discovery of a significant change of mRNA levels of AeAANATs in the abdomen and head after blood feeding is novel and suggests that these genes may be involved in behavior relevant to blood feeding. Overall, the results of this research resulted in an improved knowledge of AANATs in *Ae. aegypti*.

For future studies, detailed kinetic characterization of AeAANATs should provide further insight regarding their specific functions. Tissue/cell specific localization of individual AeAANATs undoubtedly will aid to the functional elucidation of these mosquito enzymes. Further structural studies could identify ligand-protein interactions, which can also help in studying gene regulation mechanisms. Effective knockdown/knockout studies for AeAANATs can be carried out in order to assign their specific biological functions.

## References


1. Evans, D. A. (1989) *N*-acetyltransferase, *Pharmacol Ther 42*, 157-234.

2. Klein, D. C. (2006) Evolution of the vertebrate pineal gland: the AANAT hypothesis, *Chronobiol Int 23*, 5-20.

3. Klein, D. C. (2007) Arylalkylamine *N*-acetyltransferase: "the Timezyme", *J Biol Chem 282*, 4233-4237.

4. Brodbeck, D., Amherd, R., Callaerts, P., Hintermann, E., Meyer, U. A., and Affolter, M. (1998) Molecular and biochemical characterization of the aaNAT1 (Dat) locus in *Drosophila melanogaster*: differential expression of two gene products, *DNA Cell Biol 17*, 621-633.

5. Amherd, R., Hintermann, E., Walz, D., Affolter, M., and Meyer, U. A. (2000) Purification, cloning, and characterization of a second arylalkylamine *N*-acetyltransferase from *Drosophila melanogaster*, *DNA Cell Biol 19*, 697-705.

6. Bortolato, M., Chen, K., and Shih, J. C. (2008) Monoamine oxidase inactivation: from pathophysiology to therapeutics, *Adv Drug Deliv Rev 60*, 1527-1533.

7. Tsugehara, T., Iwai, S., Fujiwara, Y., Mita, K., and Takeda, M. (2007) Cloning and characterization of insect arylalkylamine *N*-acetyltransferase from *Bombyx mori*, *Comp Biochem Physiol B Biochem Mol Biol 147*, 358-366.

8. Smith, T. J. (1990) Phylogenetic distribution and function of arylalkylamine *N*-acetyltransferase, *Bioessays 12*, 30-33.

9. Hintermann, E., Grieder, N. C., Amherd, R., Brodbeck, D., and Meyer, U. A. (1996) Cloning of an arylalkylamine *N*-acetyltransferase (aaNAT1) from *Drosophila melanogaster* expressed in the nervous system and the gut, *Proc Natl Acad Sci U S A 93*, 12315-12320.

10. Ichihara, N., Okada, M., and Takeda, M. (2001) Characterization and purification of polymorphic arylalkylamine *N*-acetyltransferase from the American cockroach, *Periplaneta americana*, *Insect Biochem Mol Biol 32*, 15-22.

11. Ichihara, N., Okada, M., Nakagawa, H., and Takeda, M. (1997) Purification and characterization of arylalkylamine *N*-acetyltransferase from cockroach testicular organs, *Insect Biochem Mol Biol 27*, 241-246.

12. Dai, F. Y., Qiao, L., Tong, X. L., Cao, C., Chen, P., Chen, J., Lu, C., and Xiang, Z. H. (2010) Mutations of an arylalkylamine-*N*-acetyl transferase, BM-IAANAT, are responsible for the silkworm melanism mutant, *J Biol Chem*.

13. Altschul, S. F., Madden, T. L., Schaffer, A. A., Zhang, J., Zhang, Z., Miller, W., and Lipman, D. J. (1997) Gapped BLAST and PSI-BLAST: a new generation of protein database search programs, *Nucleic Acids Res 25*, 3389-3402.

14. Tamura, K., Dudley, J., Nei, M., and Kumar, S. (2007) MEGA4: Molecular Evolutionary Genetics Analysis (MEGA) software version 4.0, *Mol Biol Evol 24*, 1596-1599.

15. Bembenek, J., Sehadova, H., Ichihara, N., and Takeda, M. (2005) Day/night fluctuations in melatonin content, arylalkylamine *N*-acetyltransferase activity and NAT mRNA expression in the CNS, peripheral tissues and hemolymph of the cockroach, *Periplaneta americana*, *Comp Biochem Physiol B Biochem Mol Biol 140*, 27-36.

16. Iyer, L. M., Aravind, L., Coon, S. L., Klein, D. C., and Koonin, E. V. (2004) Evolution of cell-cell signaling in animals: did late horizontal gene transfer from bacteria have a role?, *Trends Genet 20*, 292-299.

17. Nene, V., Wortman, J. R., Lawson, D., Haas, B., Kodira, C., Tu, Z. J., Loftus, B., Xi, Z., Megy, K., Grabherr, M., Ren, Q., Zdobnov, E. M., Lobo, N. F., Campbell, K. S., Brown, S. E., Bonaldo, M. F., Zhu, J., Sinkins, S. P., Hogenkamp, D. G., Amedeo, P., Arensburger, P., Atkinson, P. W., Bidwell, S., Biedler, J., Birney, E., Bruggner, R. V., Costas, J., Coy, M. R., Crabtree, J., Crawford, M., Debruyn, B., Decaprio, D., Eiglmeier, K., Eisenstadt, E., El-Dorry, H., Gelbart, W. M., Gomes, S. L., Hammond, M., Hannick, L. I., Hogan, J. R., Holmes, M. H., Jaffe, D., Johnston, J. S., Kennedy, R. C., Koo, H., Kravitz, S., Kriventseva, E. V., Kulp, D., Labutti, K., Lee, E., Li, S., Lovin, D. D., Mao, C., Mauceli, E., Menck, C. F., Miller, J. R., Montgomery, P., Mori, A., Nascimento, A. L., Naveira, H. F., Nusbaum, C., O'Leary, S., Orvis, J., Pertea, M., Quesneville, H., Reidenbach, K. R., Rogers, Y. H., Roth, C. W., Schneider, J. R., Schatz, M., Shumway, M., Stanke, M., Stinson, E. O., Tubio, J. M., Vanzee, J. P., Verjovski-Almeida, S., Werner, D., White, O., Wyder, S., Zeng, Q., Zhao, Q., Zhao, Y., Hill, C. A., Raikhel, A. S., Soares, M. B., Knudson, D. L., Lee, N. H., Galagan, J., Salzberg, S. L., Paulsen, I. T., Dimopoulos, G., Collins, F. H., Birren, B., Fraser-Liggett, C. M., and Severson, D. W. (2007) Genome sequence of *Aedes aegypti*, a major arbovirus vector, *Science 316*, 1718-1723.

18. Coon, S. L., and Klein, D. C. (2006) Evolution of arylalkylamine *N*-acetyltransferase: emergence and divergence, *Mol Cell Endocrinol 252*, 2-10.

19. Pavlicek, J., Sauzet, S., Besseau, L., Coon, S. L., Weller, J. L., Boeuf, G., Gaildrat, P., Omelchenko, M. V., Koonin, E. V., Falcon, J., and Klein, D. C. (2010) Evolution of

AANAT: expansion of the gene family in the cephalochordate amphioxus, *BMC Evol Biol 10*, 154.

20. Scheibner, K. A., De Angelis, J., Burley, S. K., and Cole, P. A. (2002) Investigation of the roles of catalytic residues in serotonin *N*-acetyltransferase, *J Biol Chem 277*, 18118-18126.

21. Marinotti, O., Nguyen, Q. K., Calvo, E., James, A. A., and Ribeiro, J. M. (2005) Microarray analysis of genes showing variable expression following a blood meal in Anopheles gambiae, *Insect Mol Biol 14*, 365-373.

22. Zilberman-Peled, B., Ron, B., Gross, A., Finberg, J. P., and Gothilf, Y. (2006) A possible new role for fish retinal serotonin-*N*-acetyltransferase-1 (AANAT1): Dopamine metabolism, *Brain Res 1073-1074*, 220-228.

23. Ferry, G., Ubeaud, C., Dauly, C., Mozo, J., Guillard, S., Berger, S., Jimenez, S., Scoul, C., Leclerc, G., Yous, S., Delagrange, P., and Boutin, J. A. (2004) Purification of the recombinant human serotonin *N*-acetyltransferase (EC 2.3.1.87): further characterization of and comparison with AANAT from other species, *Protein Expr Purif 38*, 84-98.

24. Zilberman-Peled, B., Benhar, I., Coon, S. L., Ron, B., and Gothilf, Y. (2004) Duality of serotonin-*N*-acetyltransferase in the gilthead seabream (*Sparus aurata*): molecular cloning and characterization of recombinant enzymes, *Gen Comp Endocrinol 138*, 139-147.

25. Pratt, S., and Pryor, S. C. (1986) Dopamine- and octopamine-sensitive adenylate cyclase in the brain of adult *Culex pipiens* mosquitoes, *Cell Mol Neurobiol 6*, 325-329.

26. Lee, D. W., and Pietrantonio, P. V. (2003) In vitro expression and pharmacology of the 5-HT7-like receptor present in the mosquito *Aedes aegypti* tracheolar cells and hindgut-associated nerves, *Insect Mol Biol 12*, 561-569.

27. Meyer, J. H., Ginovart, N., Boovariwala, A., Sagrati, S., Hussey, D., Garcia, A., Young, T., Praschak-Rieder, N., Wilson, A. A., and Houle, S. (2006) Elevated monoamine oxidase a levels in the brain: an explanation for the monoamine imbalance of major depression, *Arch Gen Psychiatry 63*, 1209-1216.

28. Andersen, S. O. (2008) Quantitative determination of catecholic degradation products from insect sclerotized cuticles, *Insect Biochem Mol Biol 38*, 877-882.

29. Brembs, B., Christiansen, F., Pfluger, H. J., and Duch, C. (2007) Flight initiation and maintenance deficits in flies with genetically altered biogenic amine levels, *J Neurosci 27*, 11122-11131.

# Chapter 6. Summary

This section summarizes the two important aspects of tyrosine metabolism described in this dissertation. As noted earlier, tyrosine is an aromatic amino acid that is vital for the synthesis of thyroid hormones, catecholamines and melanin. Tyrosine is involved in several physiological and biochemical functions including energy metabolism, which occurs as a result of its degradation via multiple enzymes. Additionally, tyrosine is also implicated in the synthesis of certain neurotransmitters, such as dopamine.

One of the enzymes that impacts tyrosine catabolism is tyrosine aminotransferase (TAT). TAT plays a vital role in the metabolic degradation process by catalyzing the reversible transamination of tyrosine into *p*-hydroxyphenylpyruvate. Tyrosine degradation is stimulated by glucocorticoids in the liver, which yields fumarate and acetoacetate. Fumarate is then converted to oxaloacetate, thereby stimulating gluconeogenesis. The liver can then synthesize and export glucose into plasma, after which acetoacetate is secreted and used by neurons and muscle tissue for oxidative energy production.

TAT has been found in bacteria, fungi, parasites, and humans. In mammals, TAT is primarily found in the liver, and to a lesser extent in the kidneys. Mammalian TAT is regulated by way of the ubiquitination pathway and glucocorticoids. Genetic mutations in TAT can lead to diseases such as tyrosinemia type II, which is an autosomal recessive condition that can begin in early childhood when painful circumscribed callosities develop on the pressure points of the palm and sole (i.e., hyperkeratosis). Half of all those with this disorder also suffer from some form of mental retardation.

Various biochemical differences exist between mammalian TAT and its analogue, *Trypanosoma cruzi* TAT (TcTAT), which plays a role in pathogenesis of Chagas disease. TcTAT has been shown to be over-expressed in strains of certain parasites that are resistant to benznidazole, an antiparasitic drug used to treat Chagas disease and included in selected chemotherapy regimes. Therefore, TcTAT has been suggested to have important implications for the development of new chemotherapeutic agents.

As noted, TAT has been characterized in several species. Although the structure of human TAT (hTAT) was solved, there was little discussion on its structural characteristics in literature. Given that, the objectives of our first study was (1) to conduct a comparative

biochemical and structural characterization of mouse TAT (mTAT) and (2) to differentiate between the active sites of mTAT and tcTAT via molecular dynamics simulations in order to provide further insights into substrate-enzyme interactions in human TAT/ mTAT and TcTAT.

In order to fulfill these objectives, recombinant TAT was cloned and expressed using the bacterial expression system. The protein was then purified via affinity, ion exchange and gel exclusion chromatographies. Kinetic analysis was subsequently conducted using sixteen amino acids and sixteen keto acids, which revealed that tyrosine and *p*–hydroxyphenylpyruvate are the most effective amino acid donor and acceptor for TAT, respectively. In other words mTAT has highest affinity to *p*-hydroxyphenylpyruvate and tyrosine.

For our structural studies, full-length TAT was cloned and expressed using the bacterial expression system, which failed to afford the desired crystals. However, when TAT was expressed and purified without the ubiquitin domain, we were able to obtain crystals. The subsequent diffraction of these crystals resulted in orthorhombic mTAT crystals with 2.9 Å, and whose structure was solved using the molecular replacement method. Furthermore, an active center was identified based on the presence of PLP in the center. Superimposing mTAT structure with the analogous hTAT structure resulted in a better understanding of both active sites, which were found to be identical.

One important observation we made with respect to the mTAT structure was the presence of conserved Asp247, which is vital for transaminase catalysis. Another major finding that resulted from our research is the detection of a disulfide bond between Cys144 and Cys275 residues on the surface of the mTAT structure. Because Cys144 is present in the active site, it is possible that it forms a hydrogen bond with the N1 of the pyridine ring and hinders the process of catalysis when exposed to oxidizing agent at the surface. However, in the presence of a reducing agent, this inactivation process was reversed, which points to the role of Cys144 in the regulation of mTAT activity. Furthermore, reducing agents may break the disulfide bond and change the Cys144 conformation back to an active form, which is the most likely explanation for the reversibility feature associated with TAT inactivation-activation. Future studies involving these two residues should employ site-directed mutagenesis to shed additional light on their roles in protein inactivation-activation.

This study also used molecular dynamics studies to further elucidate differences in the TcTAT and mTAT substrate profiles. Additionally, the simulations we conducted predicted that

there are hydrophobic interactions in tcTAT that may be utilized by both alanine and tyrosine during enzyme catalysis, and that tyrosine is further stabilized by hydrogen bonding to a nearby Arg419 residue. In the case of hTAT (and probably in mTAT as well), additional hydrophobic and hydrogen bonding interactions were found to promote the binding of tyrosine, but were too distant from the active site to be utilized by alanine.

Future work will employ the crystal structure of mTAT-tyrosine complex to confirm the interactions predicted by molecular dynamics studies. Mutations of the residues will be carried out, which may prove to be important with respect to the interactions between the tyrosine and enzyme complex; these results will help us understand their roles in the stability of the enzymes.

In mammals, tyrosine is involved in selected neurotransmitter synthesis, such as dopamine. In addition to its role in producing dopamine as in mammals, tyrosine is a precursor in the synthesis of octopamine in insects, which is an endogenous insect biogenic amine. It has been suggested that in insects octopamine is a substitute of norepinephrine. This amine is thought to be involved in the fight-or-flight mechanisms in insects. Another important neurotransmitter found in insects is tyramine (the decarboxylation product of tyrosine) which is associated with reproductive behaviors. Regulation of these two neurotransmitters is essential for proper functioning of the neurons. One of the mechanisms by which neurotransmission is regulated is via inactivation of neurotransmitters by enzymes. In mammals, neurotransmitters (such as dopamine) are inactivated by monoamine oxidases. In insects, however, monoamine oxidase activity has not been identified. This difference may have resulted from evolutionary changes in the enzymes, causing them to regulate neurotransmitters via other pathways.

One family of enzymes implicated in the regulation of neurotransmitters is arylalkylamine *N*-acetyltransferase (AANAT). AANATs have been shown to play a role in melatonin synthesis in mammals—but their role in insects has yet to be established. In mammals, only one copy of this gene is present, suggesting that mammalian AANAT may be associated with a specific function. In insects, however, several AANAT-like genes are present in their genome. It is difficult to predict the function(s) of the insect AANAT genes based on the characterized genes from other species due to low sequence identity. Phylogenetic analysis also separated insect AANATs from bacterial and mammalian AANAT, suggesting that insect AANAT may have very different functions.

Using *Drosophila* AANAT as a query sequence we were able to identify nine putative AANAT-like proteins in *Aedes aegypti* via BLAST search. Biochemical and molecular biology approaches were used to characterize these *Ae. aegypti* AANATs, which resulted a better understanding of the role of these enzymes in *Ae. aegypti* mosquito species. As detailed in this dissertation, most of the counterpart proteins of the AeAANATs have been found in other mosquito genera, such as *Anopheles gambiae* and *Culex quinquefasciatus*, making it easier for researchers to predict the functions of AANATs based on our study. Through substrate screening of the expressed recombinant enzymes, five out of eight expressed putative AeAANATs have been identified as true AeAANATs and among them AeAANAT1 and AeAANAT2 showed broad substrate specificity, suggesting that they have multiple functions. In contrast, other three AANATs, termed AeAANAT3, AeAANAT4 and AeAANAT7, respectively, displayed narrow substrate specificity, suggesting that they may have restricted functionality. Differences in substrate specificity suggested that there might be a difference in the active sites of these enzymes.

Discontinuous expression profiles for the AeAANATs were investigated throughout the lifecycle of *Ae. aegypti*. AeAANAT1, AeAANAT2, AeAANAT3, AeAANAT4, AeAANAT7, AeAANAT8, and AeAANAT9 show different expression patterns. For example, AeAANAT1 is primarily transcribed in the black pupae when compared to the other AeAANATs studied. AeAANAT2, AeAANAT4, AeAANAT7, AeAANAT8, and AeAANAT9 showed the highest transcription during the egg maturation stage after the blood-feeding event. Transcripts of AeAANAT2, AeAANAT4, AeAANAT7, AeAANAT8, and AeAANAT9 are down-regulated in the head following the blood-feeding event. The differences in their transcriptional profiles suggest that these genes may be under the control of different promotor.

Based on their substrate and transcriptional profiles, we believe that AeAANATs play multiple roles in various processes, including cuticular sclerotization, neurotransmitter inactivation and reproduction. These possibilities are based on several observations. For example, arylalkylamines such as dopamine (a precursor for sclerotization) can be utilized by five AeAANATs. Another possible role of AeAANATs is linked to neurotransmitter inactivation in the central nervous system, which is based on the fact most of AeAANATs are expressed in the head and are able to acetylated most of the neurotransmitters. Further, AeAANATs may

directly or indirectly play a role in reproduction because most of them showed their highest expression during egg development.

The acetylation of dopamine by five AeAANATs supports the view that acetylation of arylalkylamine is important to the biology of this organism, and that these genes have been evolved in response to specific pressures related to requirements for monoamine acetylation.

Future work will employ continuous expression profiles for these genes. Additionally, the spatial expression profiles of these genes from male and female mosquitoes from brains, fat body, antennae, testis, ovaries, legs, and wings should produce information to predict the specific functions of individual AANATs. Structural studies to identify the ligand-protein interactions should enable us to better understand their substrate specificity and catalysis. Effective knockdown studies against individual AANATs should further aid to the elucidation of their specific functions.

In summary, this dissertation describes and discusses several different aspects of tyrosine metabolism. As discussed herein, not only was the previous assumption of disulfide bond formation critically addressed, but some additional key questions—such as why there are differences in the substrate profiles of TcTAT and mTAT—were also logically explained. Another very important aspect of this dissertation is that this study represents the first attempt to systematically understand the complex roles of AANATs in *Ae. aegypti*.

# Appendix I. An attempt to Crystallize Full-length Mouse Tyrosine Aminotransferase (mTAT)

## AI.1 Statement of rational

Tyrosine aminotransferase (TAT) catalyzes the reversible transamination of tyrosine to *p*-hydroxyphenylpyruvate. Accumulation of tyrosine leads to several disorder as discussed in Chapter 2. Mutations in the TAT leads to a genetic disorder tyrosinemia type II. This attempt to crystallize full length mTAT was made as a model for human tyrosine aminotransferase.

## AI.2 Materials and Methods

**Expression and purification of tyrosine aminotransferase with ubiquitin domain (TAT-ubi)**

A full-length coding sequence of TAT-ubiquitin was amplified using mouse brain cDNA. Cloning and overexpression of TAT-ubiquitin was accomplished using pTYB12 vector (IMPACT. TAT-ubiquitin was amplified utilizing a forward primer (5'CATATGGACTCCTACGTAATCCGG 3') containing an Nde1 restriction site and a reverse primer (5' CTCGAGCTATTTGTCACACTCCTCCT 3') containing an Xho I restriction site. The amplified sequence, which encoded mTAT amino acid residues 1 to 454 (NP666326), was cloned into an Impact™-CN plasmid (pTBYB12 vector, New England Biolabs) for expression of a fusion protein containing a chitin-binding domain. Transformed *E. coli* cells were cultured at 37$^{o}$C. After induction with 0.2 mM isopropyl -1-thio-β-D-galactopyranoside, the cells were cultured at 15$^{o}$C for 24 hrs. Twenty liters of cells were harvested as the starting materials for affinity purification. The soluble fusion proteins were applied to a column packed with chitin beads and subsequently hydrolyzed under reduction conditions. The affinity purification resulted in the isolation of mTAT at approximately 80% purity. Further purification of the recombinant mTAT was achieved by Source Q ion-exchange and gel-filtration chromatography (Figure AI.1), after which the purified recombinant mTAT was concentrated to 10 mg ml$^{-1}$ protein in a 10 mM phosphate buffer (pH 7.5) containing 40 mM pyridoxial 5'-phosphate using a Centricon YM-50 concentrator (Millipore).

**Crystallization of TAT-ubiquitin domain**

Protein concentration was determined by a protein assay kit from Bio-Rad (Hercules, CA) using bovine serum albumin as a standard. The concentrated protein (10 mg/ml) was used directly in crystallization screening via the hanging drop method. (Details describing crystallization procedures are similar to those described in Chapter 3.)

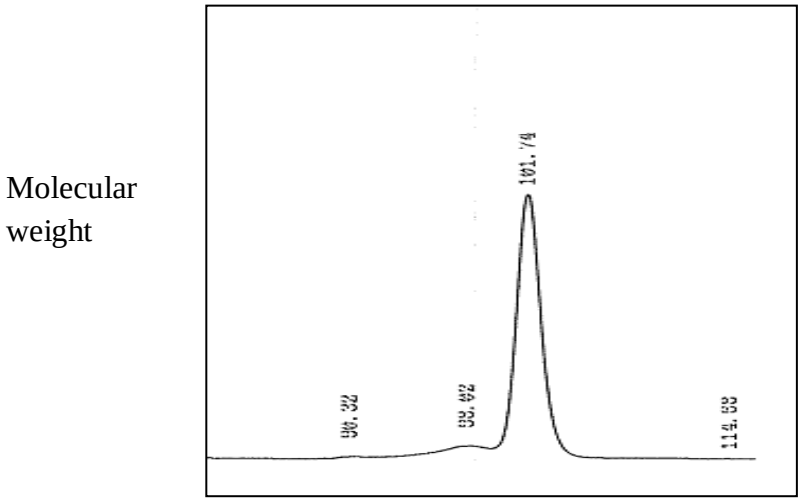


**Figure AI.1Gel filtration chromatogram of full-length mTAT.**

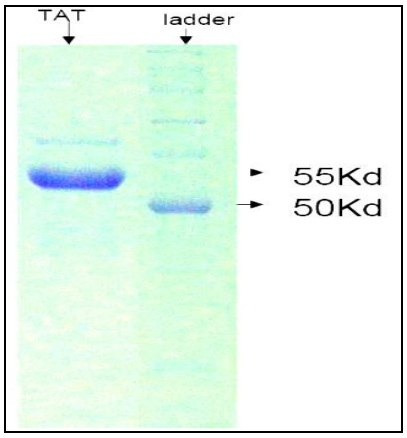


**Figure AI.2 SDS-PAGE of purified full-length mTAT.**

## AI.3 Results

Gel filtration chromatogram (Figure AI 1) revealed that the protein was a homodimer with a molecular weight of 101 kDa. Figure AI 2 show the full length mTAT on SDS-PAGE gel which was approximately 51 kDa (Figure AI 2). The full length TAT was active (data not shown). Although numerous crystallization conditions were applied we were unable to obtain crystals for full-length mTAT.

## AI.4 Discussion

The attempt to obtain the crystals for full-length mTAT was not successful. We speculate that the protein likely is highly unstable due to the presence of the N-terminal ubiquitin domain and C-terminal PEST sequence. This assumption is supported by a report which suggested these regions may play a role in the degradation of TAT (*1*). Further, these regions do not participate in activity of this enzyme (*2*). mTAT was expressed without these regions and we were successful in obtaining the desired crystals (For more information please refer Chapter 3).

## References


1. Hargrove, J. L., Scoble, H. A., Mathews, W. R., Baumstark, B. R., and Biemann, K. (1989) The structure of tyrosine aminotransferase. Evidence for domains involved in catalysis and enzyme turnover, *J Biol Chem 264*, 45-53.

2 Sobrado, V. R., Montemartini-Kalisz, M., Kalisz, H. M., De La Fuente, M. C., Hecht, H. J., and Nowicki, C. (2003) Involvement of conserved asparagine and arginine residues from the *N*-terminal region in the catalytic mechanism of rat liver and *Trypanosoma cruzi* tyrosine aminotransferases, *Protein Sci 12*, 1039-1050

# Appendix II. Examination of Catecholamines in Brain and Body Extracts by Positive-Ion Electrospray Tandem Mass Spectrometry

## AII.1 Introduction

Neurotransmission is a very important physiological process, which is characterized by three distinct stages: synthesis of the neurotransmitters; storage of the neurotransmitters, and release of these neurotransmitters (dopamine, serotonin, and octopamine). Once they are released, neurotransmitters bind to activate receptors in postsynaptic membranes. Ultimately insects must deactivate these neurotransmitters—either by the reuptake mechanism, or via enzymatic processesing. In mammal, biogenic amines, catabolizing enzymes i.e., monoamine oxidase (MAO) and catechol-*O*-methyltransferase (COMT) play a major role in their inactivation. MAO and COMT are not present in the insect nervous system (*1*). Inactivation of biogenic amines may be achieved by alternative metabolic pathways, such as *N*-acetylation and *O*-sulfation (*2, 3*). It has been hypothesized that *N*-acetylation is the pathway of monoamine inactivation in the insect brain, but to date there have been no studies that corroborate that conjecture. Based on our sequence analysis, nine hypothetical *N*-acetyltransferases have been found in *Aedes aegypti*. Our results suggest that six AeAANATs are expressed in the head, and five of them have activity toward arylalkylamines. These results provide persuasive evidence to suggest that AANATs may be the primary pathway for neurotransmitter inactivation in *Ae. aegypti*. This study attempted to demonstrate whether *N*-acetylation is the main pathway in the brain of *Ae. aegypti* for neurotransmitter inactivation. We also investigated for the presence of melatonin the circadian hormones in the brain and body extracts of *Ae. aegypti* mosquitoes. Our results suggest *N*-acetylation does occur in the brain, but we were unable to detect the presence of melatonin in the brain or body extracts. Therefore, further investigation is necessary to elucidate the role of *N*-acetylation in the brain and the subsequent outcomes.

## AII.2 Materials and Methods

Dopamine, serotonin, and melatonin were purchased from Sigma. *Ae. aegypti* mosquitoes were reared as described in Chapter 5, after which the females of this species were separated from the males. The female mosquitoes were divided into three groups one group was either fed

on dopamine (50 mM) or one group on serotonin (25 mM) for 5 hours and other group was fed on 10% sugar solution as a control. Standards for dopamine and *N*-acetyldopamine were prepared in water on the same day of the experiments.

**HPLC analysis of dopamine from tissue extracts**

The brains of the *Ae. aegypti* females were separated from the bodies and placed in 0.4 M formic acid and 0.05 M $Na_2$-EDTA. All tissues were transferred into eppendorf vials containing 200 µl of 0.1 mM formic acid with antioxidants, and placed on ice. Tissues were sonicated and centrifuged at 14,000 g for 20 min at 4 °C, and then the supernatant was collected and stored at −20 °C prior to analysis. Supernatants were chromatographed by HPLC with a reverse-phase column (C18 of 5 µm particles, 4.6 X 1100 mm), and resolved substrate and product were detected by HPLC with electrochemical detection (HPLC-ED). The biogenic amines were chromatographed in the presence of 6% acetonitrile and 50 mM of a $NaH_2PO_4$ monobasic buffer.

**Liquid chromatography (LC) and mass spectrometry (MS) analysis of dopamine and *N*-acetyldopamine from the brains and bodies of *Aedes aegypti*.**

Agilent LC pump with reverse phase column (C18, 2.1x50 mm) was used to separate the *N*-acetyldopamine and dopamine. LC separation was done using organic solvent comprised of 0.1% formic acid, 60% methanol, and 40% water as a mobile phase. The system was equilibrated for 2 min. 100 µL of prepared samples were injected for HPLC-MS analysis. *N*-acetyldopamine and dopamine were introduced into the 3200 Q-TRAP (Applied Biosystems / MDS SCIEX). Tandem mass spectrometry was used in the positive-ion interfaced with a TurboIonSpray™. Table AII. 1 shows the parameters used during this experiment. TurboIonSpray was operated at 600 ºC to introduce the LC eluent into the mass spectrometer. An enhanced product ion (EPI) scan was used to trace the *N*-acetyldopamine at (m/z 196.20). The collision gas we utilized in this experiment was nitrogen with a cell pressure of 1.1 Pa. The mass transition-dependent collision energy was 20 V for transitions *m/z* 154-137, 196-137 for the semiquantitative analysis of *N*-acetylated compounds in the brain of *Ae. aegypti*. Data were processed using Analyst 1.4.2.

**Table AII.1 Parameters used for scanning EPI spectrum.**

| | |
|---|---|
| Curtain gas | 35.00 PSI |
| Ion spray voltage (IS) | 4500 volts |
| Turbo gas temperature (TEM) | 600 ºC |
| Nebulizer gas (GS 1) | 70 PSI |
| Turbo gas (GS 2) | 60 PSI |
| CAD | High |
| DP (Declustering potential) | 40 volts |
| Detector parameter (CEM) | 2500 |

## AII.3 Results

Detection of *N*-acetyldopamine in the brain and body extracts of *Ae. aegypti* was not successful using the HPLC-electrochemical detection. Further, we used LC-MS/MS in positive mode to detect levels of dopamine and *N*-acetyldopamine. Based on the retention time, dopamine and *N*-acetyldopamine were detected in brains and body extracts of *Ae. aegypti*. *N*-acetyldopamine in the brain (Figure AII.2 and Figure AII.3) and body extracts (Figure AII.4 and Figure AII.5) of mosquitoes were detected five hours after dopamine feeding. The *N*-acetyldopamine was traced using enhanced product ion scan (linear ion trap scan mode) at m/z 196. An accumulation of dopamine and an increase in the level of the *N*-acetylated compound was also detected compared to the control (sugar) after 5 hours of feeding, thus indicating the presence of an *N*-acetylation pathway in the brain of *Ae. aegypti*. It is important to note that an attempt was made to detect serotonin, *N*-acetylserotonin, and melatonin from the brain and body extracts of *Ae. aegypti* using similar methods, but we were unable to detect these compounds in both the extracts under the conditions used in this study. It should also be noted that under our conditions melatonin and *N*-acetylserotonin were not detected from the mosquito brain and body extracts, but in the serotonin-fed samples, an increase in the level of dopamine was observed.

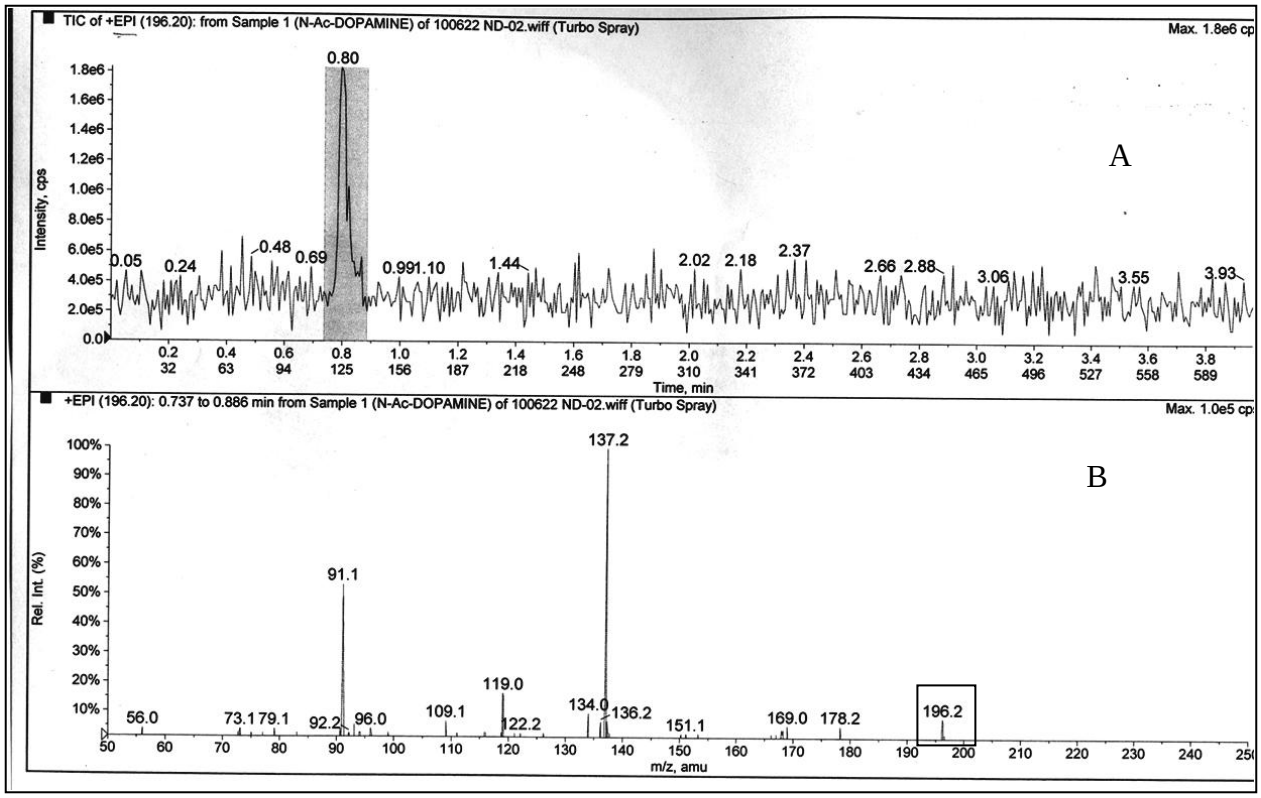


**Figure AII.1 Detection of *N*-acetyldopamine standard using the product ion spectra of protonated molecular ion with collision energy of 20 V.**

100 µM of *N*-acetyldopamine standard was injected on the LC instrument. A) Total ion chromatogram (LC-MS-TIC) of *N*-acetyldopamine. B) Electrospray ionization (ESI-MS) spectrum of molecular ion of separated *N*-acetyldopamine fragments. In Figure A X axis represents the time (min) and Y-axis represents the intensity in counts per seconds (CPS). In Figure B X-axis represents the time (Figure A) and m/z (Figure B) and Y-axis represents relative intensity in (%). 196.2 represents the precursor ion for *N*-acetyldopamine.

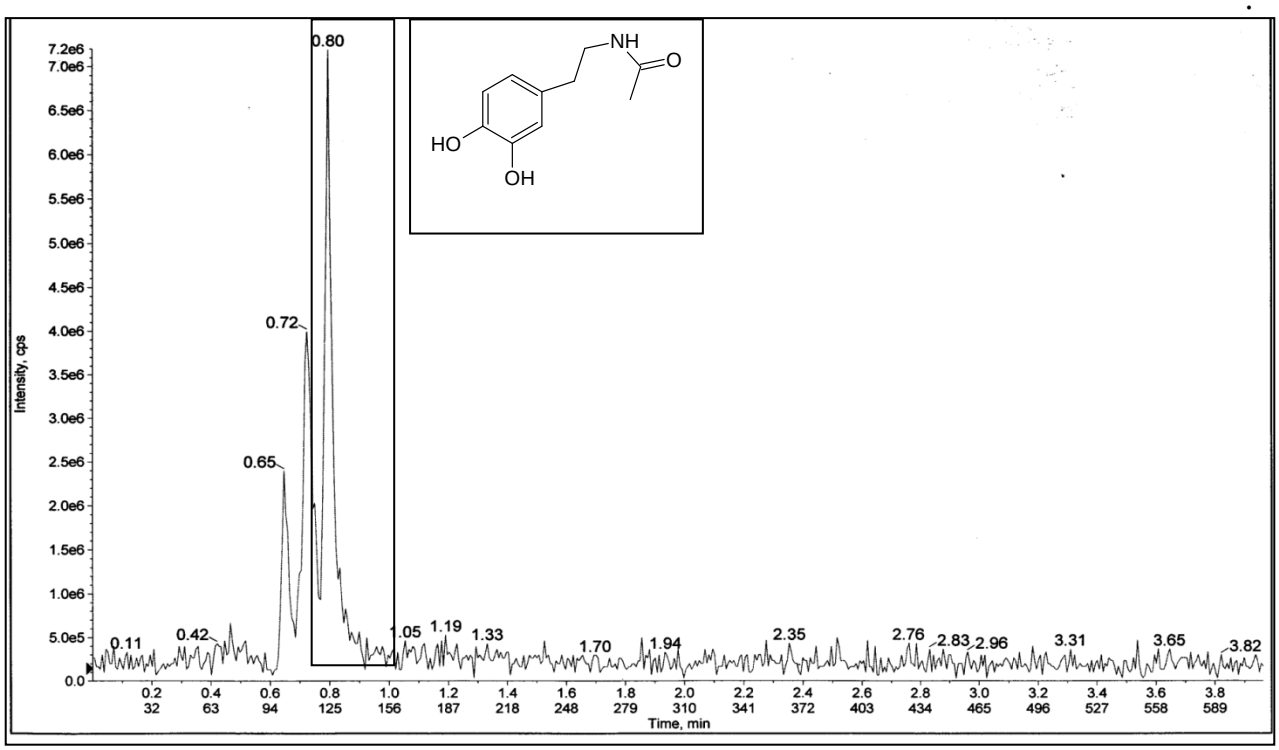


**Figure AII.2 LC-MS-TIC chromatogram of *N*-acetyldopamine from head sample.**
In this figure X axis represents the time (min) and Y-axis represents the intensity in counts per seconds (CPS).

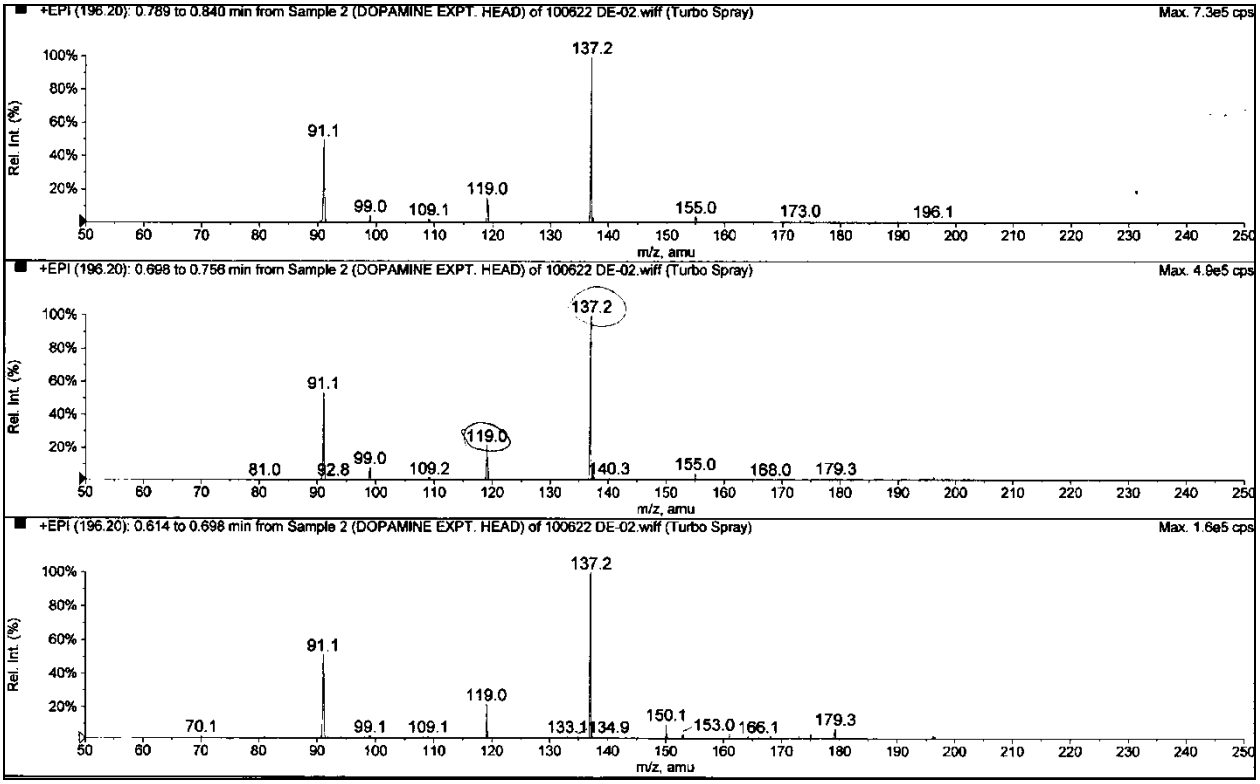


**Figure AII.3 ESI –MS spectrum of molecular ion of separated *N*-acetyldopamine fragments from head sample.**

In this figure X-axis represents the m/z and Y-axis represents relative intensity.

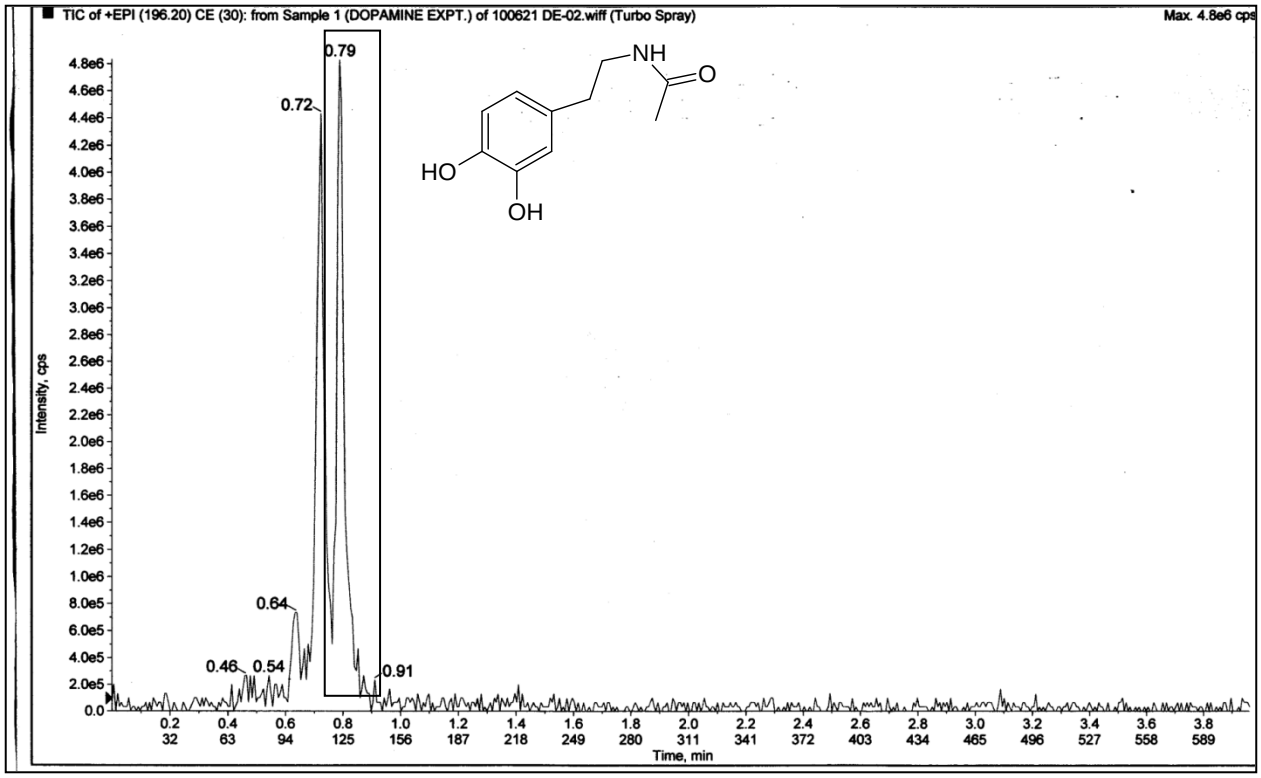


**Figure AII.4 LC-MS-TIC chromatogram of *N*-acetyldopamine from body sample.**
In this figure X axis represents the time (min) and Y-axis represents the intensity in counts per seconds (CPS).

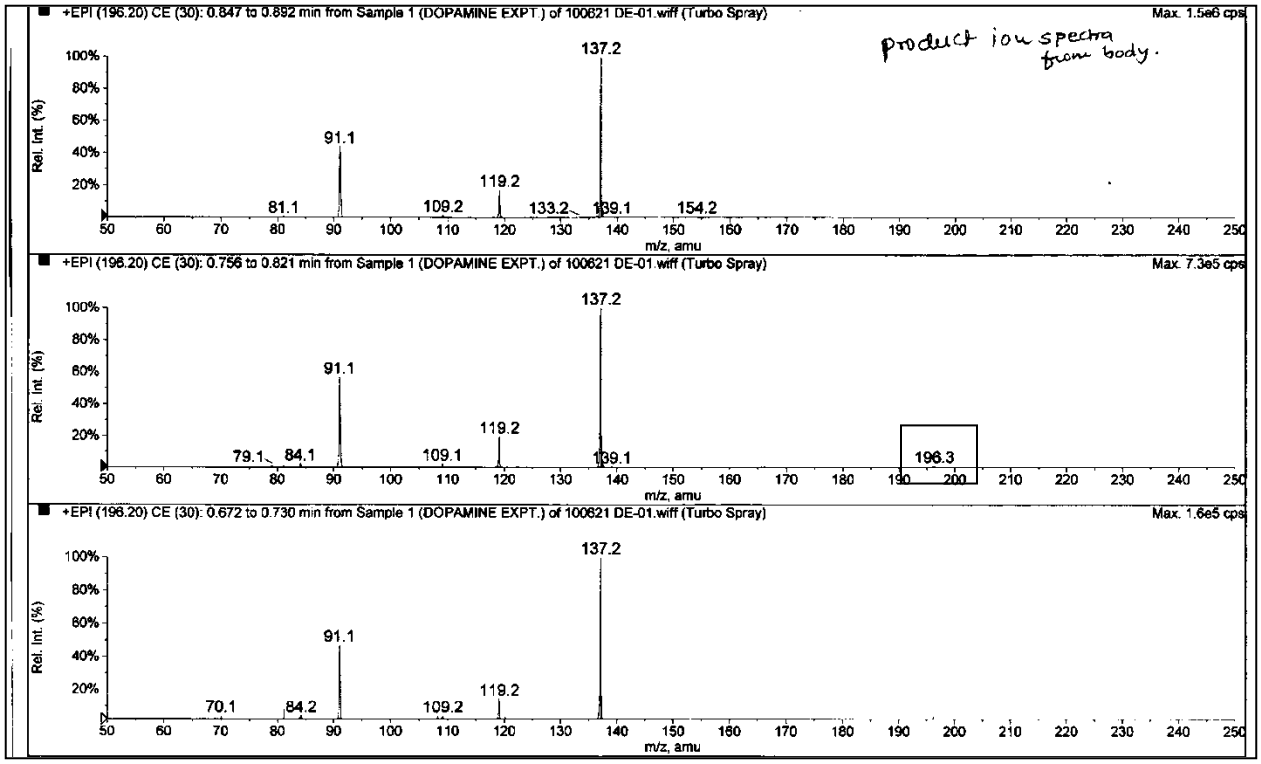


**Figure AII.5 Detection of *N*-acetyldopamine from the body of the mosquitoes using the product ion spectra of protonated molecule**.

In Figure X-axis represents the m/z and Y-axis represents relative intensity.

## AII.4 Discussion

Trace amounts of *N*-acetyldopamine were detected using the EPI method from brain and body extracts, suggesting the presence of *N*-acetylated pathways in the brain and body Inability to detect *N*-acetylserotonin or melatonin with either method in the extracts raised a question whether these compounds used in downstream pathways. This hypothesis needs to be investigated. Similarly, melatonin was not detected in either brain or body extracts from *Ae. aegypti*. This absence suggested that (1) AeAANATs in the brain may not play a key role in circadian rhythm regulation or (2) melatonin was further metabolized. We were able to detect dopamine in the serotonin-fed mosqutoes using the MRM method (data not shown), which suggests that serotonin may regulate the release of dopamine in the brain and the body of *Ae. aegypti*. A similar phenomenon has been associated with human regulatory functions, where it has been suggested that serotonin does play an important role in controlling dopamine levels in the brain (*4*).

## References


1. Sloley, B. D. (2004) Metabolism of monoamines in invertebrates: the relative importance of monoamine oxidase in different phyla, *Neurotoxicology 25*, 175-183.

2. Wright, T. R. (1987) The genetics of biogenic amine metabolism, sclerotization, and melanization in *Drosophila melanogaster*, *Adv Genet 24*, 127-222.

3. Roeder, T., Seifert, M., Kahler, C., and Gewecke, M. (2003) Tyramine and octopamine: antagonistic modulators of behavior and metabolism, *Arch Insect Biochem Physiol 54*, 1-13.

4. Di Matteo, V., Di Giovanni, G., Pierucci, M., and Esposito, E. (2008) Serotonin control of central dopaminergic function: focus on in vivo microdialysis studies, *Prog Brain Res 172*, 7-44.

This page was intentionally left blank